OPEN ACCESS

University of BRISTOL

This electronic thesis or dissertation has been downloaded from Explore Bristol Research, http://research-information.bristol.ac.uk

Author:
Dickson, Emily J

Title:
The polarised secretion of the human umbilical vein endothelial eell

General rights
Access to the thesis is subject to the Creative Commons Attribution - NonCommercial-No Derivatives 4.0 International Public License. A copy of this may be found at https://creativecommons.org/licenses/by-nc-nd/4.0/legalcode This license sets out your rights and the restrictions that apply to your access to the thesis so it is important you read this before proceeding.

Take down policy
Some pages of this thesis may have been removed for copyright restrictions prior to having it been deposited in Explore Bristol Research. However, if you have discovered material within the thesis that you consider to be unlawful e.g. breaches of copyright (either yours or that of a third party) or any other law, including but not limited to those relating to patent, trademark, confidentiality, data protection, obscenity, defamation, libel, then please contact collections-metadata@bristol.ac.uk and include the following information in your message:

• Your contact details
• Bibliographic details for the item, including a URL
• An outline nature of the complaint

Your claim will be investigated and, where appropriate, the item in question will be removed from public view as soon as possible.

The Polarised Secretion of the Human Umbilical Vein Endothelial Cell

Emily Dickson

School of Biochemistry

February 2020

Word Count: Thirty-two thousand, eight hundred and nineteen

Abstract

Endothelial cells (ECs) are polarised, allowing them to secrete different proteins into both the circulating fluid, and the underlying matrix. However, there is little understanding of how this polarised secretion occurs. Using mass spectrometry, I have examined the role liprin-α1 plays in the secretion of proteins, which had previously been identified to be involved in the secretion of fibronectin from the basolateral surface. I have shown that liprin-α1 affects the polarised secretion of a subset of proteins, particularly those involved in the assembly of the extracellular matrix (ECM) such as collagen-α1 and α2. Previous studies have suggested that atorvastatin treatment has a positive pleiotropic effect upon ECs, reducing the risk of atherosclerosis. I have shown that atorvastatin treatment affected the secretion of certain proteins from both the apical and basolateral surface of the ECs. One major group of proteins affected were proteins involved in the ECM. Dysregulation of the ECM has previously been shown to be involved in the pathogenesis of atherosclerosis. Additionally, atorvastatin treatment increased the apical/basal secretion ratio of some proteins also known to be involved in the pathogenesis of atherosclerosis, including biglycan. However, atorvastatin also increased the apical secretion of protein-glutamine gamma-glutamyltransferase 2, which is known to decrease rupture of atherosclerotic plaques. Whilst my study provides a slight insight into the polarised secretion from ECs and the role atorvastatin treatment may have in patients with atherosclerosis, further research is needed to validate these results.

Dedication and Acknowledgements

Firstly, I would like to thank my supervisor Professor Harry Mellor for his assistance, guidance and patience throughout my project. I would also like to express my gratitude to Dr Ananthalakshmy Sundararaman and Dr Haoche Wei for their support throughout my project, for teaching me new techniques, and providing suggestions and insights to allow me to develop as an individual scientist. I would like to especially extend my thanks to Haoche for generously spending his time assisting me with my initial experiments, and Ananthalakshmy for her assistance during imaging. I would also like to acknowledge the Wolfson Bioimaging Facility at the University of Bristol for access to the microscopes used throughout my project.

I would like to pay special regards to my family for supporting me throughout my entire study, and whom without none of this would be possible. They have given an enormous amount of time and dedication towards my education, and their encouragement has enabled to finish my study. I would like to thank my sister Anna for providing criticisms and feedback on my draft versions.

I would like to thank my friends for their constant support, and the University of Bristol Swimming and Water Polo club for making my time at University unforgettable.

Authors declaration

I declare that the work in this dissertation was carried out in accordance with the requirements of the University's Regulations and Code of Practice for Research Degree Programmes and that it has not been submitted for any other academic award. Except where indicated by specific reference in the text, the work is the candidate's own work. Work done in collaboration with, or with the assistance of, others, is indicated as such. Any views expressed in the dissertation are those of the author. SIGNED:
..... DATE:.....

Page of Contents

List of Tables

List of Figures

List of Abbreviations

Abbreviation	Description
ATP	Adenosine triphosphate
AJ	Adherens junction
BBB	Blood brain barrier
BSA	Bovine serum albumin
CCV	Clathrin coated vesicle
EE	Early endosome
EC	Endothelial cell
EDA-FN	Extra domain A fibronectin
eNOS	Endothelial nitric oxide synthase
ECM	Extracellular matrix
EV	Extracellular vesicle
tPA	Fibrinolytic tissue-type plasminogen activator
FN	Fibronectin
GLUT1	Glucose transporter 1
HUVEC	Human umbilical vein endothelial cell
IGF	Insulin-like growth factor
IL-8	Interleukin 8
ICAM-1	Intracellular adhesion molecule-1
ILV	Intraluminal vesicles
LSEC	Liver sinusoidal endothelial cells
LDL	Low density lipoprotein
MV	Microvesicle
MVB	Multivesicular bodies
MVE	Multivesicular endosome
NO	Nitric oxide
NOS	Nitric oxide synthase
TSP1	Thrombospondin-1
TJ	Tight junction
TGN	Trans-Golgi network
VE-cadherin	Vascular endothelial cadherin
vWF	Von Willebrand factor
wPB	Weibel-Palade bodies
ZO-1	Zona occludens 1

Chapter 1 Endothelial cells

Endothelial cells (ECs) line the internal surface of the vessels within the circulatory system, forming a thin layer called the endothelium. Initially thought to be an inert barrier, this dynamic layer of cells acts as a selectively permeable barrier, regulating the passage of molecules between the tissue and the blood or lymph stream [1]. These vessels form part of the human vascular system, which facilitate the transportation of blood and lymph around the body and are involved in the removal of waste substances such as CO_2, to maintain homeostasis, the maintenance of a constant internal environment. Within the human body there are approximately 10^{13} ECs, making up 1.25% of the average human body mass [1].

There are three main types of vessels within the vascular system: veins, arteries, and capillaries. ECs play important roles in supporting the integrity of these vessels which are each specialised to accommodate a variety of pressures and the particular demands of individual tissues [2]. Dependent on their location within the body, ECs within the vascular system have distinctive morphology and functions and can display different surface receptors, allowing them to respond to the same stimulus in different ways [1]. ECs lining larger vessels appear to be thicker and more continuous in comparison to the endothelial layer of capillaries, which are thinner and often have small openings within the cells called fenestrations, which allow rapid exchange of molecules between the tissue and the blood [3]. Surprisingly, heterogeneity of the ECs also occurs between cells in the same environment, meaning they can respond differently to the same signal [4].

The endothelium has multiple mechanisms that allow it to regulate its environment, as well as responding to external stresses, by methods such as controlling the transfer of oxygen and nutrients, secreting angiocrine factors and controlling vascular tone [5]. The endothelium plays an important role in regulating blood flow, and the ECs are able to change their surface depending on the circumstances, for example, in the case of injury ECs are able to express pro-coagulant molecules upon their surface to prevent excessive blood loss [6]. They can react in response to pathological situations such as inflammation, as well as being able to secrete vasoactive substances, which control the constriction of the blood vessel [7].

ECs act as a dynamic organ within the body, with mechanisms to regulate blood flow, control the movement of fluid, ions and other molecules between the blood and underlying tissue, as well as playing a critical role in repairing the vessel after vascular injury [6]. Dysregulation of these finely controlled processes can result in clinical disorders, such as excessive bleeding due to the low level of release of the clotting proteins by the ECs [8].

1.1 Endothelial Cell Functions

1.1.1 Transport

One of the most important functions of the endothelium is regulating transport across the vascular endothelial barrier [9]. Under normal conditions the endothelium acts as an impermeable barrier, requiring specialist mechanisms to transport solutes into the cell and the underlying tissue, to allow them to produce ATP and perform other essential processes. The endothelium is critical in facilitating the transportation of nutrients to tissues, and the removal of waste. This exchange can occur by both transcellular mechanisms, such as via specialist channels, and paracellular mechanisms via the intracellular junctions [9]. Some ECs require higher levels of transport regulation than others, such as in those within the blood brain barrier (BBB). In the BBB, there is an extremely low level of transcytosis of solutes, and the tight junctions between ECs strongly limit the paracellular flux of solutes in comparison with other ECs in other locations within the body [10].

1.1.1.1 Glucose

The endothelium is a metabolically active barrier and produces essential molecules for specialist ECs functions, such as angiogenesis. In order to produce these molecules the ECs require ATP, which can be produced through the metabolism of glucose, which is transported around the body via the circulating blood [11]. Whilst small molecules such as oxygen can diffuse through the plasma membrane of ECs, larger molecules require specific transport proteins. These transport proteins exist in both the luminal and abluminal membrane of ECs, allowing glucose and other nutrients to be transported from the blood through the ECs, for use by the parenchymal cells [12].

Transportation of glucose into the cell occurs by facilitated diffusion via the glucose transporter isoform GLUT1, which is present in the plasma membrane of the EC [1]. GLUT1 is ubiquitous between all cell types, but is expressed most highly within the endothelium of the blood brain barrier (BBB) [11]. The BBB is a highly impermeable barrier formed of ECs which prevent neurotoxins from entering the brain. ECs within the BBB have a large number of mitochondria which use the glucose to produce ATP, which is needed for the highly regulated transport mechanisms to transport ions into the ECs [13]. Defective transport of glucose across the blood-brain barrier and into the brain parenchyma is associated with developmental delay and infantile seizures, due to the reduced amount of glucose available to the brain, and the limited ability of the brain to use other fuels [14].

There is suggestion that GLUT4, another isoform of GLUT transporter is present within ECs, but evidence is still unclear. GLUT4 is an insulin regulated transporter, most commonly found within adipose tissue and striated muscle, however GLUT4 has also been shown to be in the brain microvascular endothelium [15]. It is suggested that this is the only vascular location where GLUT4 occurs, as it has not been shown to be expressed in any other vascular cells [15].

1.1.1.2 Amino acids

There are multiple transport systems that allow the influx of amino acids across the plasma membrane in ECs, where they can be used for fuels for oxidative phosphorylation [11]. In the absence of glucose, the normal fuel source for ECs, amino acids including L-glutamate and L-glutamine are rapidly oxidised to be used as an alternative fuel source [11]. When L-glutamine is absent, EC proliferation is impaired [16].

The amino acid L-arginine is required for the production of nitic oxide (NO), which is continuously synthesised by ECs [17]. NO is then released from the endothelium as a gas or attached to other molecules, and stimulates the production of cyclic guanosine monophosphate (cGMP) [17]. Smooth muscle cells within the vessel wall are affected by NO, and the subsequent production of cGMP. When NO is secreted to the underlying smooth muscle, the production of cGMP causes the relaxation of the smooth muscle cells, affecting the resistance of the blood vessel, and lowering blood pressure [17]. The production of NO can change rapidly in response to physiological changes, allowing the ECs to exert control over the vascular tone, and has been shown to be atheroprotective [16,17].

Within ECs, there are both Na^+-dependent and Na^+-independent amino acid transporters that mediate the transport of amino acids. The charge on the amino acid governs which transporter the amino acid will use. $B^{0,+}$ is an Na^+ -dependent amino acid transporter, which is highly specific for cationic amino acids, which the Na^+-independent transporters y^+, y^{+L}, $b^{0,+}$, b^+, are able to transport both cationic and neutral amino acids [11]. The amino acid L-arginine is transported into the ECs via the y^+ cationic amino acid transporter [1].

The principal amino acid transport system is y^+L system, which is involved in the Na^+-independent uptake of dibasic amino acids such as arginine and lysine [18]. The y^+L system is also capable of transporting neutral amino acids, but this process is mostly Na^+-dependent [18]. Other systems, such as the $B^{0,+}$ system have broad substrate specificity, also favour particular amino acids, such as the neutral leucine and isoleucine over other zwitterionic and cationic amino acids [18]. By being Na^+-dependent, the $B^{0,+}$ system can form gradients of its

preferred substances, and change the magnitudes of these with changes in the Na^+ and K^+ system [18].

Like glucose transporters, amino acid transporters are also located upon the abluminal surface of ECs, to allow the transcellular passage of the amino acids. In the BBB, where little passive transport of polar solutes can occur, there are high levels of specific transport proteins that regulate the passage of amino acids between the brain interstitial fluid and the blood [19].

Together, these transport mechanisms allow for effective amino acid transport, the importance of which is shown by the decrease in EC proliferation in the absence of L-glutamine, and the importance of L-arginine in regulating vascular tone.

1.1.1.3 Albumin

Within the human body, serum albumin is the most abundant circulating plasma protein, with the liver producing about 10-15g per day [20]. Albumin is a soluble protein that is involved in the transport of hydrophobic substances such as steroids through the blood, and maintains the oncotic pressure; the pull of fluid from the interstitial space into the vessel (Figure 1.1) [21]. Once albumin enters the circulatory system from the liver around 35% of the albumin remains in the blood stream, and the remainder enters the tissue space, where it later returns to the circulation via the lymphatic system.

Albumin is a negatively charged protein that has multiple ligand binding sites, and is able to bind and carry small hydrophobic molecules, including endogenous and exogenous substances such as cholesterol and drugs respectively, across the vascular endothelium from the intravascular to the extravascular space (Figure 1.1) [20,22]. Albumin is able to affect the activity and half-life of drugs such as ibuprofen, as the drug binds to albumin, reducing the rate of clearance [23].

Albumin cannot easily pass through the endothelial layer as it is too large, but instead attaches to the cell membrane surface. The plasma membrane of the EC then invaginates, which then buds off to form intracellular vesicles called caveolae [22]. Albumin is transcytosed within the cell, allowing the transport of molecules across the interior of the cell, from the luminal to the abluminal space, where it can be secreted (Figure 1.1). Within caveolae there is a specific albumin binding protein called gp60, that is selectively expressed on the plasma membrane of continuous endothelium [24]. Unlike other substances endocytosed by the caveolae, albumin internalisation by gp60 has been shown to result in transcytosis (Figure 1.1) [24]. Gp60 proteins are not present on the blood-brain barrier, to prevent albumin from passing into

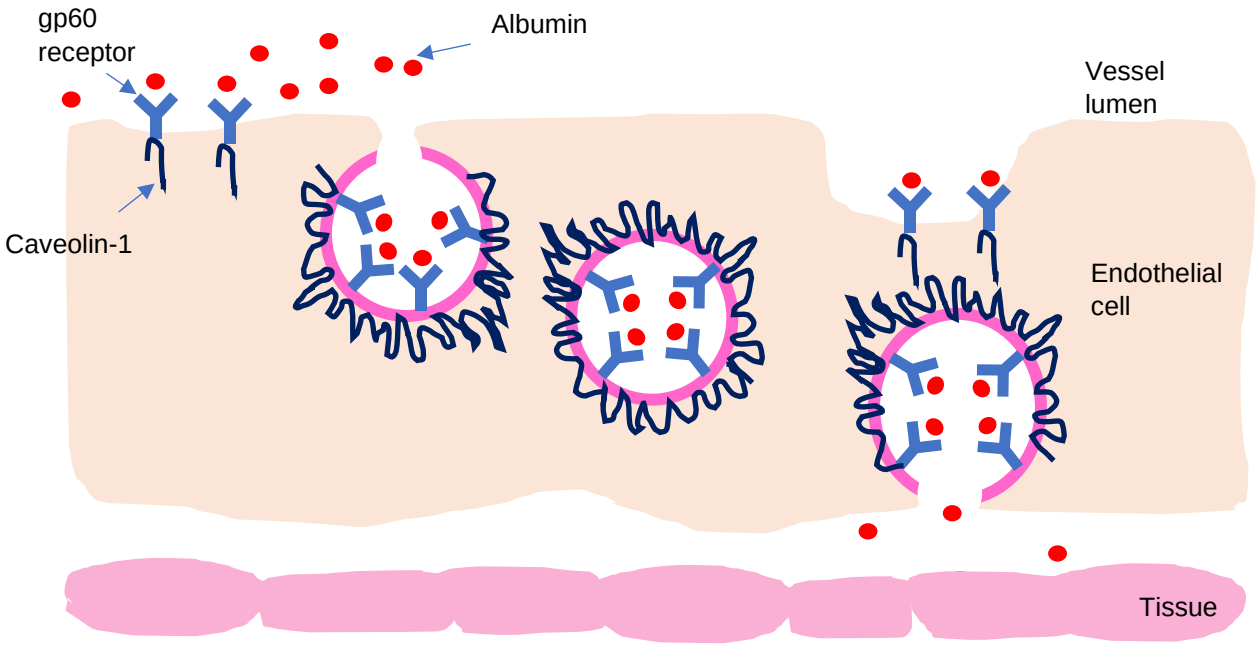

Figure 1.1 Albumin transcytosis across the endothelial cell. The albumin bound gp60 receptor is internalised from the apical plasma membrane using the scaffolding protein caveolin-1. The albumin:gp60 complex is transcytosed in caveolae carriers across the endothelial cell, and the albumin is subsequently released from the basolateral membrane into the tissue. Adapted from Impact of albumin on drug delivery – New applications on the horizon, Elsadek *et al*., Journal of Controlled Release; published by Elsevier, 2012 [231].

the brain where it could damage neuronal tissue by inducing neuronal hyperactivity, and albumin leakage has been linked to diseases including epilepsy and Alzheimer's disease [25].

1.1.2 Secretion

To perform their essential function, ECs secrete a multitude of different factors, both into the luminal space and into the tissue. The polarisation of ECs is maintained by the tight junctions, allowing ECs to secrete different factors and different concentrations of factors, from both their apical and basolateral surface. Whilst the importance of EC secretion to support their function is well known, there are few studies into the secreted EC proteome, and the mechanisms that allow for the secretion to occur.

1.1.2.1 Extracellular matrix proteins

The ECM is the non-cellular component within all tissues and organs, composed of a cross-linked network of extracellular components including collagen, fibronectin and glycoproteins [26]. The ECM provides a structural scaffold for the ECs providing structural support for the cells to grow upon, as well as modulating the cell's biochemical and biophysical behaviours [26]. Through interactions between the EC and integrins, the ECM provides an essential scaffold for maintaining the organisation of ECs into blood vessels, as well as being essential for the survival of the ECs.

The ECM underlying the ECs within a tissue consists of a basement membrane, and an interstitial matrix that is present between the cells. ECs are responsible for the synthesis and formation of the basal lamina, the primary layer of the basement membrane on which the endothelium sits (Figure 1.2).

The main protein component within the basal lamina is collagen IV, a subtype of the collagen family, which provides structural and tensile strength to the ECM [27]. The high tensile strength of collagen is due the triple helical structure of collagen, formed by three intertwined superhelices which contain one or more regions with the characteristic Gly-X-Y repeat, where X and Y can be any amino acid [27,28]. By the transition to the triple helix, collagen has higher rigidity and becomes less accessible to proteases, increasing its stability [27]. These characteristics allow collagen IV to form a network which acts as a scaffold, which can tether different extracellular molecules, including laminin and perlecan (Figure 1.2). Laminins are

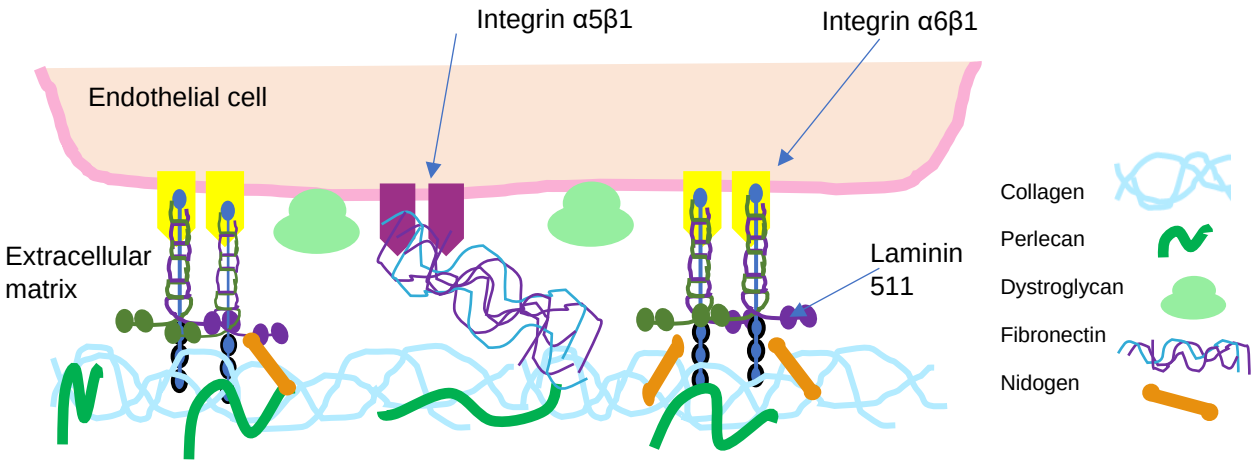

Figure 1.2 Arrangement of the basement membrane. Adapted from Vitamin A Deficiency and Alterations in the Extracellular Matrix, Barber *et al*., Nutrients; published by MDPI (2014) [232].

glycoproteins secreted by ECs, and also play a role in cell migration and adhesion, and are important for the survival of tissues [29]. Laminin provides the interaction between the EC and the basement membrane, by being anchored via transmembrane linkers called integrins at the cell surface [30]. Laminins also interact with other secreted components of the cellular matrix, including the glycoproteins nidogen and perlecan, which act to stabilise the ECM, and form cross links between components (Figure 1.2) [31]. The integrins present upon ECs, specifically the α1β1 and α2β1 integrins also bind collagen IV through specific sites within the collagen IV heterotrimer [32].

Another protein which forms part of the ECM is fibronectin, which is mainly secreted from the basolateral surface of the EC. Fibronectins are a class of glycoproteins that are present in two forms; a soluble form present in blood plasma, and insoluble present within the ECM [33]. ECs synthesise fibronectin, which is transported as dimers to the basolateral surface where it is secreted. Fibronectin is then polymerised and incorporated into the ECM. Fibronectin binds to the membrane spanning integrin $\alpha_5\beta_1$ of the EC, anchoring the cell to the ECM, and also to other ECM proteins such as collagen, creating a net to provide structural and biochemical support for the ECs (Figure 1.2) [34]. Previous studies have shown that fibronectin is predominantly polarised to the basolateral surface of ECs, in line with it playing such an integral role there [35].

Together these proteins form a stable network for the ECs to survive upon. The production of these proteins by the EC is highly regulated to prevent pathological conditions such as liver cirrhosis, where increased levels of deposition of collagen IV by liver sinusoidal ECs is clinically significant [36].

1.1.2.2 Coagulation factors

In healthy endothelium the luminal surface is both anti-coagulant and anti-thrombotic to prevent the attachment of cells and clotting proteins [6]. ECs are also able to secrete a multitude of factors which are involved in the regulation of haemostasis; encompassing the processes that control blood clotting, the activation of platelets, and vascular repair [6,37].

When vascular injury occurs, rapid pro-inflammatory and wound healing responses are triggered to repair the vessel and prevent blood loss. In healthy tissue, the endothelium expresses various anticoagulants upon its surface, such as thrombomodulin and heparin, to maintain the normal flow of blood [6]. However, when injury to the vessel occurs, the ECs become activated and the underlying cells, such as the smooth muscle cells, are exposed [6].

ECs synthesise and secrete the pro-coagulant von Willebrand Factor (vWF), a glycoprotein which can bind the coagulation Factor VIII which is involved in the activation of Factor Xa in the clotting cascade [38]. vWF is secreted from both the apical surface into the circulating fluid and from the basolateral surface into the extracellular matrix [39]. vWF secretion by ECs occurs via two pathways, one which occurs constitutively, and another triggered by exocytosis from Weibel-Palade bodies, which store vWF within the EC [40].

When the endothelial layer is damaged, the underlying collagen is also exposed to the blood, which initiates the adhesion of circulating platelets via the vWF in ECM to the exposed collagen, creating a platelet aggregate to stem blood loss [39]. Activated ECs and the smooth muscle cells express the integral membrane protein Tissue Factor (TF); which can bind the freely circulating serine protease Factor VII , which initiates the subsequent activation of other serine protease factors present within the blood, including Factor Xa [6]. Factor Xa is able to combine with another serine protease called Factor Va to proteolytically cleave the circulating coagulation factor prothrombin to form thrombin [41]. Thrombin is then able to catalyse the production of fibrin from fibrinogen, which is able to form a cross-linked fibrin mesh [41]. This cross-linked fibrin mesh, along with the platelet aggerate is able to form a stable clot, acting to plug the injury and prevent blood loss [6].

The EC surface normally expresses protease activated receptors (PAR), which initiate a cascade of cell signals upon activation by proteases such as thrombin, Factor Xa and TF:Factor VIIa complex [6]. The activation of PAR-1 by thrombin induces the activation of Weibel-Palade bodies, causing the release of vWF and Tissue Plasminogen Activator (t-PA) from the EC, as well as regulating the surface exposure of TF and triggering the release of NO from ECs, which inhibits platelet activation [40]. Once the wound is repaired, dissolution of the clot is activated by fibrinolytic agents such as t-PA, which catalyses the degradation of fibrin within the clot [6].

Under normal conditions, the secretion of vWF into the plasma is constitutive, but during acute bacterial, viral or parasitic infection secretion of vWF can increase seven-fold [40]. High levels of vWF may be an indirect indicator of atherosclerosis [42]. vWF disease is a genetic disease that results in low levels of, or non-functional vWF, of which symptoms include heavy bleeding due to the inability to clot [43].

To maintain ‘normal’ blood flow, ECs express anticoagulants upon their surface, including thrombomodulin (TM), and heparin-like proteoglycans, and secrete platelet inhibitors such as nitric oxide (NO) [6]. TM binds thrombin and acts as a cofactor to activate protein C; a vitamin K-dependent glycoprotein [44]. In studies where TM was mutated, there was limited activation

of protein C, which was shown to lead to a hypercoagulable state [45]. Protein C deficiency can result in clinical conditions including thrombus formation [46].

By secretion of these factors, the endothelium can maintain the blood in a non-coagulative state and can respond to changes, such as vessel damage, to secrete the required factors. Damage to the endothelium, such as the formation of plaques may prevent the EC from being able to regulate coagulation successfully and may contribute to the formation of a thrombus [6]. Certain diseases, including the mentioned vWF disease and protein C deficiency, are just an example of the important role the endothelium plays.

1.1.2.3 Nitric oxide

One of the roles of the endothelium is to regulate vascular tone, which it does via the production and secretion of vasoactive substances. The endothelium produces potent mediators, including NO, prostacyclin and endothelin, which are released from the EC in response to stimuli [1]. NO is a powerful vasodilator and is produced constitutively under normal conditions by type III NO synthase (eNOS), the NO synthase present within ECs.

Endothelial nitric oxide synthase (eNOS) works constitutively to produce NO. Certain chemical substances are able to alter the production of NO. When vascular injury occurs, ECs become activated, producing adhesion molecules and recruiting inflammatory cells resulting in the release of cytokines [47]. The release of cytokines causes increased production of NO by eNOS, and the cytokine inducible NOS; type II NOS [1]. NO produced by ECs can diffuse across the interstitial space to the smooth muscle, where it activates the enzyme guanylate cyclase which facilitates the conversion of GTP to cGMP, which indirectly leads to the inhibition of calcium influx into the cell [1]. This leads to the decrease in smooth muscle tension due to decreased phosphorylation of myosin light chains, causing vasodilation [1,47]. NO secretion also results in the inhibition of platelet aggregating, as well as inducing expression of chemokines and adhesion molecules on the vascular surface of ECs, and has antioxidant properties [48] .

1.1.2.4 Inflammatory mediators

Under normal conditions the endothelium is non-thrombogenic, controls the flow of blood and the passage of proteins from the blood, and inhibits inflammation [49]. However, during events such as infection, the endothelium must respond to pro-inflammatory signals such as interleukin 1. This causes the ECs to become activated, and undergo specific changes needed

for its function in the inflammatory response [50]. During changes including the upregulation of surface antigens and adhesion molecules, and the modification of the EC surface to a prothrombotic phenotype, ECs are able to react to and produce cytokines, and other inflammatory mediators [50].

One chemokine produced by ECs is IL-8, a neutrophil chemotactic factor. Within the EC, IL-8 is stored within Weibel-Palade bodies along with vWF and t-PA, and is also released upon PAR-1 activation by proteases such as thrombin [51]. The role of IL-8 within the inflammatory response is to attract neutrophils towards the site of the infection, where the neutrophils can then enter the tissue to reach the affected site [50]. IL-8 has also been shown to stimulate proliferation and migration of ECs in *vivo* [1]. Other members of the interleukin family produced by ECs include IL-1 and IL-6 [52]. IL-1 has been shown to be involved with platelet activation, and stimulating the production of NO from ECs, as well as inducing the production of other chemokines by ECs, and can stimulate the release of IL-8 [52].

Other cytokines secreted by ECs include colony stimulating factors (CSF) and growth factors. CSFs are glycoproteins that cause the proliferation and differentiation of haematopoietic stem cells into macrophages or granulocytes, which are both types of white blood cells involved in the inflammatory response [53]. Growth related oncogene-alpha (GRO-α) is another neutrophil attractant released by ECs, and has also been shown to be proangiogenic [52].

As well as secreting these cytokines, ECs also change their surface during the inflammatory response, such as expressing E-selectin and intercellular adhesion molecule-1 (ICAM-1), which mediate the adhesion of leucocytes to the ECs [1]. Another adhesion molecule released is P-selectin, which is stored within Weibel-Palade bodies with ECs [54].

1.2 The Vascular System

The vascular system, also referred to as the circulatory system, is responsible for the transport of blood and lymph throughout the body. These fluids are carried through vessels which are specially adapted, dependent on their location within the vascular system. Blood is transported through the cardiovascular system by three major vessels; arteries, veins and capillaries, which form a continuous network throughout the body. Lymph vessels carry lymph fluid that has been absorbed from tissues and returns the fluid to the cardiovascular system. The innermost surface of these vessels consists of ECs, which in veins and arteries form a continuous sheet due to tight intercellular adhesion molecules such as vascular endothelial cadherin (VE-cadherin) and zonula occludens 1 (ZO-1). However, in lymphatic vessels and some capillaries the endothelium is discontinuous which increases its permeability, increasing the transport of solutes between the vessel and the surrounding tissue. The cardiovascular and lymphatic systems work together to maintain homeostasis, the stable equilibrium of physiological processes.

1.2.1 The cardiovascular system

As previously stated, the cardiovascular system consists mainly of arteries, veins, and capillaries. Each of these vessels are structurally similar consisting of ECs surrounded by a basal lamina, and have varying amounts of connective tissue, elastic fibres and smooth muscle cells in their surrounding layers [55]. Blood vessels are typically made up of three individual layers, the tunica intima, the innermost layer of the vessel directly in contact with the blood; the tunica media, the layer underlying the tunica intima; and the tunica adventitia, the outermost layer (Figure 1.3) [56]. The composition of these layers differs between vessels, and these differences allow the vessel to be specially adapted to its role.

1.2.1.1 Arteries

Arteries generally carry oxygen-rich blood from the heart to deliver it throughout the body. There are two exceptions to this; the pulmonary artery, which carries blood away from the heart towards the lungs where it becomes oxygenated; and the umbilical artery that carries deoxygenated blood out from the foetus. After the oxygenated blood has returned from the lungs, it enters the left ventricle of the heart. The contraction of the heart, called systole, pushes the blood out of the left ventricle of the heart through the aortic valve where it enters

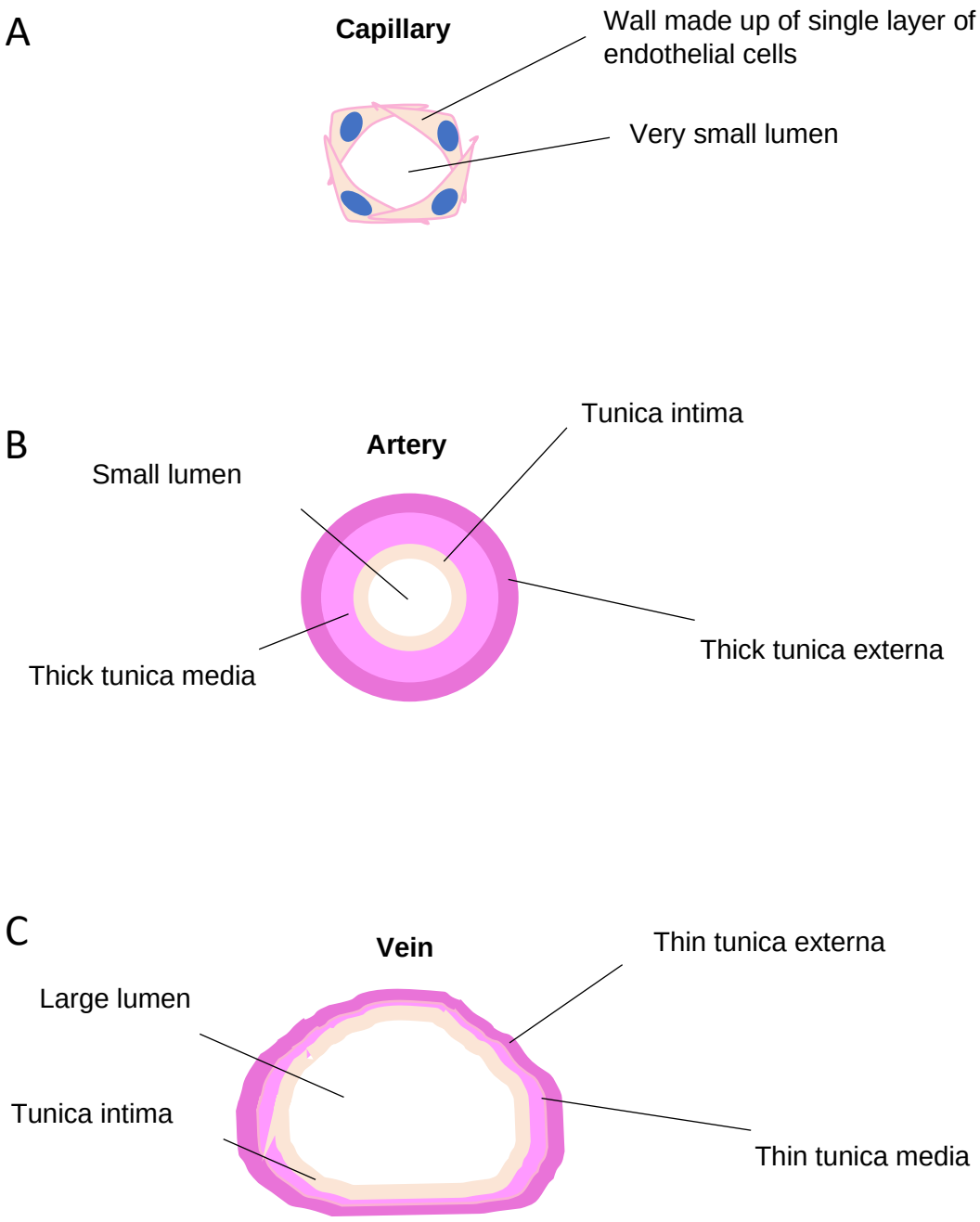

Figure 1.3. Structure of blood vessels. A) Capillaries are the smallest of the blood vessels, and their wall consists of a single layer of endothelial cells. B) Arteries have a thick tunica media made up of smooth muscles and elastic fibres, and a thick outer wall. Their lumen is lined by a layer of endothelial cells C) Veins are the largest of the blood vessels, and their tunica media consists of a thin layer of smooth muscle and elastic fibres and surrounded by a thinner outer wall. Veins have the largest lumen, which is also lined with endothelial cells. Adapted from Engineering biofunctional *in vitro* vessel models using a multilayer bioprinting technique, Schöneberg *et al*, Scientific Reports; published by Nature Research (2018) [59].

the aorta, before branching into large arteries [57]. The relaxation of the heart, called diastole, causes the aortic valve to close preventing backflow. Artery walls are specially adapted to cope with this initial high-pressure during systole and low-pressure during diastole to maintain constant pressure within the blood, by having thick artery walls which contain elastin. During systole the increase of pressure causes the artery walls to stretch, before recoiling during diastole. The elasticity of arteries results in the Windkessel effect, damping the fluctuations in blood pressure throughout systole and diastole, allowing an almost constant blood pressure [58,59].

There are two main subtypes of arteries within the body; elastic and muscular [56]. The arteries closest to the heart, including the pulmonary artery and the aorta are both elastic arteries, and contain more elastin and collagen within their tunica media than the muscular vessels, which are responsible for the distribution of blood to the smaller arteries within the body (Figure 1.3) [60]. The elastic arteries are closest to the heart and receive the highest pressured blood, and this increased elastin and collagen allows them to maintain a relatively constant pressure despite the constant pumping of the heart [60]. Muscular arteries, medium sized arteries which the blood enters after passing through the elastic arteries, contain fewer elastic fibres and more smooth muscle cells in their tunica media than elastic arteries (Figure 1.3) [56]. The increased number of smooth muscle cells allow the vascular tone to be controlled by the release of NO and other vasoactive molecules, to control and maintain blood flow and pressure [61]. The arterial system contains about 10-15% of the total blood volume.

After the blood has passed through the muscular arteries, it then enters into smaller vessels of the arterial system, called arterioles [62]. This branching causes the blood pressure to drop as the blood is transported throughout the body, due to the cumulative increase in vessel diameter as more branching occurs. Arterioles are blood vessels of between 8 and 60 micrometres, only have one to two layers of smooth muscle within their tunica media, and a thinner tunica externa than other artery types [62]. These arterioles then branch into metarterioles, which provides the link between arterioles and capillaries; the vessels which carry blood through the tissues. Unlike other vessels within the arterial system, metarterioles do not have a continuous tunica media; but instead the smooth muscle forms rings at the entrance of capillaries [56]. These rings of smooth muscle tightly regulate the blood flow into the capillaries, and open when the surrounding tissues require oxygen and the removal of waste.

On the innermost lining of all these vessels are ECs. In comparison to ECs in other vessels, arterial ECs are generally thicker, and have tighter intercellular junctions [61]. Arterial ECs are

also longer and narrower than other vessels, aligning with the direction of the blood flow within the vessels [61].

Dysfunction of the arterial ECs, characterised by a shift in ECs towards reduced vasodilation, a proinflammatory state and prothrombic properties is associated with most forms of cardiovascular disease, including atherosclerosis [63]. The formation of an atherosclerotic plaque most commonly occurs within the coronary artery, but can occur within any artery within the cardiovascular system [64]. There are multiple risk factors for atherosclerosis, including high blood cholesterol, high blood pressure and smoking [65]. These factors can cause damage to the endothelial layer, causing ECs to secrete vasoconstrictive factors including ET-1, as well as factors which cause the proliferation of smooth muscle cells [66]. The secretion of these factors causes a chemotactic effect on leukocytes and platelets, causes of the overexpression of cellular adhesion molecules such as ICAM-1 on the EC surface and the secretion of inflammatory cytokines [66]. The expression of these adhesion molecules allows leukocytes to adhere to the EC surface, where they can then migrate into the tunica intima. Inflammatory cytokines cause the EC to secrete IL-1, causing the accumulation of neutrophils which produce reactive oxygen species which further damage the endothelium [66].

These processes lead to the formation of an atherosclerotic plaque, containing ECM components, cholesterol, and cellular debris within the artery wall. Over time this plaque can build up, leading to narrowing of the artery which can cause devastating conditions, including occlusion of the artery, which could cause a myocardial infarction (heart attack) and strokes. Damaged ECs also have an impaired release of NO causing the vessel to become overly permeable, which contributes to the progression of atherosclerosis [66].

1.2.1.2 Microvasculature

After the blood has passed through the arterioles, the vascular system branches further forming a network of capillary vessels. Capillaries are vessels which have a radius of about 2-5 µM, and their wall consists of a single sheet of ECs, with a small amount of basal lamina and contractile cells called pericytes; which have a variety of functions including regulating blood flow (Figure 1.3). Networks of capillaries are present throughout tissues, supplying them with oxygen and nutrients and removing waste products including CO_2.

There are three types of blood capillaries: continuous, fenestrated and discontinuous. Dependent on the location and function of the capillary within the body, capillaries are present as one of these three types [67]. Continuous capillaries are formed of a continuous layer of ECs, with a continuous basal lamina (Figure 1.4A). These features allow the vessel to form a

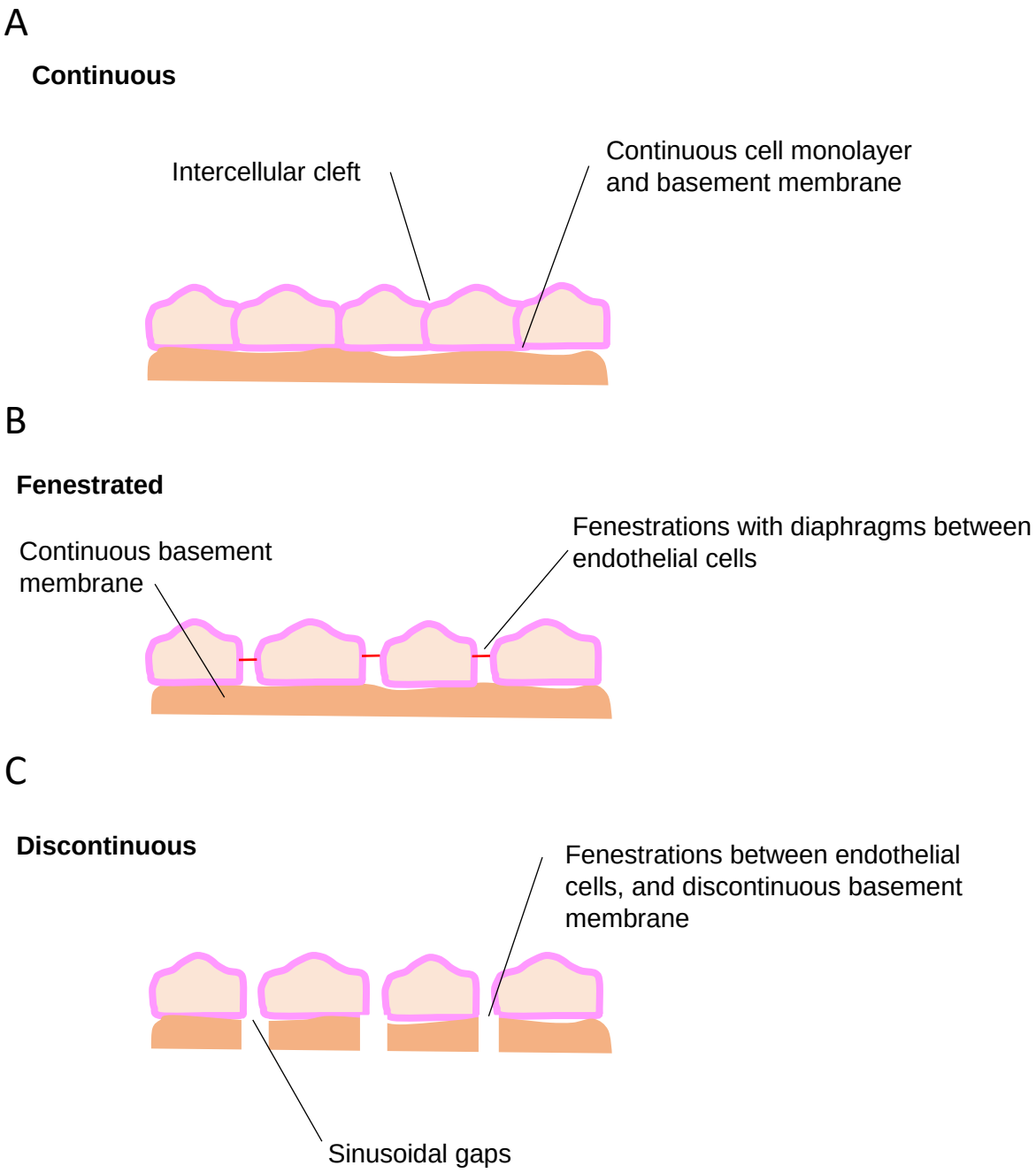

Figure 1.4. Types of capillaries. A) Endothelial cells in continuous capillaries are joined continuously to each other by junctional proteins, with no openings in the monolayer of basement membrane. Examples of tissues include the central nervous system B) Endothelial cells in fenestrated capillaries have fenestrations between cells, which are covered by a permeable diaphragm, and have a continuous basement membrane. Example tissues include the gastrointestinal tract. C) Discontinuous capillaries have large gaps between endothelial cells, and a discontinuous or absent basement membrane. Example tissues include the liver. Adapted from Organotypic vasculature: From descriptive heterogeneity to functional pathophysiology, Augustin *et al*, Science; published by AAAS (2017) [233].

permeability barrier to unwanted solutes, and form capillary networks within muscles and the brain, as well as other organs. Fenestrated capillaries also have a continuous basement membrane, but also contain fenestrations within the ECs which are about 60-70 nm in diameter [67]. These fenestrations are covered by a diaphragm, a layer of fibrils that can open to allow the passage of larger molecules (Figure 1.4B). These capillaries are found within tissues with extensive molecular exchange, such as the kidney. Discontinuous ECs, also known as sinusoidal ECs, contain openings within capillaries of around 30-40 μM in diameter between ECs. These ECs, which are present in the organs including the liver and the spleen, have a discontinuous basal lamina making these vessels very permeable, allowing the passage of red and white blood cells and serum proteins to pass through with ease (Figure 1.4C) [68].

1.2.1.3 Veins

After exchanging oxygen and nutrients with the tissue and collecting cellular waste, the blood is collected into venous system vessels called venules. Venules are very small blood vessels which facilitate the drainage of deoxygenated blood from the capillary beds into larger veins. The endothelium of venules is discontinuous, so that fluids and solutes can easily re-enter the blood stream. Veins generally carry de-oxygenated blood, however like arteries, there are two exceptions: the pulmonary and the umbilical vein. The pulmonary vein transports oxygenated blood from the lungs back to the left atrium of the heart, where it then flows into the right ventricle before being pumped around the body during ventricular contraction. The umbilical vein transports oxygenated blood from the placenta to the developing foetus. ECs within veins are generally much thinner than within arteries and are shorter and wider due to the lower venous flow rates, in comparison to arterial circulation. Veins have looser and more poorly organised intercellular junctions than arteries, especially those of post-capillary venules, which are the blood vessels that connect the capillary bed to the larger veins [61].

As well as venules, the venous system within the human body contains other subtypes of veins: deep and superficial. Deep veins are situated within the lower limbs and are normally located beside an artery with the same name, for example the femoral artery and vein [69]. Superficial veins are located close to the skin and are not paired with an artery. There are two main superficial veins within the body; the great saphenous, which transports blood up the inner surface of the calf and thigh before joining the deep femoral vein; and the small saphenous vein, which occurs on the posterior surface of the calf, and transports blood into the popliteal vein [69]. The great saphenous vein is the largest vein within the body and

contains between 8 and 20 valves, most of which occur below the knee. Superficial veins are located in the subcutaneous fat directly under the skin and are not situated near muscles. This results in blood often moving slower within superficial veins than within deep veins, due to the lack of nearby muscle for contraction [69].

Like nearly all vessels within the cardiovascular system, veins consist of three layers; the tunica intima, tunica media and tunica externa (Figure 1.3). The tunica intima of venules has an absence of elastic fibres, and the tunica media is virtually non-existent (Figure 1.3) [61]. The vessel walls of large and small veins contain elastic fibres and smooth muscle cell; however compared to arteries their tunica media is not as clearly defined or organised [61]. The tunica externa of veins constitutes the majority of the vessel wall, whilst in arteries this tunica externa is only about half the overall thickness [61]. In comparison to arteries, veins have a much thinner tunica intima, and a thin layer of smooth muscle and elastic fibres in their tunica media (Figure 1.3). This is because the vessel walls do not need to be able to withstand the high pressure unlike arterial walls. Veins have a much larger lumen than arteries, and these features together allow the venous system to accommodate nearly 75% of the blood within the body at relatively low pressures, termed high capacitance.

The blood within veins is not pressurised by the heart and therefore flows at a slower rate within the body and requires skeletal muscle contractions to return the blood to the right atrium of the heart. This slower moving blood is more liable to pooling and the occurrence of back flow, called reflux. To prevent this veins contain bicuspid valves which ensure the one-way passage of blood, and are especially important in veins that transport blood back up against gravity [70]. In absence or damage of these valves the blood pools, which can disturb the exchange of oxygen, nutrients and waste products between the tissues and the blood, which can result in chronic venous insufficiency (CVI) [71]. The failure of these valves allows the backflow of blood, resulting in venous hypertension due to the failure of reduction of venous pressure that normally occurs during exercise, leading to hypoxia and inflammation [71]. Chronic venous hypertension causes the endothelium of capillaries within the leg tissues to become more permeable, allowing fluid, proteins and blood cells to leak into the tissues [71]. The symptoms of CVI include the formation of varicose veins; swollen and enlarged veins that occur on the legs, and aching and tiredness in the legs [72]. CVI can occur primary or secondary to deep vein thrombosis (DVT). DVT is a serious condition, where blood clots occur, commonly within the deep leg veins or the deep veins of the pelvis. This can be caused by dysregulation of the ECs lining the blood vessel, causing them to release procoagulation factors into the blood, causing the formation of a thrombus. The thrombus can be transported through the venous system to the lungs, causing a pulmonary embolism, which can be fatal [6].

After blood is pushed up the vessel, the pressure falls causing the valves to close. The right atrium of the heart has a lower pressure than within the veins, providing the driving force for venous return [73]. Once reaching the right atrium of the heart, contraction of the heart causes the blood to pass through a tricuspid valve into the right ventricle, where it passes through the pulmonary artery to the lungs to be re-oxygenated. This oxygenated blood is then transported back to the left atrium via the pulmonary vein, where it enters into the left ventricle, to be pumped around the body again.

1.2.2 Lymphatic system

The lymphatic system is an open circulatory system composed of structures and vessels that drain lymph fluid from tissues and return it to the circulatory system. The lymphatic system has three main roles: the removal and filtration of interstitial fluid from tissues, fatty acid absorption from the digestive system, and immune function [74–76].

Interstitial fluid builds up in tissues due to the hydrostatic and osmotic pressure exerted by capillaries from the cardiovascular system forcing fluid into the tissues. The lymphatic system drains this excess fluid and large extracellular molecules from the tissues into its own lymphatic vessels. The initial vessels of the lymphatic system are blunt-ended capillary vessels that are conjoined to the surrounding organs via anchoring filaments [76]. Here, the ECs overlap and are joined together by the adhesion protein VE-cadherin in button-like arrangement, which act as mini valves allowing fluid to enter the capillaries [76]. When the accumulation of interstitial fluid is at a greater pressure than within the lymph vessel, these mini valves open, allowing fluid to enter the capillary before closing to prevent lymph backflow. In comparison to blood capillaries, lymph vessels are larger and have a greater oncotic pressure, which causes fluid to flow into the capillaries after the proteins in the lymph [77].

As lymph capillaries have no smooth muscle, the increase of pressure during lymph accumulation pushes the lymph fluid into larger lymphatic vessels. These larger vessels are surrounded by fibrous tissue including collagen, which is used to anchor vessels within the body [78]. These larger vessels contain internal valves, like those within veins, and have a thin layer of smooth muscle, allowing lymph to be propelled along the vessels and preventing backflow [78]. When the pressure of the fluid within the lymph vessel increases to a certain point due to increased fluid accumulation, muscular contraction pushes the lymph fluid through the valve into the next chamber, called a lymphangion; the space between two semilunar

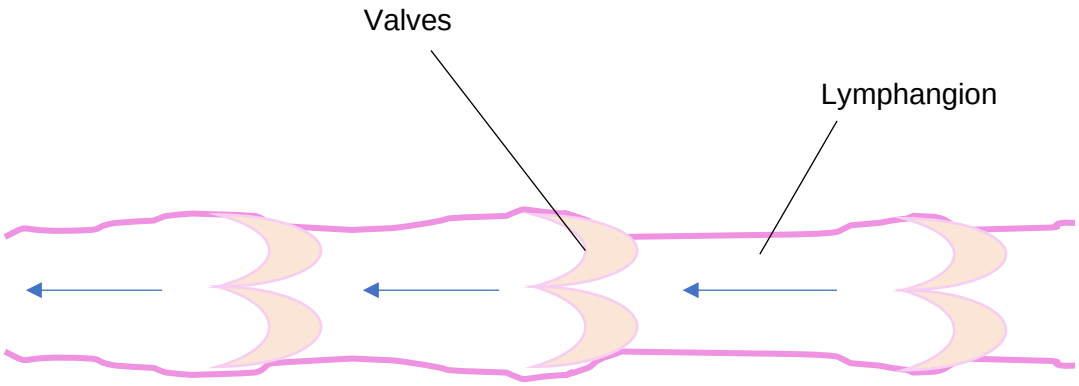

Figure 1.5 Valves within lymphatic vessels. Lymph vessels contain valves that prevent the backflow of the lymph fluid. Upon pressure, the valves open allowing forward transport of the lymph. As the pressure of the vessel decreases, the valves close preventing backflow. Adapted from Anatomy and roles of lymphatics in inflammatory diseases, Al-Kofahi *et al*, Clinical and Experimental Neuroimmunology; published by British Society for Immunology (2017) [234].

valves in a lymphatic vessel (Figure 1.5) [78]. As the pressure falls, these valves close preventing the fluid from flowing back into the vessel [78].

Throughout the body the lymph is filtered, removing pathogens and other abnormal solutes. This occurs through lymph nodes, which are formed of bundles of lymphoid tissue [79]. Unfiltered lymph fluid enters these nodes, which are more densely located around areas including the neck, chest and groin, through afferent vessels, and the filtered fluid flows back out of these nodes using efferent vessels [80]. The role of these nodes is to filter pathogens and other foreign bodies from tissues, where they are presented to lymphocytes to trigger the adaptive immune response, and the lymphatic system allows the transport of immune cells [75].

Fats which have been digested into fatty acids by the digestive system are emulsified and converted into lipoproteins called chylomicrons in intestinal cells [74]. The lymph drainage vessels that line the intestine absorb these into the lymph fluid, where the chylomicrons then enter the blood circulation where they interact with high density lipoproteins before being broken down in the liver [74].

One of the main principal functions of the lymphatic system is to gather the lymph fluid and return it to the blood system for blood homeostasis. If this fluid is not returned to the blood system at the same rate it enters the vascular system, the fluid pools and can lead to lymphedema [81]. This occurs when there is insufficient lymph drainage, resulting in a build-up of fluid in the tissues [82]. Lymphedema is a chronic condition, resulting in the dilation of the main lymphatic vessels, normally occurring in the legs. This disease cannot be cured, however methods, such as compression garments to increase the pressure within the vessel, aiding circulation can alleviate symptoms. Lymphatic ECs are affected during lymphedema, and excess strain upon the ECs can result in altered collagen deposition, and the release of inflammatory cytokines [83].

Together, these vessels allow for the efficient transport of fluid within the body, maintaining the body in homeostasis. Within these vessels, ECs play an important role in all processes, ensuring only the correct solutes enter and leave the vessel and maintaining vessel integrity. As these processes described are so crucial for the body to maintain equilibrium, slight dysregulation of these can have serious pathological effects, which can affect a range of other systems within the body, causing serious clinical diseases including strokes. External factors, such as smoking, causes injury to the vessel, and affects the function of the EC within the vessel, which can lead to issues including coronary artery disease and thrombus formation.

1.3 Endothelial cell subtypes

Despite the endothelium being originally thought of as a homogenous cell layer providing a barrier between blood and tissue, more recent studies have discovered that there are multiple subsets of ECs, dependent on their location within the vascular system. ECs can differ substantially in their morphology, gene expression and antigen presentation, as well as their function. Their properties can differ between organs, between different sections of the organ, and even between neighbouring cells within the same organ and blood vessel type [84].

1.3.1 Specific differences between endothelial cells

Typically, ECs are thought of as long, flat cells. However, their thickness can substantially differ dependent on their location, from less than 0.1 μM in capillaries and veins, to 1 μM thickness in the aorta [85]. There are other differences between ECs; including basal and inducible permeability throughout the vascular tree, the expression of coagulation mediators, and the regulation of leukocyte trafficking [84].

1.3.1.1 Continuous endothelium in the blood-brain-barrier

The blood-brain-barrier (BBB) is a highly specialised structure that separates the blood from the brain and cerebrospinal fluid [86]. The properties of the BBB are mainly determined by the EC junctions; tight junctions (TJ) and adherens junctions (AJ) [87]. TJs allow the EC to form a continuous blood vessel, which is important in ensuring the low permeability of the BBB by reducing paracellular diffusion; the diffusion between ECs [88]. AJs are important for the maintenance of cell-cell contacts between ECs [89]. This barrier creates a polarised cell with distinct luminal and abluminal areas, to prevent the free movement of drugs, and other circulating compounds [10].

ECs in the BBB express ATP-binding cassette efflux transporters, that are required to transport lipophilic compounds across the BBB [90]. In other types of ECs, these lipophilic molecules can generally pass through the EC membrane, therefore not requiring an efflux transporter [90]. Efflux transporters are polarised to the luminal surface of the ECs, and transport substances including hormones, phospholipids and cytokines across the plasma membrane into the blood using ATP [90]. ABC transporters are expressed by most cells, but are most highly expressed in barriers, including the BBB, and excretory and absorbing tissues,

such as the liver and intestine [90]. ABCB1 is a transporter protein that is highly expressed upon the apical surface of the BBB, and has a wide substrate specificity, allowing the transporter to be an effective defence against a wide range of xenobiotics and therapeutic drugs [91]. The ABCB1 transporter is thought to be the most important ABC transporter in neuroprotection, as it limits the entry of exogenous molecules into the brain [91]. Reduced expression of ABCB1 is associated with neuropathologies including Alzheimer's disease, where the expression of ABCB1 was shown to be significantly inversely correlation with the deposition of β-amyloid plaques by Vogelgesang *et al* (2002) [92]. Other types of ABC transporters include the ABCC family, which are efflux transporters involved in multi-drug resistance, and show preference for anionic substrates [90]. Evidence has shown that oxidative stress and xenobiotics increase the expression of these transporters at the BBB [90].

1.3.1.2 Discontinuous endothelium in the liver

The liver is an organ within the human body that is involved in multiple processes, including digestion, detoxification, and immunity. The liver is involved with processing nutrients absorbed from the small intestine. Liver cells, also called hepatocytes secrete bile, a fluid composed of water, bile salts, cholesterol and other substances, that are involved in the digestion of lipids in the duodenum. The liver is also able to convert potentially toxic lipophiles into more water-soluble metabolites, that can be excreted from the body via urine [93]. As the liver is exposed to bacteria from the gut, and toxins within the body, the liver contains specialised Kupffer cells; specialised macrophages that line the walls of sinusoids, discontinuous capillary vessels [94].

As previously mentioned, discontinuous capillaries have open spaces between ECs and a discontinuous or absent basement membrane (Figure 1.4). These sinusoids act as a selective barrier between the blood, which contains molecules containing nutrients and bile acids on ECs luminal side, and hepatocytes involved in metabolism on their abluminal side [95]. Liver sinusoidal ECs (LSECs) are the most permeable ECs within the human body, due to their fenestrae, absence of a diaphragm and lack of an underlying basement membrane [95]. Metabolites, plasma proteins and drugs, amongst other solutes present within the vessel are able to pass through these gaps to be transported into the hepatocytes surrounding the capillary. LSECs have one of the highest endocytic capacities, and strong lysosomal activity, allowing LSECs to clear pathogens and macromolecules from the blood [95]. LSECs are able to rapidly endocytose these compounds from the blood through scavenger and mannose receptors, working alongside Kupffer cells which clear larger particles by phagocytosis [96].

During liver cirrhosis, the scarring of the liver caused by long-term damage which can be causes by excess alcohol consumption or hepatitis, LSECs lose their fenestrae and a basement membrane forms [97]. This reduces the permeability of these cells, which can cause serious health problems including jaundice, and can be fatal [97].

1.3.1.3 Fenestration endothelium in the kidney

The kidneys are excretory organs that remove toxins from the body by filtering the blood, resulting in the production of urine. The kidneys are also involved in other processes, such as regulating the body's water balance controlling blood pressure, ensuring the blood is not too acidic or alkaline, and produce the hormone EPO, which promotes the formation of red blood cells by the bone marrow [98]. The filtration of blood occurs within the glomerulus, a network of blood capillaries that are located at the beginning of nephron, the functional unit of a kidney. Unusually for capillaries, the glomerular capillary wall consists of three layers; highly fenestrated endothelium; glomerular basement membrane (GBM); and the foot processes of glomerular epithelial cells which wrap around capillaries leaving slits between them, as well as providing support to the vessel [99]. The endothelium that makes up the capillaries of the glomerulus is extremely fenestrated, with pores covering 30% to 50% of its surface area which are covered by diaphragms (Figure 1.4) [100]. In comparison to other ECs, ECs within the glomerular filtration barrier are also extremely flat, and the luminal surface of the glomerular ECs is covered by a glycocalyx with a high heparan sulphate content [99,101].These adaptions allow for the high permeability of the capillary to water and small solutes through the 60- to 80-nm fenestrae, whilst preventing the passage of cells and large proteins such as albumin through the capillary wall as they cannot fit through the pores [100]. Vascular endothelial growth factor (VEGF) plays a role in the formation of EC fenestrations [102].

Patients with type 2 diabetes mellitus; a metabolic disease that causes high blood sugar levels due to the insensitivity to insulin, can develop diabetic nephropathy. This cause the overproduction of reactive oxygen species that can damage the glomerulus, and upregulated production of the enzyme heparanase, which degrades the glycocalyx of the glomerular ECs [103]. The GBM also thickens, and the podocyte foot processes detach from the GBM, increasing the permeability of the glomerular filtration barrier [101]. This results in the passage of large proteins including albumin to pass through the capillary walls, and be present within the urine, an early indicator of kidney damage [103]. If this disease becomes advanced, and the kidneys are unbale to effectively filter the blood, treatment can include kidney dialysis,

where the blood passes along a tube into an external machine for filtration to effectively remove toxins from the blood.

1.3.2 Mechanisms of endothelial cell heterogeneity

ECs require different properties, dependent on their location within the vascular tree. Until the late 1990s, the differences between ECs was thought to be dependent on the exposure of cells to flowing blood. However, more recent investigations have shown that EC heterogeneity is not only due to their environment, but also has a genetic component that may play a role before the differentiation of angioblasts into ECs [102].

During the early stages of embryogenesis during the development of blood vessels, signalling molecules are thought to be important in the initial decision of whether the ECs should be arterial or venous. During development, high levels of VEGF induce arterial specification by activating phospholipase C (PLC), which activates the mitogen-activated protein kinase (MEK) and extracellular signal regulated protein kinase pathways (ERK) [102]. These pathways activate subsequent signalling molecules, including upregulation of Notch and Nrp-1 to proceed arterial specification [102]. When the ERK pathway is supressed due to low levels of VEGF, and the protein kinase B (AKT) pathway induces COUP-TFII, a protein that downregulated the Notch and Nrp-1, causing the expression of venous-specific markers [102]. A subgroup of these venous ECs are specified into becoming lymphatic ECs, by expressing Sox18 and Prox1 [102]. Where Notch signalling is deficient, Hill-Felberg *et al* (2015) found that zebrafish lose their expression of Eph B2, a ligand that is the marker for arteries, but instead ectopically expresses Eph B4, which is normally associated with veins [104]. When Notch signalling is either reduced or constitutively active, arteriovenous malformations (AVM) can develop [104]. These AVMs can be asymptomatic, but if the AVM occurs in the brain, symptoms such as epileptic seizures and headaches can occur [104].

Despite this early molecular specificity of the ECs final identify, ECs have plasticity for further differentiation dependent on their location within the body. For example, variable blood flow in the aorta results in a non-uniform distribution of atherosclerotic plaques [105]. Laminar blood flow in the aorta induces the expression of eNOS and thrombomodulin, conferring an anti-thrombotic and anti-inflammatory properties to the endothelium [105]. Non laminar flow, such as at areas where the arteries branch reduces the expression of eNOS, but induces the expression of vascular cell adhesion molecule-1, causing a pro-inflammatory endothelial phenotype [105].

However, as well as properties of the ECs being controlled by their microenvironment, ECs are also able to be controlled via epigenetics: heritable changes in gene expression that do not alter the DNA sequence [85]. Epigenetic modifications are semi-conserved during mitosis and meiosis, but can also occur in response to signals from the surrounding environment, or in response to pharmacological intervention [106]. There are two types of epigenetic modification: DNA methylation, and histone modification, which can positively or negatively influence gene expression [84]. By analysing gene expression and methylation patterns of vascular ECs and lymphatic ECs, a significant set of genes were identified with different methylation patterns and gene expression [107]. For example, the lymphatic specific gene promoter IL-7 is differentially methylated between these lymphatic and vascular endothelial subtypes. IL-7 is upregulated in lymphatic ECs where the gene is hypomethylated, compared to blood ECs [107].

1.4 Secretory Pathway

1.4.1 Epithelial secretion

The term ‘epithelial cell’ encompasses cells which line both the internal and external surfaces of the body, therefore ECs are a subset of epithelial cells [108]. The majority of epithelial cells, including ECs have a defined apical and basal membranes, which differ in their structure, composition and function, for example ciliated epithelium in the respiratory tract only has cilia on the apical surface of the cell [108,109]. Epithelial cells interact with the extracellular matrix (ECM) via integrins, transmembrane proteins which anchor cells to the ECM (Figure 1.1) [108]. The molecular mechanisms that determine apicobasal polarity in ECs are unclear, however, important insights may come from the extensive studied polarisation of epithelial cells [110].

Cellular polarisation underlies processes including cell-cell signalling, cellular division, and cell migration, and is therefore important for almost every cell type [111]. The polarisation of epithelial cells is maintained by protein complexes which are localised at the apical membrane and is essential in maintaining apicobasal polarity [112]. There are three main protein complexes involved in regulating epithelial cell polarity, Crumbs, Par, and Scribble [113]. The Crumbs and Par complexes are located apically, and the Scribble complex is basolaterally located [113]. The composition, cellular location and function of these complexes is evolutionary conserved [112]. Whilst is it is not exactly known how these complexes define the polarity, the antagonism between these complexes excludes Crumbs and Par from entering the basolateral domain, and Scribble from entering the apical domain [113,114]. This antagonism occurs by methods including phosphorylation of components of the Scribble complex, preventing its accumulation at the apical surface [111]. This establishment of polarity allows the segregation of certain organelles such as the nucleus to the basal side and cellular extensions such as cilia present on the apical surface. Tight junctions separate the apical and basolateral compartments of epithelia by prevent the lateral diffusion of intramembrane components [115].

The apical and basolateral plasma membrane domains differ in their protein and lipid composition, with certain transporters, ion channels and enzymes are specifically enriched in apical or basolateral membranes [116]. The apical membrane of epithelial cells is enriched with glycolipids and cholesterol, whilst the basolateral membrane contains many cell adhesion proteins [117]. The lipids and proteins need to be sorted to the correct target location to maintain polarity.

There are three main types of epithelial cell: squamous, cuboidal and columnar, which can be only one cell layer thick (simple), or two or more layers thick (stratified). Squamous epithelial

cells appear as flattened cells, with an almost oval shapes nucleus. ECs are a type of specialised squamous epithelium tissue, as are mesothelial cells, which line the body's cavities [118]. Mesothelial cells secrete a non-adhesive protective surface for the body's internal surfaces and unlike ECs, can consist of several cell layers [119]. Cuboidal ECs have a large spherical nucleus which is central within the cell. This type of epithelium is found in the ducts of glands and is actively involved in the secretion and absorptions of molecules. In smaller glands, this epithelial tissue is often squamous, with stratified epithelial tissue in larger glands such as salivary glands [120]. Columnar epithelial cells are rectangular shaped cells, with their nucleus located toward the basal side of the cell and contain lots of Golgi and endoplasmic reticulum [118]. Columnar epithelial cells are commonly found within the digestive tract where the cells express features upon their apical surface such as microvilli, to increase the surface area for absorption, or cilia to waft mucus, which has been secreted by a type of modified epithelial cells called goblet cells [118].

The apical surface of epithelial cells is often covered in microvilli and contains most of the proteins required for functions such as digestion, and nutrient absorption [114]. The apical membrane is also generally enriched in sphingomyelin-containing glycolipids, and glycolipid-anchored proteins [114]. The basolateral cell surface is enriched in plasma membrane proteins such as transferrin and low-density lipoprotein receptors, and Na^+K^+ATPase, which are required for fundamental cellular processes [121]. One of the major roles of epithelial cells is secretion. In the intestine epithelial cells need to secrete molecules into the gut, such as digestive enzymes to break down food, and mucus into the lumen to lubricate the gut lining to aid the passage of material along the gut. These molecules are secreted from the apical surface of the epithelial cells, whilst endocrine epithelial cells in the gut secrete hormones from their basolateral surface.

One of the major roles of epithelial cells is polarised secretion of proteins. The destination of these proteins is known by the addition of sorting signals, which are recognised by specific cellular sorting machinery at the TGN and in recycling endosomes before incorporation into apical and basolateral sorting vesicles [122]. Apical sorting signals include N- and O- linked glycans, and glycophosphatidylinositol (GPI)- anchors which are attached to the protein [117]. During the translocation and elongation processes of the polypeptide chain during protein synthesis by ribosomes, N-linked glycans are attached to an asparagine residue within an N-X-T/S consensus sequence within the polypeptide chains [123]. There is not currently an O-linked glycosylation consensus sequence. After the N-linked glycans have been correctly modified by glucosidases and α-mannosidases, and the polypeptide chain has been correctly folded in the endoplasmic reticulum (ER), the protein is exported to the Golgi. Within the Golgi, the plasma membrane proteins are further glycosylated, before being trafficked to the apical

cell surface. The mechanism by which N-linked glycans are apically sorted is weakly understood. The mannose-binding lectin VIP36 and the galactose-binding lectin, galectin-3 are potential sorting receptors for N-linked glycans [123]. VIP36 is predominantly expressed in the *cis*-Golgi and the ER-Golgi intermediate compartment (ERGIC), and has been found to promote sorting of several apical glycoproteins [124]. Over expression of VIP36 in MDCK cells increased the apical content of VIP36 and VIP36-recongised glycans [124]. Galectin-3 has been shown to directly interact with certain apical glycans, and depletion of galectin-3 in MDCK cells results in the mis-sorting of these apical glycans to the basolateral membrane [125]. Galectin-3 is also suggested to be able to sort O-linked glycans [123].

The abundance of several proteins within the apical membrane has been shown to decrease when N-glycans are removed. For example, when some of the 7 N-glycosylation sites of the gastric H-K-ATPase β-subunit in LLC-PK_1 were mutated, the distribution of the protein changed [126]. Normally, the correctly glycosylated β-subunit is 40% detected in the ER, and 60% amongst the plasma membrane, Golgi, and endosomes [126]. Removal of the N1, N3 and N5 increases the amount of protein retained in the ER, and removal of N7 leads to virtually total retention in the ER [126]. The O- linked glycan sorting signal works in a similar mechanism [125].

Basolateral sorting does not involve the addition of glycans but involves the recognition of signal sequences. The most common sorting signals for basolateral proteins include tyrosine peptide motifs, which has the consensus sequence NPXY or YXXØ, or dileucine motifs which have the consensus sequence D/EXXXLL within their cytoplasmic domain [127].

At the TGN, proteins are sorted into membrane bound vesicles destined for their required location. Lipid rafts have been suggested to be sorting platforms within the TGN for delivery of proteins to the apical membrane [128]. Lipid rafts are subdomains of the plasma membrane that contain higher levels of cholesterol and glycosphingolipids than other areas of the PM, increasing their stability. GPI anchored proteins oligomerise into lipid rafts, however, it is uncertain whether GPI-anchoring alone is sufficient to specify proteins to the apical membrane, and may require N-linked glycans [127]. However, apical trafficking using N- and O- glycans can also be lipid raft independent [128]. Another type of transporting apical proteins is by first transporting them to the basolateral surface, where they then undergo transcytosis to the apical surface [129]. This indirect pathway is commonly used within hepatocytes [129].

The basolateral sorting motifs are very similar to those that interacts with clathrin-adaptor complexes in endocytosis and lysosomal sorting, giving rise to suggestions that clathrin may be involved in basolateral sorting [129]. For some proteins targeted to the basolateral surface, such as transferrin receptors, have shown to be indirectly transported via endosomes [129]. If

these basolateral sorting signals are removed, basolateral proteins are generally transported to the apical surface, and if the sorting sequences were moved to the cytoplasmic domains of apical proteins, the proteins were transported to the basolateral surface [121].

The membrane of secretory vesicle are enriched in proteins such as Rab11a, Rab8a, and Rab27, which are able to recruit v-SNAREs, for example Slp4a [116]. Slp4a binds to the t-SNARE syntaxin-3 on the plasma membrane, along with the Sm protein Munc18-2 to allow fusion to the plasma membrane [116]. Another v-SNARE protein present within the secretory vesicle membrane is Vamp7, which is also able to interact with syntaxin-3 on the plasma membrane [116]. This docking brings the vesicle into close proximity, where it can fuse and secrete its contents outside of the cell. Exocytosis can be either constitutive, where secretion occurs continuously, or regulated, for example regulation via Ca^{2+} concentration [130].

An example of where polarised secretion is important is within the small intestine. Here, the polarisation of epithelial cells allows the epithelial intestinal cells to be specialised for absorption of nutrients, whilst providing a barrier against pathogens. The small intestinal epithelial cells form villi and crypts, increasing the surface area of the small intestine. The intestine contains multiple different types of simple columnar epithelial cells; including the secretory goblet cells, Paneth cells, and enteroendocrine cells; as well as absorptive enterocytes, and tuft cells [131]. The villi are formed of enterocytes, which have microvilli upon their apical plasma membrane to maximise surface area, and goblet cells secrete mucus to protect the intestine wall from acids and gases produced by gut bacteria. The base of the intestinal crypts contain Paneth cells, which secrete antimicrobial peptides including alpha-defensins into the crypt lumen via merocrine secretion [132]. Paneth cells are specialised secretory cells, with their nucleus towards the basal side of the cell, containing extensive ER and Golgi, and accumulate secretory granules towards the apical surface of the cell [132]. The intestinal crypts also contain stem cells and goblet cells. Many of the digestive enzymes present within the small intestine are produced by the pancreas. The pancreas contains exocrine acinar cells, which are highly polarised with their apical pole densely packed with digestive enzymes, including trypsin, lipase and amylase to secrete via exocytosis [133]. These enzymes enter the small intestine via the pancreatic duct, which is lined by ductal cells [134].

The small intestine is also an endocrine organ, meaning it can secrete hormones directly into the blood and tissue. Finger like apical projections expressed by enteroendocrine cells (EECs), can detect specific nutrients present in the intestinal lumen. This detection causes the secretion of peptide hormones contained in secretory granules from the basal surface, which can then activate receptors on proximal cells, enter the blood, or stimulate receptors on

neurons [135]. These secreted hormones include cholecystokinin (CCK), which is secreted by enteroendocrine cells within the intestine in response to a meal, and causes the release of digestive enzymes from the pancreas, as well as mediating satiety, and histamine which increases acid secretion [135].

Disruption in the polarity of epithelial cells can have a significant effect upon the organisms. If the apical proteins are disrupted, malnutrition occurs due to inability to absorb nutrients across the apical membrane, and mislocalisation of the basolateral proteins is associated with cancer development and inflammatory bowel disease [131].

1.4.2 Extracellular vesicles

Intracellular communication is an essential function of multicellular organisms. Cells communicate in numerous different ways, including cell-cell contact, intracellular transfer of secreted molecules and intracellular transfer of extracellular vesicles (EVs). EVs are an important mechanism of intracellular communication and are released by cells under both physiological and pathological conditions, and dock at the membrane of a target cell causing a response [136]. These EVs have a variety of functions, including the transport of DNA, RNA, and miRNA [137]. Two types of EVs are exosomes and microvesicles (MVs) (Figure 1.6). ECs are able to release both exosomes and MVs [136]. One major challenge in the study of exosomes and MVs is the difficulty discriminating between these two types of EVs, as size and morphology does not allow a clear distinction [136].

1.4.2.1 Exosomes

Exosomes are 40-100 nm extracellular lipid vesicles, which are released as a consequence of multivesicular endosome fusion with the plasma membrane (Figure 1.6) [138]. Intraluminal vesicles (ILVs) are formed by invagination of the endosomal membrane, and endosomes accumulate ILVs within their lumen, forming multivesicular bodies (MVBs) (Figure 1.6) [138]. Not all MVBs containing ILVs become exosomes, and other fates include fusion with lysosomes, the generation of specialised organelles such as wPB, or fusion with the plasma membrane [138]. Whilst it is currently unknown how the fate is decided, the cholesterol levels of the MVB membrane appear to play a role, with cholesterol-poor MVBs fusing with lysosomes, and cholesterol-rich MVBs fusing with the plasma membrane [138]. If MVBs fuse

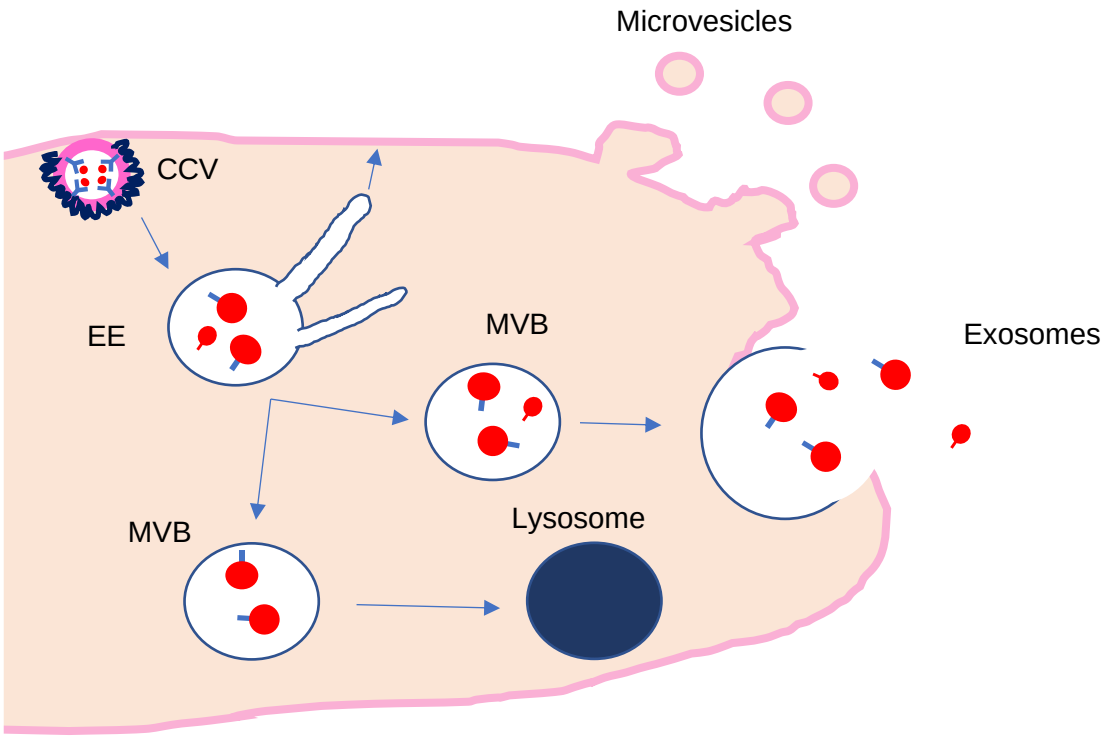

Figure 1.6. Release of microvesicles and exosomes. Microvesicles are released directly by budding off from the plasma membrane. The release of exosomes occurs by interluminal vesicles fusing with EEs, before being released by the fusion of MVBs with the plasma membrane. Other MVBs fuse with lysosomes. Adapted from Extracellular vesicles: Exosomes, microvesicles and friends, Raposo and Stoorvogel, Journal of Cell Biology; published by Rockefeller University (2013) [136].

CCV: Clathrin coated vesicle, EE: Early endosome, MVB: Multivesicular body

with the plasma membrane of the cell, the contents is released to the external environment as exosomes (Figure 1.6) [138].

Exosomes were initially thought to be involved in removing cellular waste, but recently it has been found that exosomes capable of carrying proteins, lipids and DNA amongst other substances [138]. Exosomes are released from nearly all eukaryotic cells, and are thought to be involved in many cellular processes, including immune response and cell-cell communication [139].

The study of exosomes is a recent advancement and there has been increasing interest on their biological significance, and the implications of exosomes in disease states [140]. One study by Davidson *et al* (2018) investigated whether exosomes released by ECs could be cardioprotective [141]. In hypoxic conditions, co-culture with HUVEC and cardiomyocytes decreased cell death when compared to cardiomyocytes culture alone, suggesting that HUVEC can release cardioprotective factors, which they later confirmed as exosomes by transmission electron microscopy and flow cytometry [141]. This study, as well as other studies using different cell types suggest that exosomes could be used as therapies [142]. When there is a high level of blood sugar within the body, which can occur during diabetes mellitus, ECs can become activated meaning they express proinflammatory and procoagulant proteins upon their surface. In one study by Sáez *et al* (2019) exosomes were found to be able carry molecules involved in EC activation such as the cellular adhesion ICAM-1 [143]. This study showed that exosomes may deliver ICAM-1 to monocytes, and exosomes may increase the expression of these adhesion molecules, inducing and maintaining the activation of both cell types during hyperglycaemia [143]. Exosomes have also been proposed as useful tool for drug delivery, due to their ability to cross the BBB [144].

1.4.2.2 Microvesicles

Microvesicles (MVs) are another type of extracellular vesicle released from the cell membrane that are involved in cell-cell communication, and are approximately 0.1 – 1 μm in diameter (Figure 1.6) [136]. Unlike exosomes, which are formed in MVBs, MVs occur by direct budding from the plasma membrane (Figure 1.6) [136].

Like exosomes, MVs are capable of transporting molecules including mRNA and proteins. The content of microvesicles depends on the microenvironment and the triggers preceding the release of the microvesicles. The shedding of MVs occurs from micro-domains within the plasma membrane called lipid-rafts, regions of the plasma membrane which contain high

concentrations of cholesterol [145]. Many cells are capable of releasing MVs from their plasma membrane, including ECs. MVs are released under physiological conditions in ECs, such as cell growth. The amount of microvesicles released by ECs increases during EC activation, which occurs due to conditions such as cell injury, hypoxia and shear stress [145]. Dependent on the condition that MVs are released, such as between shedding and apoptosis, MVs have express a different repertoire of surface receptors and cytoplasmic components [145]

Endothelial MV can be indicators of diagnosis and prognosis of health conditions [140]. The process of MV release is thought to be highly regulated and occurs in many cell types, with MVs being detected in blood and other bodily fluids [146].

However, like exosomes, the exact mechanism of formation and secretion of MVs is unknown, however the release of MVs shows similarities to that of viral budding [146].

1.4.3 Endothelial cell secretion

As previously discussed, the ECs act as a dynamic organ, interacting with both the circulating fluid and the underlying tissue. Whilst most of the mechanisms are similar to other cell types, ECs have unique features, due to their roles within processes such as blood haemostasis [147].

Von Willebrand factor (vWF) is synthesised within ECs and is either secreted directly, mainly as low molecular weight VWF through the constitutive pathway, or stored within Weibel-Palade bodies (WPB) (Figure 1.7) [148]. Within ECs, vWF is initially formed as a monomer within the ER consisting of a signal sequence, pro-peptide and the mature protein, before being dimerised using disulphide bonds [147]. The dimerised vWF is transported to the Golgi; an organelle associated with the modification and transport of proteins, where O- glycosylation occur, and vWF becomes a multimer [147]. These vWF multimers then have two fates; either to be constitutively secreted by the EC or stored with WPBs.

WPBs are endothelium specific organelles and contain chemokines such as IL-8 and endothelin-1, as well as vWF. The formation of the WPBs starts at the TGN, and is dependent on the adaptor protein AP-1 and clathrin [147]. During maturation, WPBs recruit other components including Rab GTPases (Rab27A, Rab3B/D, and Rab15) and Rab effectors (MyRIP, Slp4-a and Munc13-4), which allow the WPB to become ready for secretion [149]. SNARE complex proteins, molecular machines that are involved in the exocytosis of secretory vesicles, interact with these proteins [149]. The assembly of these SNARE proteins brings the vesicle and the plasma membrane into close proximity. Once stored in WPBs, vWF can be

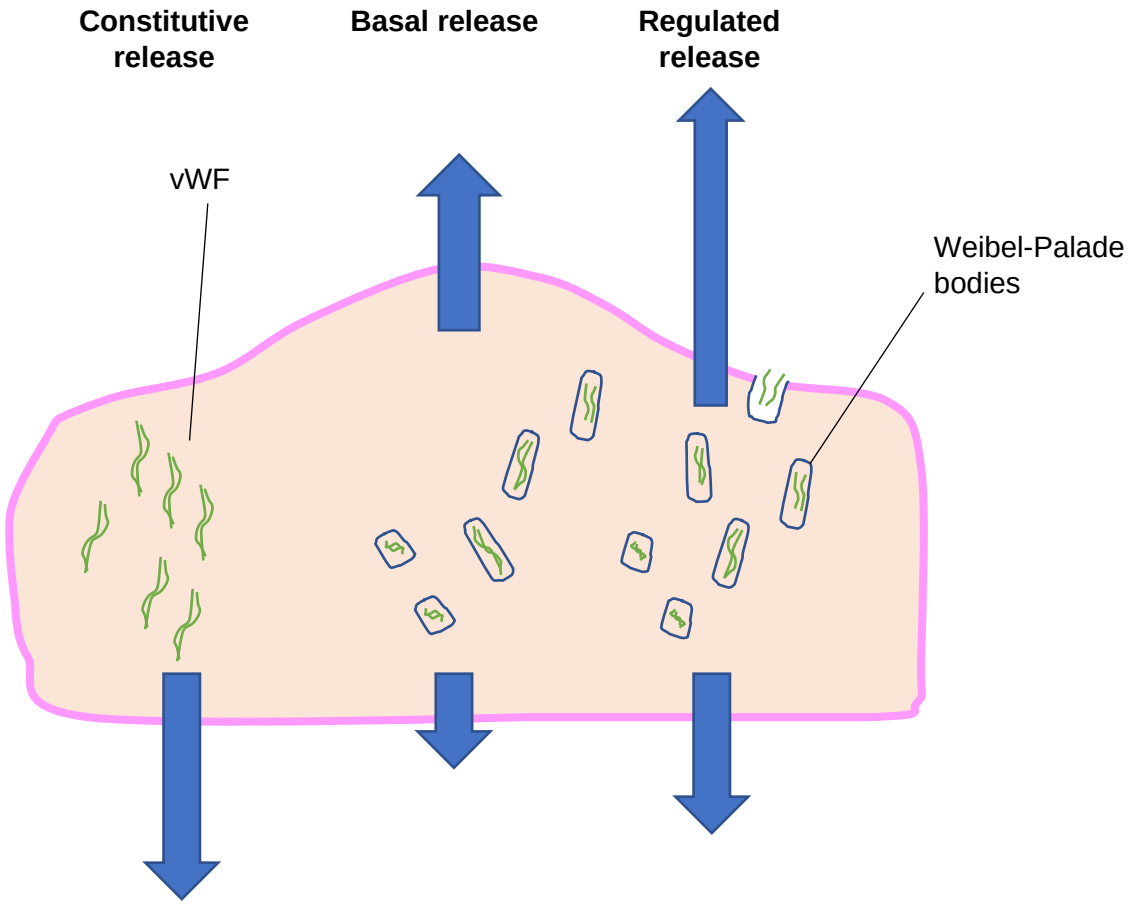

Figure 1.7. Release of vWF from endothelial cells. Von Willebrand factor (vWF) is constitutively released from endothelial cells solely from the basolateral surface. Under basal and regulated release, secretion of vWF occurs predominantly apically, with little vWF secreted via these methods from the basolateral surface. The secretion of vWF via the basal and regulated secretion occurs from Weibel-Palade bodies. The length of the arrow correlates the relative secretion of vWF. Adapted from Von Willebrand Factor multimerization and the polarity of secretory pathways in endothelial cells, Lopes da Silva and Cutler, Blood; published by ASH (2016) [150].

secreted as high molecular weight vWF when the EC is activated, but also under basal conditions [148].

The largest amount of regulated VWF is secreted as long strings of vWF polymers apically into the blood vessel lumen where it can recruit circulating platelets; an important stage in coagulation [150]. However, constitutive release of vWF is exclusively targeted to the basolateral surface (Figure 1.7). AP-1 is involved in the delivery to the basolateral surface, however, how AP-1 is involved in this targeting is uncertain [150].

In steady state most ECs are quiescent, meaning they are not actively dividing, and favour tumour dormancy. However, ECs are able to be rapidly activate in response to physiological stresses such as hypoxia, inflammation, and the upregulation of angiogenic factors. These stresses can cause the ECs to secrete specific molecules. Other important molecules secreted by ECs include matrix metalloproteinases (MMPs). One specific MMP, MMP-14, has shown to be of vital importance during development in lung ECs. MMP-14 is required for alveolarization, and MMP-14 KO mice have decreased alveolar surface area which results in decreased lung function [151]. The secretion of ECs can also change in response to injury and play an important role in repair of the vessel. ECs in the lung capillary secrete MMP-14 after surgical removal of part the lungs, which allows activation of EGF-like ligands, promoting repair to the lungs by stimulating the proliferation of epithelial progenitor cells [152]. Liver sinusoidal ECs (LSECs) are also involved in tissue regeneration. After a partial hepatectomy LSECs established a vascular niche that releases angiocrine growth factors, such as the bone morphogenic proteins BMP2 and 4, involved in organ regeneration [153].

Other stresses, including shear stress are able to induce secretion of other factors from ECs. Shear stress refers to the force of the flowing blood on the EC surface stimulate EC cell signalling pathways such as the MAPK and PI3K transduction pathways, resulting in the secretion of subset of molecules, including platelet derived growth factor (PDGF) [154]. PDGF is a powerful mitogen for vascular smooth muscle cells causing them to switch from a contractile to proliferative state, so is involved in the regulation of cell growth and proliferation, especially within angiogenesis [155]. Whilst the secretion of these molecules can have practical results, such as repair of tissue, they can also be implicated in pathogenic complications. For example, PDGF is a potent chemoattractant for smooth muscle cells, which is a critical event in atherosclerosis [154]. PDGF causes migration of smooth muscle cells into the tunica intima of arteries, which form part of the fibrous cap of the atherosclerotic plaque [65]. This invasion of smooth muscle cells into the arterial tunica is also aided by the secretion of proteolytic MMPs from ECs, especially MMP-9. Under basal conditions MMP-9 is not produced by ECs, but is induced by cytokine activation of ECs [156]. MMPs are involved in

the degradation of the extracellular matrix, allowing smooth muscle cells to enter the tunica intima [66].

ECs are also able to synthesise and secrete vasoactive substances, including the vasodilators NO and prostaglandins, hyperpolarisation factors, and vasoconstrictors angiotensin and endothelin 1 (ET-1) [157]. Under normal conditions ET-1 is produced in small amounts, regulating blood pressure and reducing the heart rate, however in pathological conditions the production is increased [158]. The secretion of ET-1 is stimulated by factors such as thrombin, hypoxia and adrenaline, and may decrease eNOS expression reducing NO production [159]. ET-1 is involved in endothelial dysfunction, as ET-1, the ET receptors and the biological effects controlled by ET-1 become more pronounced during cardiovascular disease [158].

The substances secreted by ECs are of considerable importance. However, these factors need to be secreted from the correct surface of the ECs, to ensure they can perform their required function.

1.4.4 Polarised EC secretion

ECs can secrete different proteins from the apical and basolateral surface of the cell, such as the secretion of IL-8 from the apical, and MIC-1 from the basolateral surface [160]. Whilst there have been vast studies into the polarised secretion of epithelial cells, there are few studies into the polarised secretion of ECs and the sorting mechanisms used [33,114,123,160,161]. Some studies have suggested that the mechanism used within epithelial cells are not the same as used within endothelial cells, highlighting the need for further investigations into this area.

One protein which has been shown to be involved in the HUVEC polarised secretion is liprin-α1. Liprin-α1 is involved in a method of trafficking vesicles from the Golgi to the basolateral membrane in a Rab11B-dependent pathway, which uses microtubules for vesicle transportation. Cells are anchored by to the ECM via large macromolecular assemblies on the basolateral membrane called focal adhesions (FAs), which transmit mechanical force and regulatory signals between the ECM and the cell. The assemblies contain integrins, which anchor the cell to the ECM via their extracellular region, and their cytoplasmic tale is connected to the actin cytoskeleton.

One of the protein complexes involved in anchoring microtubules to the FAs is the cortical microtubule stabilising complex (CSMC) [1]. The CSMC interacts with plus-end trafficking proteins of microtubules such as KIF21A, and associate with FAs proteins such as talin [1].

One of the proteins involved in the CSMC is liprin-α1, which interacts with the protein tyrosine phosphate receptor type f polypeptide (PTPRF) and localises it to the FAs [2].

Liprin-a1 is a member of the leukocyte common antigen related (LAR)-interacting family, alongside other liprin-α and liprin-β cytosolic adaptor and scaffold proteins [3]. The liprin-α proteins have mainly been previously studied in neurons, where they are involved in synapse functions [3]. In non-neuronal cells, including ECs, liprin-α1 proteins have been shown to have roles within cell adhesion, cytoskeleton organisation and signal transduction, as well as FA dynamics [3].

A study by Mana *et al* (2016) showed that liprin-a1 was involved in the trafficking of FN to the basolateral surface of ECs [2]. Within the cell, FN dimers are proposed to associate with the α5β1 integrin in vesicles and be transported to the basolateral plasma membrane in a Rab21 dependent pathway. Mana *et al* (2016) showed when liprin-α1 was depleted, the secretion of FN from the basolateral surface was depleted.

In order to maintain the non-thrombogenic surface of ECs, ECs polarise secretion of basement membrane components to the basolateral surface of ECs, including fibronectin (FN). In newly confluent cultures, Kowalczyk *et al* (1990) found that FN was secreted equally from both the apical and basolateral surface of ECs of pre confluent and newly confluent cultures, whilst in post-confluent cultures FN was predominantly secreted from the basolateral surface [33]. This study showed that ECs also have binding sites for FN upon their confluent basolateral surface, where polymerisation can occur [33]. This suggests one possible method of ensuring FN polymerisation only occurs upon the basolateral surface of ECs [33].

In epithelial cells, N-glycans normally direct proteins to the apical membrane, however a study by Jurczyluk *et al* (2003), found no evidence for this sorting mechanism in ECs [160]. IL-8 and GM-CSF were predominantly secreted from the apical surface, and MIC-1 from the basolateral surface. However, the study found that the N-glycosylated proteins IL-8 and pro-MIC-1 were sorted to both the apical and basolateral surfaces of HUVEC, suggesting sorting may not be related to glycosylation within ECs [160].

Other cytokines show polarised secretion in ECs. A study by Verma *et al* (2006) found that IL-6, GM-CSF and TNF-α were secreted from the apical and basolateral surface of ECs, whilst IL-1α and IL-10 were found to be solely secreted from the apical surface from microvascular brain endothelial cells (MBEC) [161]. This study also found that stimulation by lipopolysaccharide to either surface of the EC can stimulate polarised cytokine release, supporting the results that MBEC release [161].

As vasoactive substances act upon the smooth muscle cells underlying the ECs, it would imply that these substances were released form the basolateral surface of ECs. The vasoactive substance endothelin-1 released from ECs has been shown to be predominantly secreted from the basolateral surface of cultured HUVEC, with 80% of the total amount being found in the basal media [162].

This polarisation ensures the secretion of substances to the desired location. If molecules are not accurately sorted and secreted from the correct surface of the EC, there can be significant physiological consequences, including atherosclerosis [65].

1.5 Statins

There are a number of drugs that have been shown to affect ECs, including angiotensin-converting enzyme (ACE) inhibitors which are used to treat hypertension, and beta blockers, which reduce the heart rate [163]. Another drug thought to affect ECs are statins, which are suggested to have an anti-inflammatory effect. Statins are predominantly used for reducing high blood cholesterol levels, which is one of the most important risk factors in the development of coronary heart disease [164]. However, they may also have additional roles that are not yet appreciated [164].

Statins affect the cholesterol synthesis pathway, by competitively inhibiting 3-hydroxy-3-methylglutaryl coenzyme A (HMG-CoA) reductase, which converts HMG-CoA to mevalonate. This inhibition results in increased expression of cell surface LDL receptors, therefore increasing cellular uptake of LDL and reducing circulating cholesterol.

The formation of an atherosclerotic plaque is a complex multifactorial process, involving the build-up of cholesterol, inflammation, and EC dysfunction. The inhibition of HMG-CoA reductase also inhibits other downstream products of the mevalonate pathway, including the synthesis of isoprenoid intermediates such as farnesylpyrophosphate (FPP) and geranylgeranylpyrophosphate (GGPP) [165]. These intermediates serve as lipid attachments for various intracellular signalling molecules, including the small GTP-binding proteins Rho, Rac and CDC42 [165]. The inhibition of these proteins is thought to play an important role in the positive biological effect of statins on endothelial cells.

The inhibition of Rho and Rac prenylation by statins has been shown to improve EC dysfunction, by increasing the production of NO by increasing the expression of eNOS [166]. This promotes vasodilation, which can be impaired by other known risk factors for atherosclerosis, including hypertension and high blood sugar [166].

1.6 Aims of Project

The aims of my project are to analyse the normal HUVEC polarised secretome, and to investigate the changes that occur in different conditions. I will be comparing the normal HUVEC polarised secretome to the polarised secretome where liprin-α1 is silenced and examining which proteins secretion is changed. As there is currently very limited information about the mechanisms EC use for secretion, this investigation will allow me to suggest which proteins involve liprin-α1 in their secretion. This information will allow further investigations to be performed to aid elucidation of the mechanisms of EC secretion.

I will also be comparing how atorvastatin addition affects the polarised secretome of HUVECs. Atorvastatin is one of the most commonly prescribed drugs for reducing cholesterol, which acts by inhibiting the HMG-CoA reductase pathway. In my study, I aim to investigate whether atorvastatin changes the polarised secretome of HUVEC, and whether atorvastatin has any, previously unknown pleiotropic effects. These effects could possibly highlight other disease conditions that atorvastatin may have therapeutic potential for. This study could also highlight counterindications where atorvastatin should not be given as treatment. As statins are such an important drug within the UK health system, my study will provide valuable information about the effects of statins upon EC secretion.

Chapter 2 Materials and Methods

2.1 Reagents

2.1.1 Cell Culture

Mammalian cell line	Source
HUVEC	Human umbilical vein endothelial cells, Lonza, CC-2519, pooled donors

Cell culture media type	Components
EBM-2	Endothelial cell basal medium-2, Lonza, CC-3156
Endothelial cell growth medium (EGM-2)	Endothelial cell basal medium (EBM-2) supplemented with BulletKit minus vascular endothelial growth factor, Lonza, CC-4176
HIFA	EBM-2 (supplemented with hydrocortisone, ascorbic acid and GA-1000 (gentamicin-amphotericin) according to manufacturer's instructions: 10 ng/mL human recombinant fibroblast growth factor (FGF)/carrier free, R&D 233-FB-025 10 ng/mL insulin growth factor (IGF)/carrier free, R&D 8335-G1-200

2.1.2 General reagents

Reagent	Supplier
Human fibronectin (0.1%)	Sigma-Aldrich, F0895
Bovine type I collagen (2.8 mg/ml)	Advance BioMatrix, 5409
Bovine gelatin (2%)	Sigma-Aldrich, G1393
Trypsin-EDTA (0.05%)	Life technologies, 25300-062
Dulbecco's Modified Eagle's Medium/Nutrient Mixture Ham's F-12 (DMEM/F-12) + 10% Fetal Bovine Serum (FBS) +1% Penicillin Streptomycin (P/S)	Sigma-Aldrich, D8062
Ammonium persulphate (APS)	Sigma-Aldrich, A3678
Acrylamide: bisacrylamide (37.5:1, 30% (w/v) acrylamide	Bio-Rad, 161-0158
Amersham ECL western blotting detection reagents	Promega, W1015
Amersham Hyperfilm	GE healthcare, 28-9068-44
N,NM'N'- tetramethyl ethylenediamine (TEMED)	Fisher Scientific, BP150-20
Immobilon-P polyvinyl fluoride (PVDF) membrane	Merck Millipore, IPVH00010
4',6-diamidino-2-phenylindole (DAPI)	Life technologies, D21490
1,4-diazabicyclo[2.2.2]octane (DABCO)	Sigma-Aldrich, D2522
Mowiol 4-88	Calbiochem, 475904

Triton X-100 (0.2%)	Sigma-Aldrich X100
Sodium borohydride	Sigma-Aldrich 452882
Bovine serum albumin (BSA)	Sigma-Aldrich, A9647

2.1.3 General solutions and buffers

Solution/Buffer	Components
10 x Phosphate-buffered saline (PBS)	27 mM KCL 1.4 M NaCl, 18 mM KH_2PO_4, 100 nM Na_2HPO_4, pH 7.4.
10x Tris-buffered saline (TBS)	50 mM Tris Base 140 mM NaCL pH 7.6
10 x SDS-PAGE running buffer	192 mM glycine 25 mM Tris 1.0% (w/v) SDS
1x Transfer buffer	25 mM Tris 192 mM glycine pH 8.5
Blocking solution	5% (w/v) dry skimmed milk 1x TBS-T
2x Laemmli sample buffer	25 mM Tris-HCL pH 6.8 2% (w/v) SDS 10% (v/v) glycerol 0.2% (w/v) bromophenol blue 20 mM DTT
Tris buffered saline – Tween (TBS-T)	1L TBS 0.1% Tween 20 (Sigma Aldrich, P1379)

2.1.4 Antibodies

(IB: Immunoblotting, IF: Immunofluorescence)

Primary Antibody	Species	Application/Dilution	Supplier
PPFIA1	Rabbit	IB-1:1000	Protein Tech, 14175-1-AP
Tubulin	Mouse	IB-1:5000	Sigma-Aldrich, T5168
VE-cadherin	Mouse	IF-1:200	BD Biosciences, 55-7H1
EDA-fibronectin	Mouse	IF - 1:200	Santa Cruz, sc-59826
Fibronectin	Rabbit	IF - 1:400	Protein Tech, 15613-1-AP
Zonula Occludens-1	Rabbit	IF - 1:400	Thermofisher, 61-7300

Secondary antibodies	Species	Dilution	Supplier
Anti-mouse HRP	Donkey	IB: 1:10000	Jackson, 715-035-150
Anti-rabbit HRP	Donkey	IB: 1:10000	Jackson, 711-035-152
Mouse Alexa Fluor 594	Donkey	IF: 1:400	Invitrogen, A21203
Rabbit Alexa Fluor 488	Goat	IF: 1:400	Invitrogen, A11034

2.1.5 siRNA oligonucleotides

Target Gene	Sense strand (5'-3')
PPFIA1	siRNA A: AGUUUAGACCAAAGGACAUUCGUGG siRNA B: GCAUGACCUCAAUGAUAAACUUGAA siRNA C: CCAAGGUACAAACUCUUAAUGAGCA

2.1.6 Statins

Statin	Supplier
Simvastatin, 98%	Acros Organics, 458840010
Atorvastatin calcium	Sigma-Aldrich, PH41422-1G

2.2 Cell Biology

2.2.1 Mammalian cell culture

HUVEC were obtained from Lonza (CC-2519, pooled donors), and maintained in Endothelial Growth Medium (EGM-2, CC-3162, Lonza) and incubated at 37 °C in 5% CO_2. HUVEC were split after reaching approximately 80% confluency. To do this, the medium was removed, and cells were washed twice in PBS before incubation with Trypsin-EDTA (approximately $1/10^{th}$ of media volume) at 37 °C until detached. DMEM/F12 + 10% FCS was added at a 4:1 ratio with Trypsin-EDTA to neutralise the trypsin. Cells were centrifuged at 400x g for 3 minutes, before the pellet was resuspended in EGM-2 media, and cells were counted using a haemocytometer. HUVEC were generally used for experiments between passage 2 and 6.

2.2.2 Coating of tissue culture dishes

Prior to plating, tissue culture dishes were coated with fibronectin at a concentration of 10 µg/mL in PBS for 30 min at room temperature. Glass coverslips were coated with fibronectin at the same concentration in tissue culture dishes. Transwell (Costar, 3460) inserts were coated with a triple coat of 100 µl PBS, 5 µl gelatin, 5 µl fibronectin and 1 µl collagen per well for an hour at 37°C prior to plating.

2.3 Biochemistry

2.3.1 Preparation of materials

2.3.1.1 siRNA transfection

HUVEC were cultured onto tissue culture dishes as in 2.2.1. Cells were seeded at 7 x 10^4 /mL onto dishes and incubated at 37°C 5% CO_2 (v/v). After 24 hours cells were washed three times in room temperature OptiMEM I reduced serum medium (Gibco, 31985-047), and following the third wash samples were resuspended in half the normal volume. SiRNA transfections were made up as according to the table below.

	Tube A		Tube B	
Dish/Plate	OptiMEM (µl)	20 µm siRNA (µl)	OptiMEM (µl)	GeneFECTOR (µl)
12 – well plate	48.5	1.5	47	3
6 – well plate	97	3	94	6
6 cm dish	242.5	7.5	235	15
10 cm dish	485	15	470	30

siRNA transfections were carried out using GeneFECTOR (Venn Nova, R-0001-01) according to the manufacturer's instructions. Three siRNA oligonucleotide duplexes targeting liprin-α1 were synthesized by Origene Technologies (Herford, Germany), and a control siRNA duplex (#SR30004). Tube A was added to Tube B before incubating at room temperature for 5 minutes. The mixture was then added dropwise to cells whilst swirling plates, and plates were incubated at 37°C 5% (v/v). After 3 hr, cells were refreshed with EGM-2, before being incubated at 37°C 5% CO_2 (v/v) for 48 prior to experimental use.

2.3.1.2 Statin preparation

Statins were made up to a 1 mM solution by dissolving the statin powder in DMSO and stored at – 20°C until use.

2.3.2 Western Blotting

2.3.2.1 Sample preparation

HUVEC were plated onto 6 cm tissue culture dishes as in 2.2.1. After 48 hours, cells were washed in PBS at room temperature, then ice cold PBS before 200 µL of 2x Laemmli lysis

buffer was added. After 2 minutes, cells were scraped and transferred to a centrifuge tube, and spun for 10 minutes at 10000x g. The supernatant was collected, and the pellet discarded.

2.3.2.2 Sodium-dodecyl sulphate polyacrylamide gel electrophoresis (SDS-PAGE)

Gels were typically made using a 10% resolving gel and a 6% stacking gel. Resolving gels were prepared using 30% acrylamide/0.8% bis-acrylamide, 10% SDS, H_2O, 1M Tris (pH 8.8) as according to the table below. TEMED and 10% APS were added just prior to pouring gel. The resolving gel was poured between two glass plates leaving enough space for the stacking gel, and overlaid with H_2O, before being allowed to set at room temperature until set. The stacking gel was creating using 30% Acrylamide/0.8% bis-acrylamide, 10% SDS, H_2O, 1M Tris (pH 6.8) as according to the table below. Just before pouring, 10% APS and TEMED was added. The resolving gel overlay was removed, and the stacking gel was added on top of the resolving gel between the glass plates, and an appropriate comb was inserted. After polymerisation of the gel the comb was removed. Samples were heated to 95 °C for 5 min, then loaded onto the gel. Samples were electrophoresed at 10 mA until the bromophenol blue entered the separating gel, when the voltage was increased to 150 volts.

	Resolving gel (10%)	Separating gel (6%)
Stocks	Volume	Volume
30% acrylamide/ 0.8% bis-acrylamide	5 mL	667 µL
1M Tris-Cl	5.625 mL (pH 8.8)	625 µL (pH (6.8)
10% SDS	150 µL	50 µL
H_2O	4.05 mL	3.6 mL
10% APS	150 µL	50 µL
TEMED	8 µL	5 µL

2.3.2.3 Western blotting

An Immobilon-P polyvinyl fluoride (PVDF) membrane was activated by placing in methanol for 20 seconds, then equilibrated in the transfer buffer for 10 minutes. The PVDF membrane was placed onto a layer of a filter paper then fibre pad, and the SDS-PAGE gel was placed on top and covered by filter paper then a fibre pad. This was then placed in a gel cassette holder. Cassettes were placed into a Bio-Rad Mini Trans-Blot electrophoretic transfer unit with cooled Western transfer buffer for 1 hr at 50 V at 4°C. After transferring, the cassette was disassembled, and the membrane was rocked gently for 1 hr in 20 ml 5% blocking solution, then washed in 1x TBS-T. The membrane was then incubated in the primary antibody in

blocking solution overnight at 4°C on the rocker, then rinsed twice in TBS-T, before washing on the rocker three times in TBS-T. The membrane was then incubated with the secondary HRP-conjugated antibody in blocking solution for 1 hr 30, then again rinsed twice in TBS-T before washing three times in TBS-T on the rocker. The TBS-T was drained before covering with ECL reagents before incubation for 5 min at room temperature. Signal was detected by exposure to Hyperfilm for an appropriate amount of time based on signal strength.

2.3.3 Permeability assay

2.3.3.1 siRNA Transwell culture

Nine hours after siRNA transfection on tissue culture dishes, HUVEC were passaged onto Transwell inserts at $2x10^5$/mL. After 24 hours, the media was removed from the Transwell lower chamber and washed with PBS, and then from the upper chamber and washed in EBM-2 three times. After the third wash, all media was removed from the lower and upper chambers and refreshed with HIFA.

2.3.3.2 Statin Transwell Culture

Cells were cultured on Transwell inserts as in 2.2.1 at $2x10^5$/mL. After 24 hours, the media from the lower compartment was removed was washed with PBS, and then from the upper chamber and washed in EBM-2, which was repeated three times. After the third wash, all media was removed from the lower and upper chambers and refreshed with HIFA, and 50 µl of statin:DMSO solution was added to the upper Transwell chamber at the required concentrations, and 130 µl of the same concentration was added to the lower chamber, and again after 24 hours. Statins were made up to a 1 mM solution in DMSO and diluted accordingly.

2.3.3.3 Addition of FITC-dextran

After incubation in HIFA for 24 hours, 20 µl of fluorescein isothiocyanate-dextran (Sigma-Aldrich, FD40S) was added at a final concentration of 1 µg/mL to the upper compartment of the Transwell at a final concentration of 1 µg/mL. At 24 hours after addition, 50 µl of medium from the lower compartment was diluted in 950 µL PBS, and 100 µL of the solution was added

into a black 96 well plate. The absorbance was measured in a fluorimeter at 480 nm excitation, 520 nm emission and 67 gain using Tecan Infinite m200 i-control fluorometer.

2.3.4 Mass spectrometry

2.3.4.1 Mass spectrometry

HUVEC were cultured onto Transwell inserts at 2 x 10^5 cells per insert, and after 24 hours refreshed with HIFA as according to 2.2.1. After 48 hours, conditioned media from the upper and lower compartment of the Transwell inserts was transferred to separate microfuge tube and the media from the upper compartment of the Transwell was made up to 1.3 mL using HIFA. The samples were then centrifuged at 300 x g for 5 minutes at 4°C to remove any cells present, and media was transferred to a fresh centrifuge tube. Aliquots of the media were then transferred to separate Amicon Ultra 0.5 mL centrifugal filters (Merck Millipore, R8HA86271), and centrifuged at 16400x g for 15 minutes at 4°C, and filtered media was discarded. After concentration of media inside the filter to about 50 µL, filters were reverse centrifuged at 1000x g for 2 minutes into a fresh microfuge tube to allow the proteins to be eluted. Samples were kept on ice between steps.

2.3.4.2 Proteomic analysis

Proteomic analysis was performed by Dr Kate Heesom of Bristol Proteomics Facility. An equal volume of each sample was digested with trypsin and then labelled with Tandem Mass Tag (TMT) ten plex reagents according to the manufacturer's protocol (Thermo Fisher Scientific. The labelled samples were pooled and analysed by nano-LC MSMS using an Orbitrap Fusion Tribrid Mass Spectrometer. The raw data files were processed and quantified using Proteome Discoverer software v1.4 (Thermo Scientific) and searched against the UniProt Human database using the SEQUEST algorithm. Peptide precursor mass tolerance was set at 10ppm, and MS/MS tolerance was set at 0.6Da. Search criteria included oxidation of methionine (+15.9949) as a variable modification and carbamidomethylation of cysteine (+57.0214) and the addition of the TMT mass tag (+229.163) to peptide N-termini and lysine as fixed modifications. Searches were performed with full tryptic digestion and a maximum of 1 missed cleavage was allowed. The reverse database search option was enabled, and all peptide data was filtered to satisfy false discovery rate (FDR) of 5%.

2.3.5 ELISA

Cells were transfected with siRNA as described in 2.3.1 and were cultured on Transwell inserts as described in 2.2.1. After 24 hours, the media was removed from the Transwell lower chamber and washed with PBS, and then from the upper chamber and washed in EBM-2 three times. After the third wash, all media was removed from the lower and upper chambers and refreshed with HIFA. 48 hours after seeding onto Transwell inserts, all media was removed from both the lower and upper chamber of the Transwell, and the media from the upper compartment was made up to 1.3 mL using HIFA. Reagents and samples were prepared as according to the R&D human fibronectin Quantikine ELISA kit (R&D, DFBN10) sandwich enzyme immunoassay technique. 100 µL of assay diluent was added to each of the wells, and 50 µL of the standard, control, or sample was added to each well. The plate was covered with a plate seal and incubated on a horizontal orbital microplate shaker at room temperature for 2 hours. Each well was then aspirated and washed with the provided ELISA wash solution four times. After adding 200 µL of the provided conjugate to each well, the plate was covered with a new plate sealer, and incubated at room temperature for 2 hours on the shaker. After again aspirating and washing four times, 200 µL of the provided Substrate Solution was added to each well and the plate was incubated at room temperature in the dark for 30 minutes. After this time, 50 µL of the provided Stop Solution was added to each well, and the plate was read at 450 nm with a wavelength correction of 540 nm. A standard curve was created using the provided fibronectin standard, to allow concentrations of fibronectin to be determined.

2.3.6 Immunofluorescence microscopy

Cells were seeded onto Transwell inserts at 2 x 10^5 cells/mL, or glass coverslips at 1 x 10^5/mL as according to 2.2.1 and incubated at 37 °C overnight. After this, the growth media was removed, and samples were washed three times in PBS, before 4% (w/v) paraformaldehyde (PFA, Fisher Scientific, 30525-89-4)/PBS was added to samples for 15 minutes to fix the samples, then removed. Samples were washed twice with PBS before 0.2% Triton was added to permeabilise the cells, and samples were incubated at room temperature for 5 minutes before washing three times in PBS. 0.1% sodium borohydride solution was then added for 5 minutes at room temperature to quench autofluorescence, before incubating, before samples were washed three times in PBS. Samples were then incubated with 1% BSA for 20 minutes, before 30 µL of the primary antibody:BSA solution was added to the Transwell insert for 1 hr. Cells were then washed three times in PBS, and 30 µL of the secondary antibody:PBS solution was added to the Transwell and incubated for 45 minutes in the dark

at room temperature. If coverslips were used, the protocol was followed the same until addition of the primary antibody, where coverslips were inverted onto 80 µL of the primary antibody:BSA solution and incubated at room temperature for one hour, before washing three times in PBS. Coverslips were then again inverted onto 80 µL of the secondary antibody:PBS solution for 45 min. Samples were washed twice in PBS to remove the secondary antibody, then DAPI (1:5000) was added and samples were incubated at room temperature for 5 minutes. For Transwell inserts, cells were washed four times in PBS, and the Transwell membranes were excised using a blade, and were mounted onto glass slides using 5 µL of Mowiol mounting solution containing 2.5% (w/v) DABCO. Slides were left to dry overnight in the dark at room temperature, and then stored at 4°C in the dark. If using glass coverslips, cells were washed four times before 5 µL of Mowiol mounting solution containing 2.5% (w/v) DABCO was added to the slide before coverslips were inverted onto slides. Images were taken using a Leica SP5-AOBS confocal laser scanning microscope attached to a Leica DM I6000 inverted epifluorescence microscope.

2.4 Statistical analysis

Wherever possible, a minimum of three biological repeats were performed for each experiment with the appropriate controls. Quantitative data was expressed as mean +/- SEM and P-values were calculated using the appropriate statistical test, typically a one-way ANOVA with repeated measures, with a Dunnett's multiple comparison post hoc test, unless specified in the Figure legend. A P-value of <0.05 was considered statistically significant. The statistical package PRISM was used for all analyses.

Chapter 3 The HUVEC polarised secretome

3.1 Introduction

Currently, there are few studies that have analysed the proteome of endothelial cells (ECs), and fewer still that have analysed the secretome of ECs [167]. It is well known that ECs are polarised and therefore have different secreted proteins at their apical and basal surfaces; however previous studies have only focused on the entire secreted proteome [167]. Transwell permeable supports enable the separation of apical and basal conditioned media and therefore of the proteins secreted from each surface, allowing them to be individually analysed. This technique allows the user to gain an insight of the difference in the protein secretion from each surface to allow a deeper understanding of the role of ECs.

The polarised secretome of ECs relies on the different intracellular transport mechanisms of vesicles to the cell surface membrane, allowing different proteins and in different amounts to be secreted separately from the apical and basal surface. The apical and basal membrane differ in their lipid and protein composition, allowing the polarised transport and secretion of molecules [168].

Recent studies have focussed on the polarised secretion of fibronectin (FN) in ECs, a glycoprotein involved in the extracellular matrix (ECM) of cells. FN is transported along microtubules to the basolateral surface, where it is then secreted to form part of the ECM in confluent human umbilical vein ECs (HUVEC) [33]. Whilst there has been little data on the regulation of polarised protein secretion by ECs, recent studies have shown that knocking down liprin-α1, a protein involved in microtubule docking at the cell periphery, disrupts the transport of FN to the basolateral surfaces of ECs [35]. To explore the function of liprin-α1, I used siRNA mediated silencing to deplete expression of the protein, to allow an insight in to whether other proteins that are transported to the basolateral surface by this mechanism. The dysregulated secretion of FN is of clinical significance, as it is implicated in diseases such as atherosclerosis [169]. FN is one of the earlier ECM proteins that is deposited at the sites of atherosclerosis plaque sites, and may promote plaque formation [170].

My study used HUVEC, obtained from the major vein of human umbilical cord, which is otherwise discarded after childbirth. These primary cells are the most commonly used ECs when modelling ECs *in vitro,* as in early passages retain their physiological and morphological properties [171]. HUVEC provide an ideal model system, allowing the investigation of many aspects of endothelial function and disease. ECs are involved in a large variety of different functions, such as angiogenesis and blood coagulation, and these processes can, as well as

being viewed under normal conditions, be manipulated to induce disease states for medical research purposes [7].

My research had three objectives

1) To investigate the normal polarised secretome of HUVEC
2) To examine the polarised secretion of FN with liprin-α1 siRNA, to compare results with the study by Mana *et al* (2016) in the paper 'PPFIA1 drives active α5β1 integrin recycling and controls fibronectin fibrillogenesis and vascular morphogenesis'
3) To use liprin-α1 siRNA to decrease expression of liprin-α1 in HUVEC, and to explore whether any proteins of the normal polarised secretome are affected

These investigations will give a deeper insight into the mechanisms involved in EC secretion. The data provided by the mass spectrometry will give insight into other proteins secreted via the same pathway as FN. Like FN, some of these proteins could also be implicated in disease, and the information gained from my study could provide a starting point for further investigations.

3.2 Results

3.2.1 Analysis of the HUVEC secreted proteome

In order to successfully study the polarised secretion of ECs, there needs to be a separation of the apical and basal layer. For all the experiments on the secretion of proteins in my experiments, Transwell inserts are used in order to separate the medium, and therefore the secreted proteins. Transwell inserts are permeable supports, that allow cells to be cultured upon their surface. Small molecules are able to pass through the 0.4 µm pores within the support from the apical surface to the basal media, and vice versa. The pores within the permeable membrane inserts allow protein secretion from the basal surface to pass through to the basal chamber, whilst EC monolayer prevents leakage of apical proteins.

In order to investigate the polarised secretion of protein, mass spectrometry of the conditioned media of the separate apical and basal compartment was performed. These samples were prepared for mass spectrometry by Dr Haoche Wei. The samples were obtained by extracting the media from the upper compartment and transferring to a centrifuge tube, and the same with the media from the lower compartment (Figure 3.1A). The media from the upper compartment was diluted to the same volume as the lower compartment, by the addition of HIFA (Figure 3.1A). The data obtained from this study was then given to me by Dr Wei, for my own analysis.

I firstly analysed this data to gain an initial understanding of the polarised secretion of ECs. I calculated the ratio of apical/basolateral secretion and used a log2 transformation of these values (Figure 3.1B). Proteins which were apically polarised, where a higher amount protein was secreted from the apical surface of the EC than the basolateral surface, would have positive log2 values. Proteins which were basolaterally polarised, where a higher amount of the protein was secreted from the basolateral surface than the apical would have a negative log2 value. I found that the secretion of the majority of proteins within my data were apically polarised.

I performed further analysis of the secreted proteome of HUVEC, by plotting the apical/basolateral ratio of the protein against the P-value (Figure 3.2A). In this analysis, P-values were calculated by comparing the apical/basolateral ratio of protein secretion against the assumption that there was no polarisation, with the value 1. P-values indicate the significance of results, and P-values below a certain value (typically 0.05) are classed as being statistically significant, and therefore the null hypothesis should be rejected. The proteins

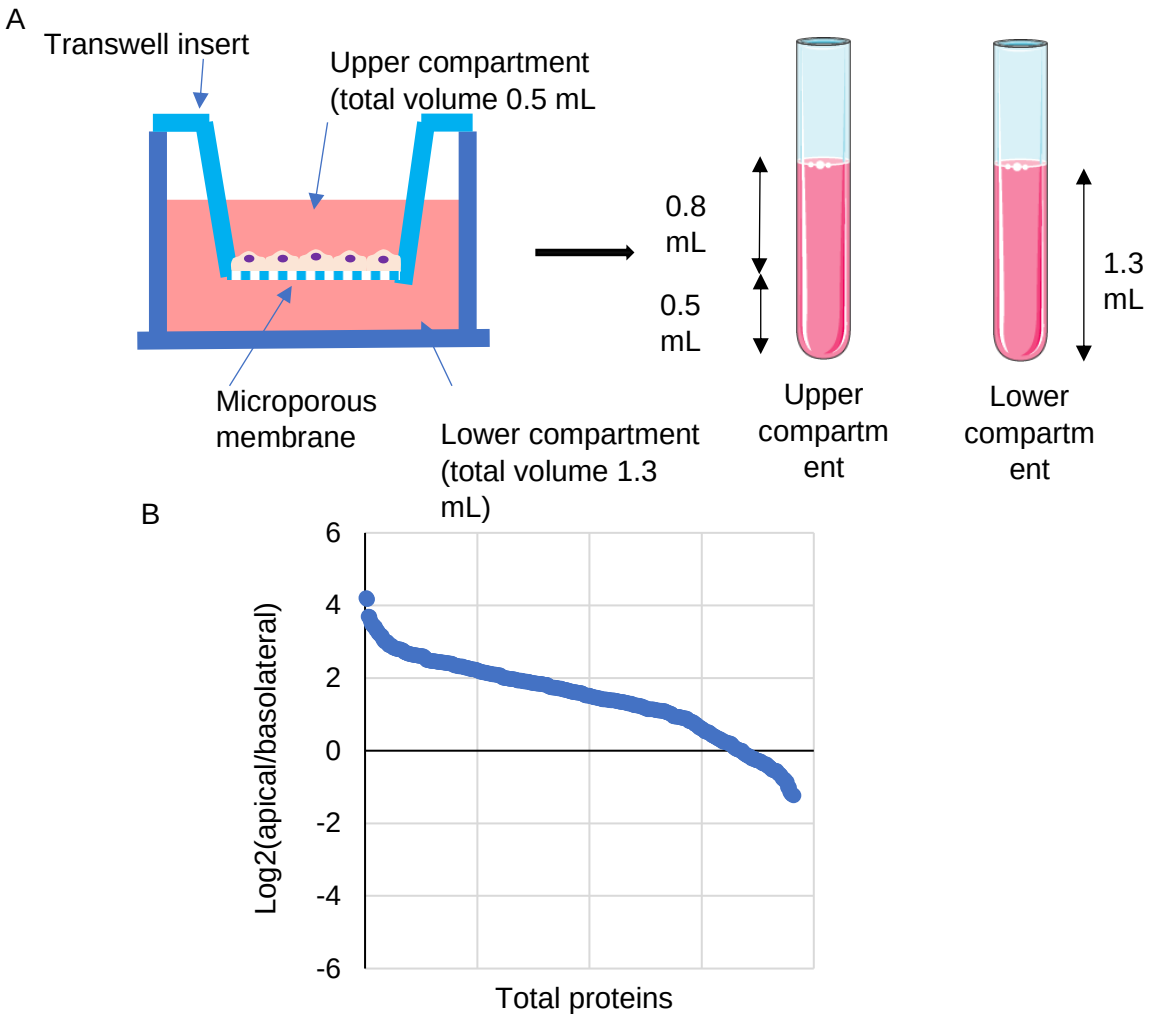

Figure 3.1 Analysis of the HUVEC secreted proteome. A) The media was collected from the upper and lower compartment of the Transwell, and the upper compartment was made up to 1.3 mL using HIFA. The media was then centrifuged using ultra centrifugal filters until concentrated to 50 µL, and then analysed by mass spectrometry. B) The distribution of proteins secreted from the apical membrane and the basal membrane, shown by plotting the data on a log2(apical/basolateral) scale graph. Proteins with a positive log2 value were secreted apically, and proteins with a negative log2 value were secreted from the basal membrane. The majority of the proteins were secreted apically.

A

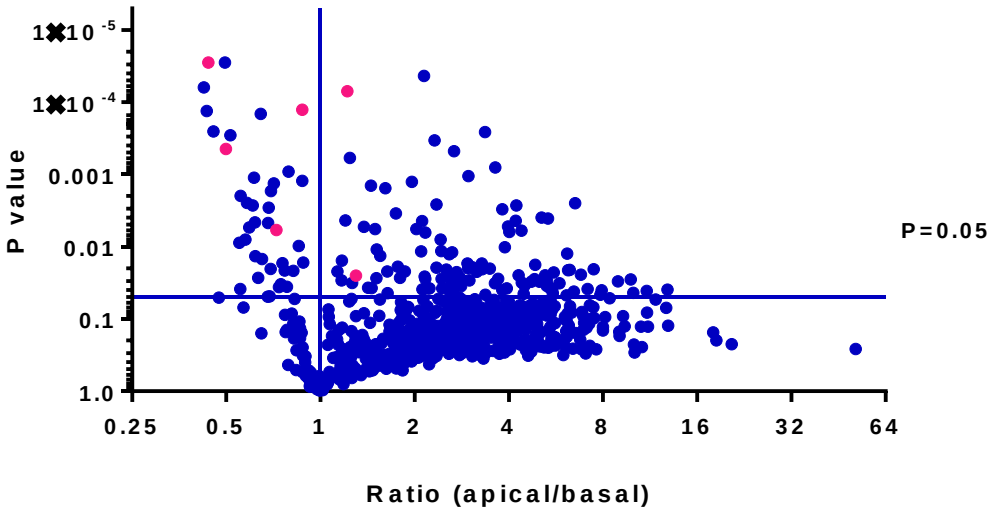

B

Apical < Basal

Gene name	Protein	Ratio (apical/basal)	P-value
COL4A1	Collagen-α1	0.875	0.000126
FBN1	Fibrillin-1	0.723	0.005868
FN1	Fibronectin 1	0.498	0.000441
HSPG2	Perlecan	0.438	0.000028

Apical > Basal

Gene name	Protein	Ratio (apical/basal)	P-value
LAMB1	Laminin subunit γ1	1.297	0.025075
NID1	Nidogen	1.219	0.000070

Figure 3.2 HUVEC display polarised secretion. A) Further analysis of the proteome by volcano plot of the ratio of apical/basolateral against the P-value achieved. Values above 1 on the x-axis are polarised apically, and values below 1 are polarised basolaterally. P-values below 0.05 were considered be statistically significant. Proteins of interest which were known to be secreted and have significant P-values have been highlighted and are marked pink within the graph. B) The table contains known secreted proteins that have been shown to be important from the volcano plot which notably change their polarization with liprin-α1 depletion. The corresponding data point in the volcano plot has been highlighted in pink.

were analysed using UniProt, and those known to be secreted and with significant P-values on the graph were marked pink (Figure 3.2A). The proteins corresponding to these points are shown in Figure 3.2B. The proteins which are polarised basally are generally components of the ECM (Figure 3.2B). The protein collagen α1 is basolaterally polarised with an apical/basolateral ratio of 0.8745, and P-value of 0.00126 (Figure 3.2B). Collagen α1 is a protein which forms part of the ECM, a network of certain proteins that provides structural and biochemical support to the ECs [26]. The other secreted proteins basolaterally polarised include perlecan and FN, which are both other known components of the ECM (Figure 3.2B) [26]. However, other known components of the ECM including nidogen and laminin subunit γ1 are both shown to be polarised apically (Figure 3.2B). My study showed that laminin subunit γ1 had a significant P-value of 0.025075, suggesting it is significantly apically polarised, however other studies have found that laminin is not secreted apically in corneal ECs [172].

From the proteins found to have a significant P-value in the volcano plot in Figure 3.2, these proteins were further analysed to see which proteins were true secreted proteins by analysis using UniProt (Figure 3.3). These proteins were then subdivided into their function and shown in the pie-chart (Figure 3.3A). Almost 70% of the proteins are those involved with the ECM, such as the protein perlecan, a large proteoglycan that is involved in cross linking the ECM and other cell surface molecules [173]. Other secreted proteins with significant P-values include the enzyme lysyl oxidase homolog 2, which is basolaterally polarised. Lysyl oxidase homolog 2 is involved in crosslinking collagen type IV in the basement membrane, and involved in the regulation of angiogenesis [174]. Other secreted proteins were found to be involved in the binding of growth factors, and angiogenesis (Figure 3.3A). The secreted proteins and their corresponding ratios and P-values are shown in Figure 3.3B.

3.2.2 Transfection of HUVEC with Liprin-α1 siRNA can affect monolayer permeability

In order to gain accurate data about the polarised secretion of proteins, the HUVEC monolayer must have high integrity, showing strong cell-cell junctions in order to ensure proteins cannot freely pass between the cells. One way to measure the integrity of the HUVEC monolayer is by the addition of fluorescein isothiocyanate (FITC)-dextran, a fluorescent probe that can pass through the HUVEC monolayer. If the cell-cell junctions of the HUVEC are poor, more FITC-dextran will be able to pass through the monolayer. This means when the fluorescence of the lower compartment is measured by fluorescence absorbance spectrometry, the result will be higher than if the monolayer junctions are well maintained. Ideally, the HUVEC will form a confluent monolayer, as this is most comparable to ECs in a non-diseased state *in vivo*. Also,

A

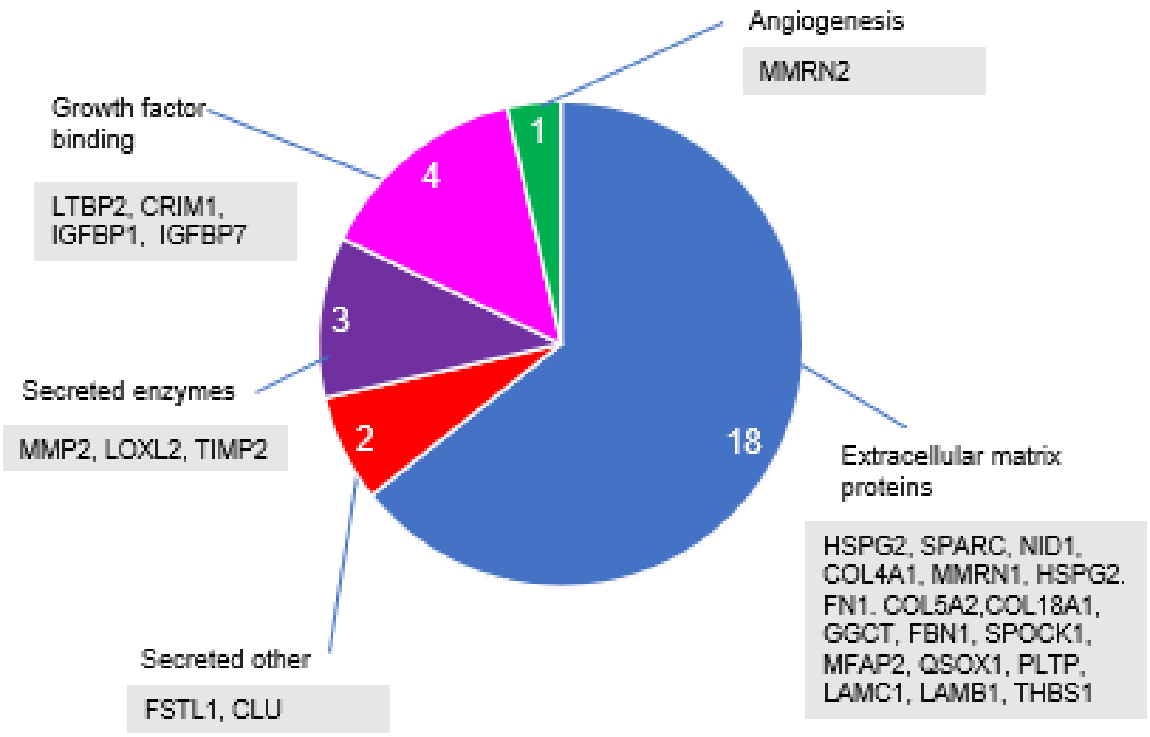

B

Gene name	Protein	Ratio	P-value
HSPG2	Perlecan	0.438333	0.000028
SPARC	Osteonectin	0.495	0.000028
NID1	Nidogen-1	1.219333	0.00007
COL4A1	Collagen alpha-1	0.8745	0.000126
MMRN1	Multimerin-1	0.433	0.000132
FSTL1	Follistatin-related protein	0.644	0.000144
HSPG2	Basement membrane-specific heparan sulphate	0.454333	0.000252
MMP2	Type IV Collagenase	0.515	0.000285
FN1	Fibronectin 1	0.498	0.000441
COL5A2	Collagen alpha-2	0.694	0.001696
TIMP2	Metalloproteinase inhibitor 2	0.555	0.001963
LOXL2	Lysyl oxidase homolog 2	0.581667	0.002475
COL18A1	Collagen alpha-1(XVIII) chain	0.684	0.002869
LTBP2	Latent-transforming growth factor beta-binding protein 2	0.617667	0.004568
CLU	Clusterin	0.591667	0.005375
GGCT	Gamma-glutamylcyclotransferase	1.494	0.005687
FBN1	Fibrillin-1	0.723	0.005868
SPOCK1	Testican-1	0.576	0.007895
MFAP2	Microfibrillar-associated protein 2	0.6185	0.013461
QSOX1	Sulphydryl oxidase	0.650667	0.01469
PLTP	Phospholipid transfer protein	0.7565	0.016825
LAMC1	Laminin subunit gamma-1	1.297	0.025075
CRIM1	Cysteine-rich motor neuron 1 protein	1.508	0.027169
MMRN2	Multimerin-2	1.1685	0.029299
IGFBP7	Insulin-like growth factor-binding protein 7	0.747333	0.032984
LAMB1	Laminin subunit beta-1	1.421	0.036799
THBS1	Thrombospondin-1	0.688667	0.048337
IGFBP4	Insulin-like growth factor-binding protein 4	0.678667	0.049154

Figure 3.3 Function of proteins identified in the HUVEC secretome Analysis of secretome identified using TMT mass spectrometry was performed using UniProt (www.uniprot.org). The table shows the secreted proteins with their corresponding ratios and P-values. P-values<0.05 are included.

the confluent monolayer will reduce the likelihood of proteins being able to diffuse through the cell monolayer, which could cause incorrect polarised secretion values. By exploiting the traits of the Transwell, I was able to effectively measure the permeability of the monolayer. After 48 h of culture on Transwell insert, FITC-dextran was added to the upper chamber of the Transwell (Figure 3.4). Following 24 h after FITC-dextran addition, media was removed from the lower chamber of the Transwell, and the media transferred into a well of the 96 well plate before the fluorescence intensity of the media was read and presented as an absorbance value (Figure 3.4).

My assay found that the permeability of HUVEC was not significantly affected by transfection with liprin-α1 siRNA C or the control siRNA (Figure 3.5A). However, transfection of HUVEC by liprin-α1 siRNA B caused a statistically significant increase in permeability of the HUVEC (Figure 3.5A), with a P-value of 0.0009.

In order to support these permeability values and investigate the integrity of the cell membranes, HUVEC were transfected with liprin-α1 siRNA and seeded onto glass coverslip for 48 h before fixing and staining for ZO-1 and VE-cadherin. ZO-1 is a component of tight junctions, and VE-cadherin of adherens junctions, two of the main junctions in ECs which are important in maintaining vascular integrity [175,176]. In comparison to the control, HUVEC transfected with liprin-α1 siRNA C showed no noticeable difference in the distribution of these proteins (Figure 3.5B). Using the data gained in this experiment, as well as the permeability data in the liprin-α1 siRNAs (Figure 3.5A), I was able to confidently use liprin-α1 siRNA C for the mass spectrometry experiments as it did not have a significant effect on the permeability.

3.2.3 Liprin-α1 controls the sorting of a subset of proteins to the basolateral surface

Liprin-α1 is a part of the cortical microtubule stabilising complex, which localises microtubules to focal adhesions. Mana *et al* (2016), showed that the protein PPFIA1, which is also known as liprin-α1 was responsible for the recycling of the integrin α5β1. This integrin is trafficked with FN, a protein which forms part of the ECM, suggesting that liprin-α1 is involved in the trafficking of FN to the basolateral surface of the cell. Mana *et al* (2016) showed that by suppressing the expression of liprin-α1 the secretion of ED-A FN, the endogenous FN secreted by ECs, is severely impaired [35].

A key stage in the formation of an atherosclerotic plaque is the expansion of the ECM, and FN is one of the earliest proteins deposited at the atherosclerosis-prone region [177]. Elevated

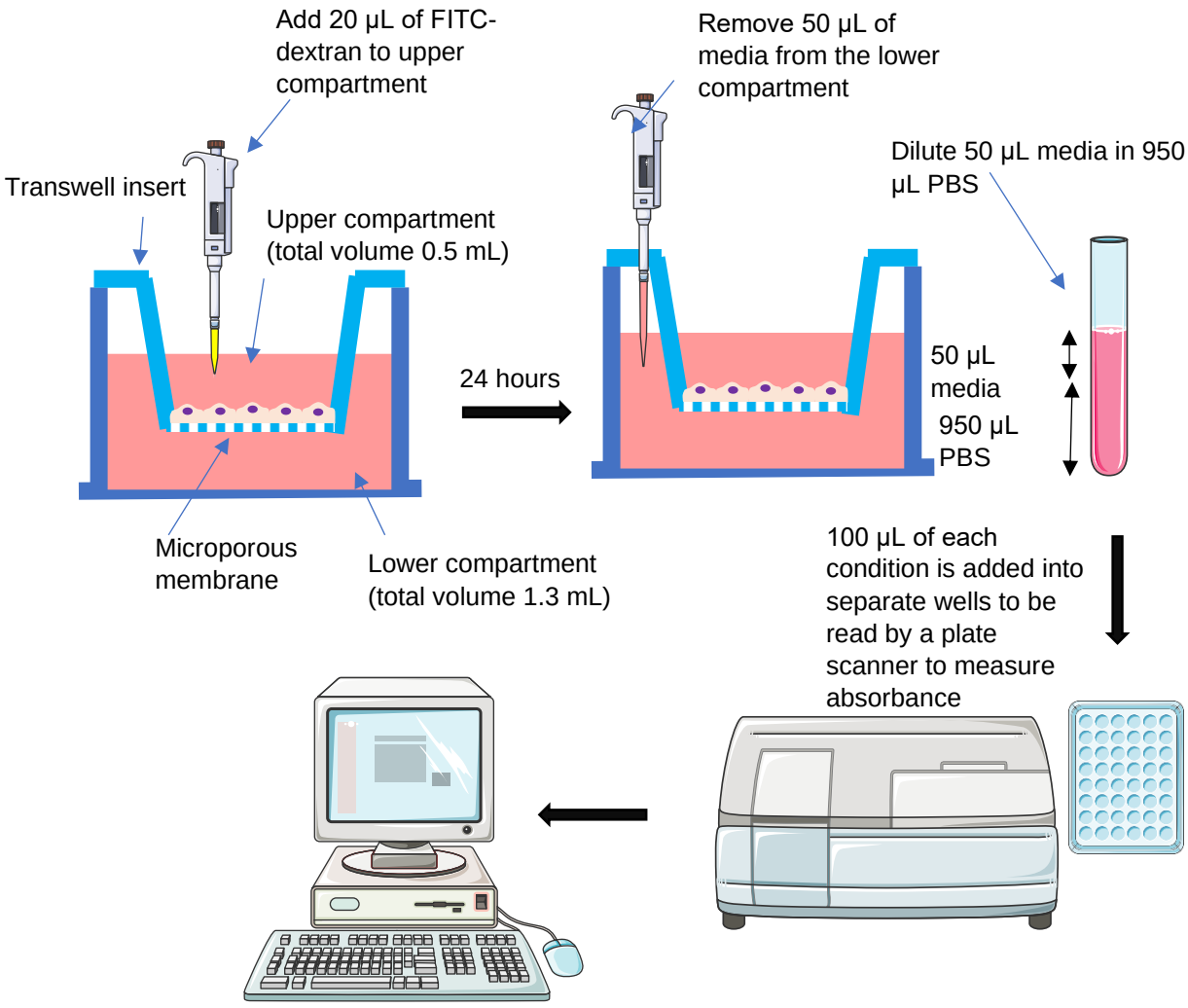

Figure 3.4 Method of obtaining permeability data. After being cultured for 48 hours on Transwell inserts, 20 µL of FITC-dextran is added to the upper compartment of the Transwell insert. 24 hours after addition, 50 µL of media from the lower compartment is diluted in 950 µL PBS. 100 µL of this solution is added into a well of the 96 well plate, of which the fluorescence intensity is measured, which outputs absorbance values.

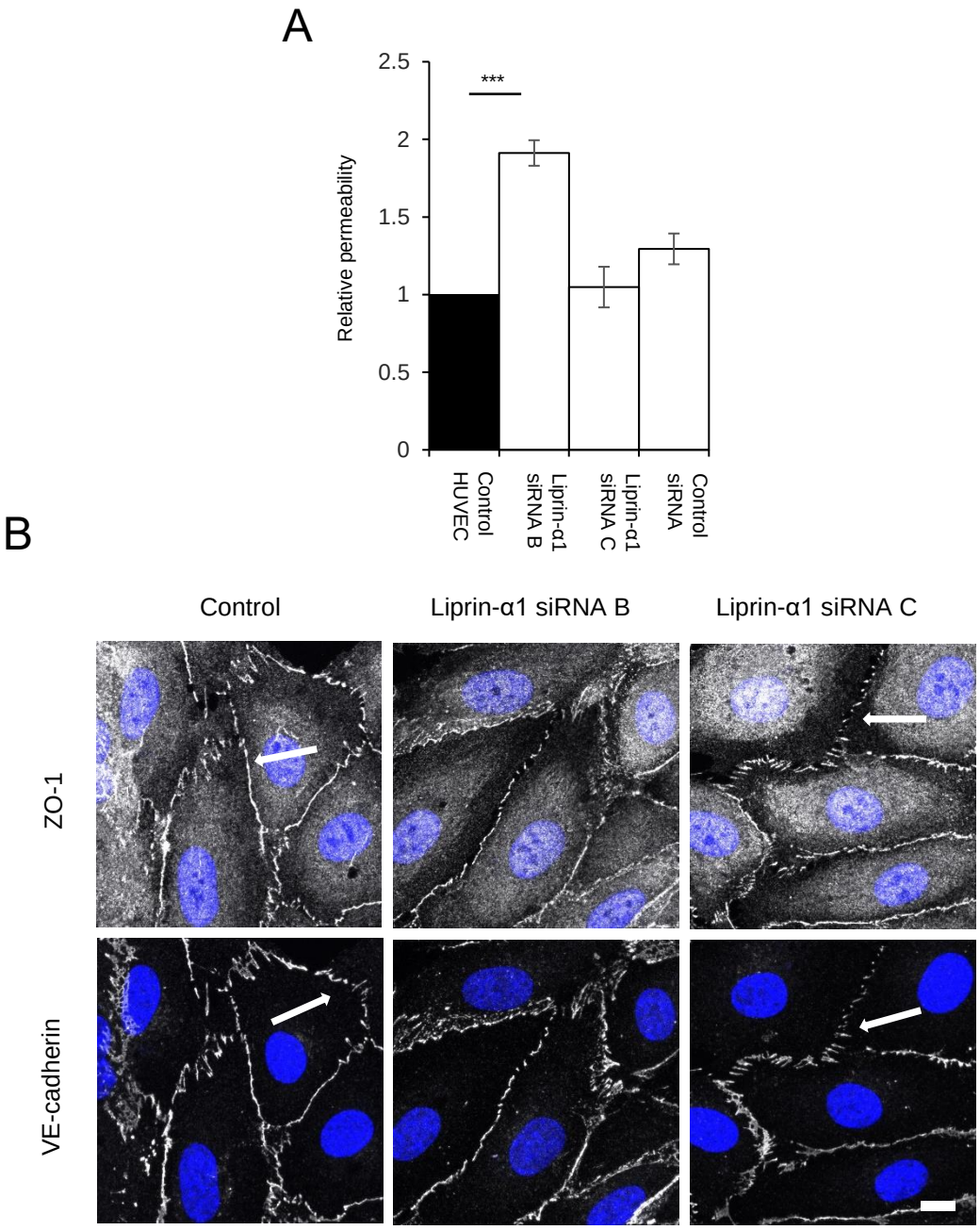

Figure 3.5 Liprin-α1 siRNAcan affect HUVEC monolayer A) Liprin-α1 siRNA C showed no significant difference in permeability compared to the control, whilst siRNA B showed a statistically significant difference (P-value = 0.0009). Permeability experiments were performed by culturing transfected HUVEC onto Transwell inserts for 48 hours, before adding FITC-dextran to the apical compartment. The fluorescence absorbance of the media from the lower compartment was measured after 24 hours. Statistical analysis performed using a one-way ANOVA and Dunnett's multiple comparison post hoc test and P-values below 0.05 were considered to be statistically significant. Graphs are plotted as means ± SEM (n=4), and data is normalised to the control. B) Liprin-α1 siRNA were transfected 24 h prior to seeding onto coverslips, and control mock transfected HUVEC were seeded at the same time. After a further 48 h the cells were fixed and stained for ZO-1 and VE-cadherin. Cells were then imaged using confocal microscopy. Liprin-α1 siRNA transfected cells show a slight difference in ZO-1 and VE-cadherin distribution in comparison to the control, especially liprin-α1 B. Arrows show differences in distribution of ZO-1 and VE-cadherin between control and liprin-α1 sirRNA C. Scale bar = 10 μm.

levels of FN have been found in atherosclerotic regions [169]. ED-A FN, a variant of FN that contains an extra A domain, is a form of FN has been suggested to support atherogenesis, the formation of arterial fat deposits, and high levels of ED-A FN are seen during atherosclerosis [169]. Impaired blood flow, which occurs in plaque formation causes the deposition of FN by ECs into the vessel wall [169]. As one of the leading causes of death in the western world, this disease and its contributing factors, including FN deposition are of high clinical importance [169,178]. High levels of ED-A FN are seen in the plasma samples of patients at high risk of developing coronary artery disease, including atherosclerosis compared with the low levels seen in patients at low risk, and this high level is believed to be involved in inflammation and disease progression [177].

Figure 3.6A shows the mechanism of FN trafficking from the synthesis of FN dimers in the trans-Golgi network (TGN) to the basolateral membrane. Upon leaving the TGN, FN dimers are transported to trans Golgi carriers, associated with the integrin α5β1 to the cell membrane where it is exocytosed (Figure 3.6A). Liprin-α1 is an adaptor protein that forms part of the cortical microtubule stabilising complex, which is involved in the tethering of microtubules to the membrane and localises them close to focal adhesions (Figure 3.6B).

To further explore the function of liprin-α1, siRNA mediated silencing was used to decrease expression of liprin-α1. HUVEC were cultured and transfected with liprin-α1 siRNA. Figure 3.7A shows a Western blot of the expression of liprin-α1 within the HUVEC. Each of the liprin-α1 oligonucleotide duplexes gave significant depletion of the protein, with liprin-α1 siRNA B and liprin-α1 siRNA C showing the highest depletion at 97% (Figure 3.7A). These two siRNAs were then used for subsequent experiments.

Following on from the study by Mana *et al* (2016), I analysed the effect of liprin-α1 depletion on the secretion of FN using ELISA. By culturing liprin-α1 siRNA transfected HUVEC on Transwell polyester membrane inserts, the apical and basolateral conditioned medium, and therefore the polarised secretion of ED-A FN could be separated. My data showed that, supporting the data by Mana *et al* (2016), the suppression of liprin-α1 led to the decreased basolateral secretion of FN (Figure 3.7B). I showed that the basolateral secretion of ED-A FN was strongly impaired by the depletion of liprin-α1, however, the apical secretion is not affected in confluent cultured HUVEC (Figure 3.7B). This result was also seen by Mana *et al* (2016) in their ELISA.

To investigate whether the depletion of liprin-α1 affected any other proteins, I used mass spectrometry. Transfected HUVEC were cultured on Transwell inserts for 48 hours, then the apical and basal condition media was removed and prepared for mass spectrometry. Liprin-α1 siRNA C was selected for use in mass spectrometry, due to its high successful depletion

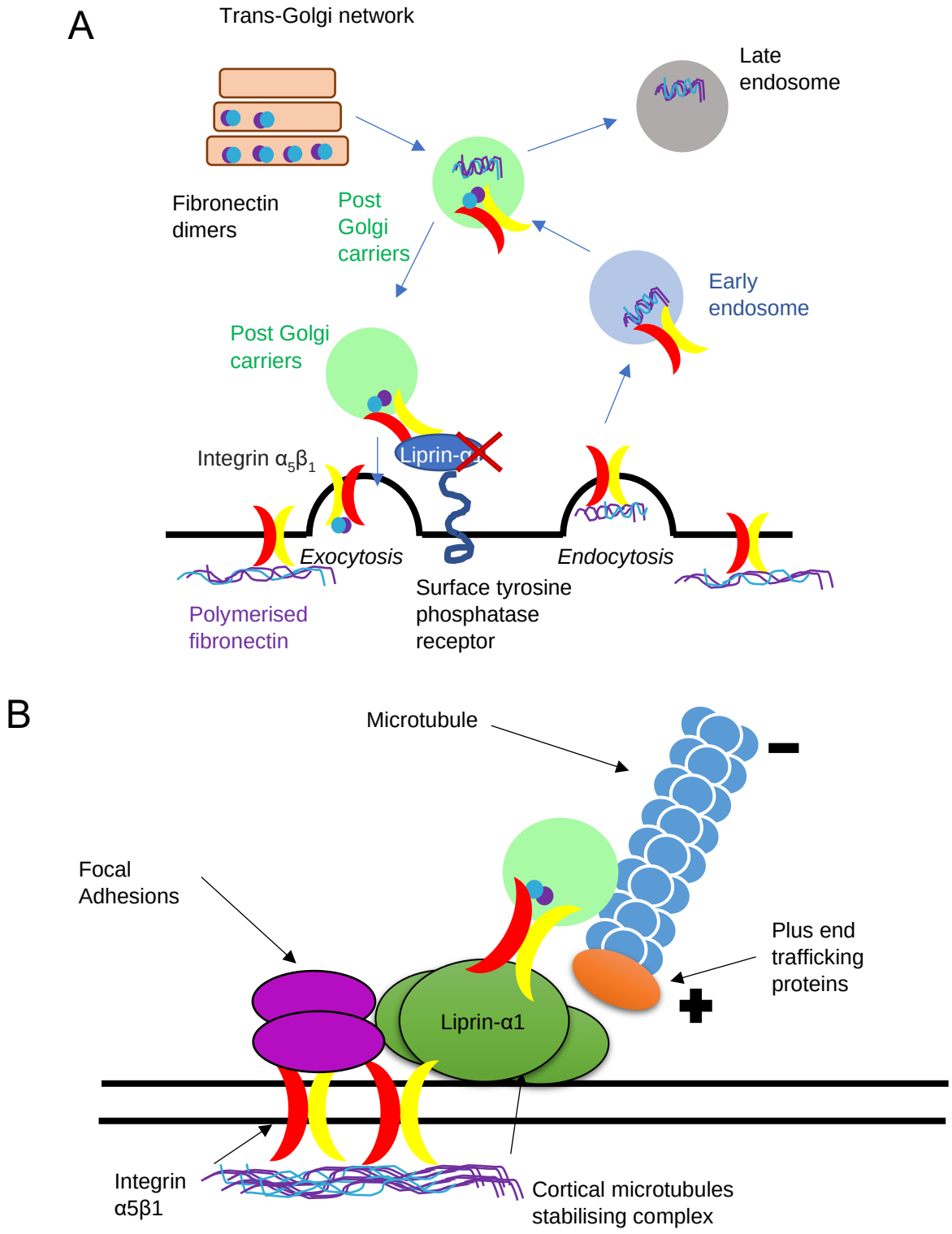

Figure 3.6 Liprin-α1 localises to focal adhesions, by binding directly to the β1 tail of integrins. A) Mechanism of fibronectin transport to the basolateral surface of ECs. Figure adapted from supplementary figure by Mana *et al* (2016). B) Liprin-α1 forms part of the microtubule stabilising complex to anchor microtubules at the basolateral surface. Figure adapted from Garcin and Straube (2019).

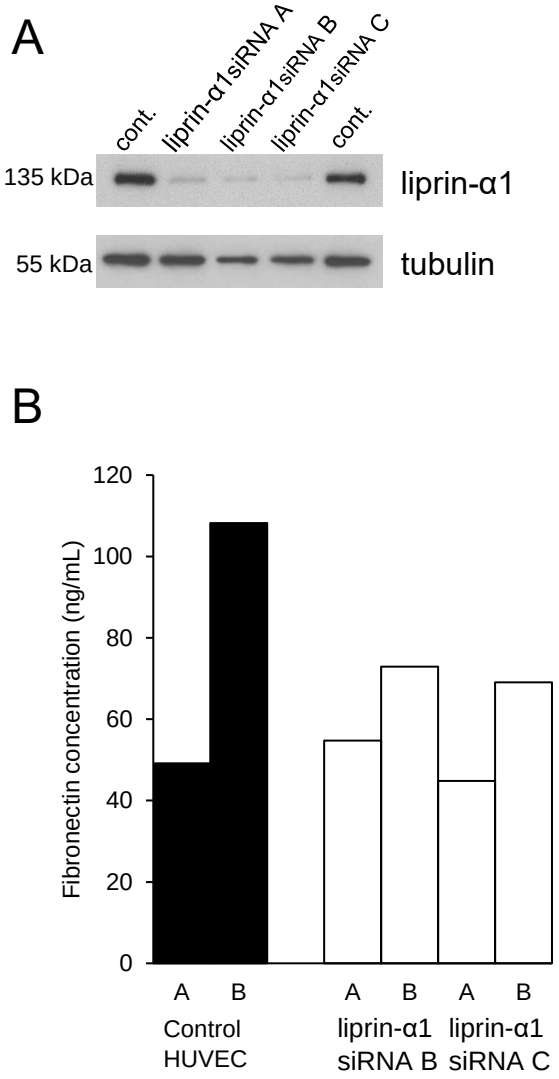

Figure 3.7 Liprin-α1 affects the polarised secretion of fibronectin from the basolateral surface. A) Liprin-α1 siRNA showed significant depletion of liprin-α1 (94%, 97% and 97% respectively) in comparison to the control. Analysis was performed 48 hours after transfection of HUVEC using western blot, and silencing calculated using ImageJ. B) The literature showed that Liprin-α1 siRNA decreased the polarised secretion of fibronectin from the basolateral surface, and analysis of fibronectin secretion was performed using ELISA. Control HUVEC were seeded directly onto Transwell inserts. Liprin-α1 siRNA B and C HUVEC were transfected before seeding onto Transwell inserts. Media from the upper and lower compartment of the Transwell insert was collected from each of the conditions and analysed using ELISA. A – Apical secretion, B – Basolateral secretion. The silencing of liprin-α1 using siRNA was shown to strongly decrease the secretion of fibronectin in the basolateral secreted media of the siRNA transfected HUVEC in comparison to the control HUVEC, with little effect on the apical secretion.

of liprin-α1 in HUVEC. Generally, the depletion of liprin-α1 by siRNA did not affect the polarised secretion of proteins (Figure 3.8A). R^2 values are a statistical measure of how well the data fits a regression line, with a higher R^2 value meaning that a high amount of the secreted proteins in the liprin-α1 siRNA transfected HUVEC sample show the same secretion ratio as the proteins in the control HUVEC, and a lower R^2 value showing that few of the secreted proteins in the liprin-α1 siRNA transfected HUVEC show the same secretion ratio as the secreted proteins within control HUVEC. With an R^2 value of 0.7691, the relationship between the control HUVEC and liprin-α1 siRNA transfected HUVEC shows a strong correlation between the ratio of proteins secreted both by liprin-α1 siRNA transfected HUVEC and control HUVEC, showing generally liprin-α1 does not control secretion of proteins from the basolateral membrane (Figure 3.8A). Particular proteins affected by the depletion of liprin-α1 are highlighted in pink in Figure 3.8A, and their corresponding ratio for both the control HUVEC and liprin-α1 siRNA transfected HUVEC are shown in Figure 3.8B. Most of the proteins which are affected by liprin-α1 siRNA transfection are proteins which are secreted basolaterally by ECs into the ECM, including collagen I α1 and α2, and nidogen-1. In the control HUVEC, these proteins were apically polarised, whilst in the liprin-α1 transfected siRNA these became more basolaterally polarised. This data conflicts current understanding of these proteins, as previous studies have found these proteins were secreted into the ECM [31]. However, the control sample only had one repeat, in comparison to the three repeats of the liprin-α1 siRNA transfected HUVEC, meaning any differences between the control samples could not be seen and a mean could not be taken. To verify this further, a repeat of the mass spectrometry with more samples of the control would need to be performed. Included in the table in Figure 3.8B are the ratios of FN, both in the control and in the liprin-α1 siRNA transfected HUVEC, which is highlighted in yellow in Figure 3.8A. Compared to the data obtained by my ELISA (Figure 3.7B) where the basolateral secretion of FN decreased noticeably, the change shown in my mass spectrometry is not as noticeable.

3.2.4 Liprin-α1 siRNA transfection of HUVEC does not affect the distribution of EDA-FN when analysed using mass spectrometry

The current evidence from my study provides differing results on the secretion of FN in liprin-α1 siRNA transfected HUVEC. My ELISA data supports the paper by Mana *et al* (2016), and my mass spectrometry data showed that the secretion of FN becomes slightly more apically polarised with the depletion of liprin-α1. However, mass spectrometry analysis only provides an estimation of the apical/basolateral ratio, rather than the actual concentration. In order to

A

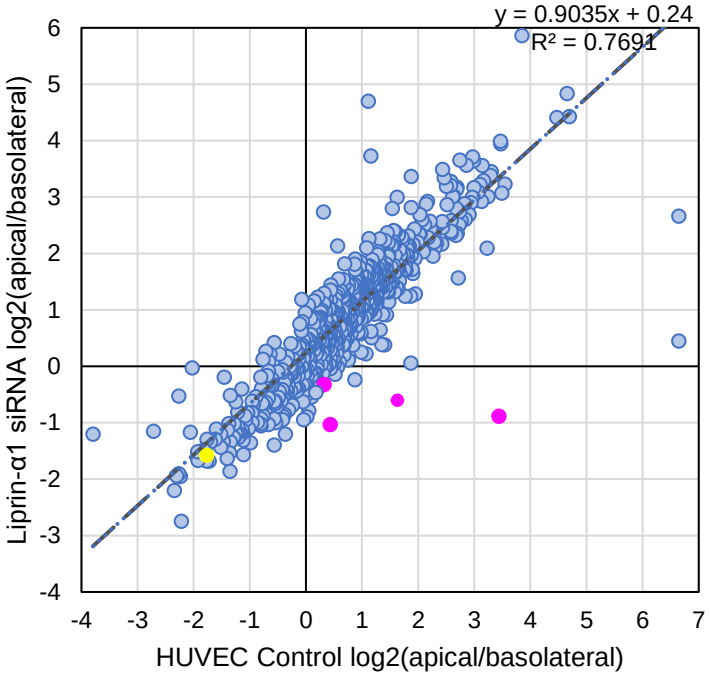

B

Gene name	Description	Apical /basolateral ratio control	Apical/ basolateral ratio liprin-α1 depletion
COL4A1	Collagen I α1	10.877	0.540
COL1A2	Collagen I α2	3.109	0.659
ECAM-1	Epithelial cell adhesion molecule-1	1.353	0.487
NID1	Nidogen-1	1.016	0.710
FN1	Fibronectin	0.293	0.312

Figure 3.8 Liprin-α1 siRNA affects the polarised secretion of certain proteins. A) The apical/basolateral ratio of the control HUVEC were calculated, and log2 values were plotted against the Liprin-α1 silenced apical/basolateral log2 values. An R^2 value is a measure of how well the data fits the regression line, and an R^2 value of 0.7691 shows a moderate positive correlation between the two conditions, suggesting that Liprin-α1 knockdown does not affect the polarised secretion of all proteins. However, there a few proteins which are affected, with highlights included in the table below. Fibronectin, the secretion of which has previously shown to be affected by liprin-α1 silencing is highlighted in yellow, as the mass spectrometry data found secretion became slightly more apical in the polarised secretion of fibronectin. B) The table compares the ratio of the secretion of particular proteins, and the change liprin-α1 silencing has on the secretion. A value above 1 means the protein is secreted more apically than basally, and a value below 1 means a protein is secreted more basally than apically. These proteins were highlighted as they are known secreted proteins and show a considerable difference in their secretion with Liprin-α1 knockdown. The ratio of fibronectin is also shown in the table, to show there was a small difference in the mass spectrometry of the polarised secretion, becoming slightly more apically polarised.

try and elucidate the true effect of liprin-α1 silencing on the secretion of FN, HUVEC were transfected with liprin-α1 siRNA and seeded onto glass coverslips, before fixing and staining for ED-A FN. The distribution of ED-A FN is similar whether transfected with control siRNA and liprin-α1 siRNA, suggesting that the depletion of liprin-α1 does not affect EC secretion of ED-A FN (Figure 3.9). This conflicts with the study by Mana *et al* (2016), which showed using immunofluorescence the secretion of ED-A FN is decreased with liprin-α1 silencing [35].

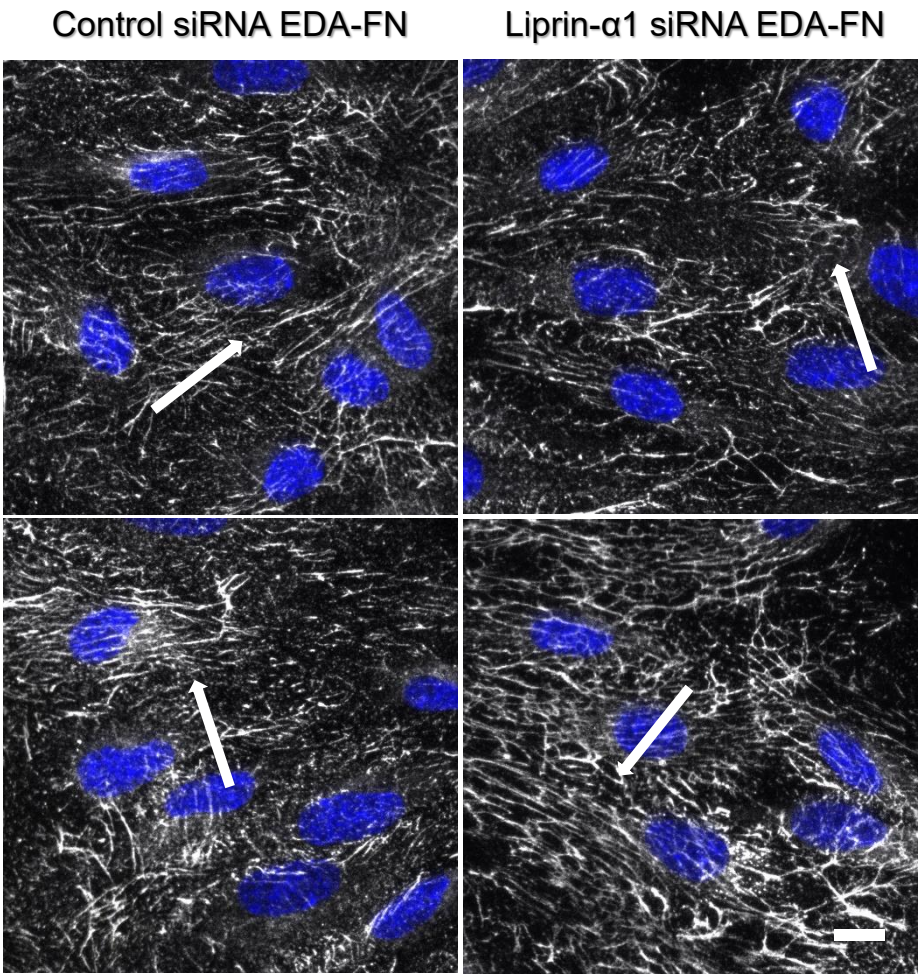

Figure 3.9 Liprin-α1 has no effect on the secretion and distribution of EDA fibronectin. A) HUVEC were transfected using siRNA and grown on coverslips for 48 hours, before fixing and staining for EDA-fibronectin. Cells were then imaged using confocal microscopy. There was no noticeable difference in the secretion of EDA-FN between either of the conditions. Similar observed densities are shown with white arrows. Scale bar = 10 μm.

3.3 Conclusion

Whilst polarised secretion of ECs is essential to their function, the mechanisms by which this sorting occurs is poorly understood. Throughout my study, I aimed to examine the role of the liprin-α1 in the basolateral secretion of proteins, as it had previously been shown to be involved in the targeted secretion of fibronectin [35].

Initially I analysed the polarised secretome of HUVEC, which showed that secreted proteins were mainly apically polarised. Using statistical analyses (one-way ANOVA and Dunnetts post hoc test) to generate P-values, I examined the secretome and found that the majority of proteins with statistically significant P-values were basolaterally polarised proteins involved in the ECM, such as perlecan and collagen α1. My analysis showed there are differences in the roles of proteins secreted from the apical and basolateral surface of ECs, with the secretion of ECM proteins significantly polarised to the basolateral surface of ECs.

After analysing the normal polarised secretome of HUVEC, I investigated the polarised secretome of HUVEC where I had silenced the expression of liprin-α1. I initially investigated whether depleting liprin-α1 expression using siRNA in HUVEC affected the integrity of the HUVEC monolayer.

In a non-disease state, HUVEC form a continuous cobblestone-like monolayer which lines the lumen of blood vessels. This monolayer acts as a selective barrier to the passage of solutes between the blood and the underlying tissue, whilst allowing essential small molecules such as ions, nutrients and water to flow across [179]. HUVEC are commonly used in experimental systems, due to their ability to form the so-called cobblestone phenotype, mimicking the *in vivo* phenotype of ECs [180].

After isolation from umbilical veins, HUVEC can be propagated by using endothelial specific media, supplements [180]. Coating of the membrane HUVEC are grown upon in ECM components such as collagen and fibronectin, promotes EC attachment [181]. During cell culture HUVEC form the characteristic markers of ECs, such as the polygonal shape, and tight and adherens junctions, responsible for integrity of the monolayer. A study by Jiménez *et al* (2013) showed that HUVEC cultured on ECM components form a tight monolayer, replicative of the human umbilical vein endothelium *in vivo* [180].

The integrity of the EC monolayer in *vitro* can be measured by several different methods, including by Transwell permeability assays. In this study, the passage of 70 kDa FITC-conjugated dextran was used to measure the monolayer integrity, which has been used in multiple studies in the literature [179]. FITC-dextran was added to the upper chamber of the Transwell, and after 24 hours a sample was removed from the lower chamber, and the

absorbance was read in a fluorometer. The more permeable the HUVEC monolayer, the higher the absorbance of the media from the lower chamber will be. In this study, the HUVEC monolayer after treatment, by either siRNA or statin was compared a control HUVEC monolayer. For each independent experiment, the raw control monolayer absorbance was given the value 1, with the treated HUVEC absorbance value calculated relative to this. To support my analysis of the absorbance values, I also used immunofluorescence microscopy to stain for ZO-1 and VE-cadherin, both markers of endothelial cell-cell junctions. As well as measuring the absorbance of a control HUVEC monolayer, I could also have measured the passage of FITC-dextran across a blank Transwell insert. This would allow me to know the maximum value of transmission and allow me to be more confident with my HUVEC monolayer values showing integrity.

Another method which could be used to investigate membrane integrity is by measuring the transendothelial electrical resistance (TEER). When HUVEC have formed a tight monolayer, they should resist the passage of electrical current, and provide a quick and real time evaluation of the monolayer [182]. The resistance of the can be measured with an ohmmeter, and a calculation can provide an integrity value [182]. Unlike when using FITC-dextran, where HUVEC were discarded after the media from the lower chamber was removed, using the non-invasive TEER method would allow me to continue to use the cells in the same experiment. This would have been especially effective for my mass spectrometry experiments, as I did not know the integrity of the monolayer which may have had a direct impact upon my results. By using a TEER value, I would have known the integrity of my monolayer, which would have allowed me to be more confident in my results.

If the monolayer was disrupted, proteins may be allowed to pass between gaps in the cell-cell junctions to the opposite media, meaning I would be unable to identify whether proteins were apically or basolaterally secreted. By performing both permeability assays and confocal microscopy I was able to select the liprin-α1 siRNA that affected the HUVEC monolayer the least, as shown by a lower level of FITC-dextran permeability.

To measure the efficiency of my siRNA as depleting liprin-α1, I used a Western blot, with tubulin as a loading control. The purpose of a loading control is to indicate an equal loading of samples. However, liprin-α1 is involved in stabilising microtubules, which are formed of tubulin. Therefore, it is possible that the use of liprin-α1 affected the levels of tubulin inside my HUVEC, and therefore would appear as different intensities in my Western blot. In my Western blot (Fig 3.7A), the level of tubulin appears decreased when HUVEC were treated liprin-α1 siRNA. This means the assumption that the siRNA was effective at depleting the expression of liprin-α1 at up to 97% may be inaccurate, as the tubulin levels appear different. Therefore, I cannot be

confident that the siRNA reduced the expression of liprin-α1 by levels of up to 97%, or whether a loading error between the controls and the siRNA occurred. In future experiments, another loading control such as calnexin could be used to ensure the effect on liprin-α1 levels is solely caused by the effects of the siRNA.

I demonstrated in my ELISA, as in the study by Mana *et al* (2016), the basolateral secretion of fibronectin (FN) decreased with the depletion of liprin-α1 [35].

To investigate this further, I used mass spectrometry to find out the apical/basolateral ratio of secreted protein. Liquid chromatography with tandem mass spectrometry, followed by database interrogation is a common bioanalytical technique which is able to identify peptides, and their relative abundances within a sample [183]. Proteins are identified by matching their observed spectra to the predicted spectra of that protein. My mass spectrometry assay had peptide precursor mass tolerance at 10 ppm, meaning that if my precursor peak was not with 0.01 Da of the theoretical mass, the sequence was not accepted, and disregarded in the analysis. This is to reduce the possibility of false positive errors, which can result in false protein identification [183]. My mass spectrometry also had a MS/MS tolerance of 0.6 Da, which allows for errors in the masses detected by the instrument, and values which do not fall within the limit are again excluded. However, some of the excluded values may in fact be correct, whilst other identified as correct, may still be false positives. These can lead to discrepancies between data, especially when performing multiple repeats. My experimental design also accounted for other possible differences, such as post-translational modifications, but there is still the possibility of false data. Differences in the data can also occur for other reasons, such as differences in preparation or loading of the samples, or contamination by foreign bodies.

The mass spectrometry data obtained in this study is n=1, with three technical repeats in each. This means that the secretion of some proteins may have been falsely identified as being affected by the depletion of liprin-α1, whilst other important proteins may have been overlooked. This means I cannot draw any clear conclusion from my analysis. By having three separate biological repeats of the mass spectrometry analysis and comparing the results, the chance of these errors occurring would be reduced, as I would be able to identify any anomalous results. This would improve the validity and accuracy of my results, meaning that they could be used to investigate other mechanisms of polarised secretion in ECs.

I found that the ratio of apical/basolateral secretion increased when liprin-α1 expression was depleted, further supporting the study by Mana *et al*. As well as this, mass spectrometry provided me with data that showed that depletion of liprin-α1 affected the sorting and delivery of a subset of proteins to the basolateral surface. These proteins included nidogen-1, collagen

α1 and collagen α2, which are components of the ECM. I found that these proteins became more basolaterally polarised with the depletion of liprin-α1, which could potentially be due to the cell being aware of the reduction of FN secretion, and therefore increasing the basolateral secretion of these proteins. However, I found that many other basolaterally secreted proteins were not affected by liprin-α1, showing there are other mechanisms of polarised trafficking other than the mechanism using liprin-α1.

Whilst dysregulated secretion of FN is a known contributing factor in atherosclerosis, one major aim of this research was to discover the other proteins involved [184]. This research has provided the background for further investigations of the proteins highlighted in the mass spectrometry data, to further elucidate the full role of EC dysregulation in disease.

Chapter 4 Effect of statin treatment on HUVEC

4.1 Introduction

Cardiovascular disease (CVD), comprising of strokes, angina and heart attacks, is the leading cause of mortality in the world, attributed to over a quarter of global deaths [178,185]. One major risk factor for CVD events is high blood cholesterol, and therefore reducing cholesterol levels is of clinical importance. Statins are the first choice of treatment for reducing blood cholesterol and are one of the most commonly prescribed drug within the UK health system [186]. Statins act by inhibiting the enzyme HMG-CoA reductase, a rate-limiting enzyme involved in the cholesterol synthesis pathway, therefore reducing the production of cholesterol. Statins are structurally similar to HMG-CoA, the biological substrate for rate-limiting enzyme HMG-CoA reductase, so act by competitive inhibition [166]. This inhibition reduces the ability of HMG-CoA to produce mevalonate, the next molecule in the cholesterol cascade [166]. Most of the circulating cholesterol in the body is produced internally by the liver via the cholesterol synthesis pathway, rather than from the diet. This in turn reduces the levels of blood cholesterol, and thus reduces the risk of CVD events. As well as directly affecting HMG-CoA reductase in the liver, statins have also been shown to have pleiotropic effects, including on the vascular endothelium. Previous studies have suggested that statins can affect endothelium vascular tone, and can inhibit inflammatory responses [187]. By inhibition of the HMG-CoA reductase pathway, statins also inhibit specific prenylation, the addition of hydrophobic prenyl group involving either farnesyltransferase or geranylgeranyl transferase, and the prenylation of Rab proteins which may be responsible for the other biological effects seen by statins [166]p.

The aim of this work was to investigate the pleiotropic effects of statins, by performing mass spectrometry on the HUVEC polarised secretome after statin treatment.

In order to gain accurate results from the mass spectrometry, it was necessary to ensure that the permeability of the ECs was not negatively affected by the statin treatment. If this was the case, and the ECs had leaky junctions I could not know whether proteins were truly secreted by the apical or basolateral membranes, as proteins may pass through the permeable layer.

Therefore, I performed permeability assays at various concentrations, as well as confocal imaging of VE-cadherin and ZO-1; two proteins involved in the formation of different cell-cell junctions. VE-cadherin is an endothelial specific adhesion molecule, and is a main component of adherens junctions [188]. ZO-1 is tight junction-associated protein, and the integrity of both these junctions are a marker for endothelial junction integrity [189]. This is important when studying the polarised secretome, to ensure secreted proteins cannot pass between cells to the opposite surface.

The data from these studies allows a therapeutic plasma value of statin treatment to be selected, to perform mass spectrometry which has clinical significance.

This research had three objectives:

1) To investigate whether statins treatment affects the monolayer formation of HUVEC, by performing permeability assays using FITC-dextran, and immunofluorescence, to quantitatively measure the permeability of the HUVEC monolayer, and to visually assess the cell junctions respectively
2) To use the data obtained from the first objective to choose the appropriate concentrations of statin to perform mass spectrometry of the HUVEC secreted proteome
3) To analyse the secretome provided by mass spectrometry, and examine whether the secretion of any important proteins change after statin treatment

With statins being one of the most commonly prescribed drug in the UK, further studies into the off-target effect of these drugs is of great importance to the health system and may indicate other disease conditions that statins may have therapeutic potential for.

4.2 Results

4.2.1 Measurement of the effect of statins on endothelial permeability

Two of the most commonly prescribed statins with the UK are atorvastatin, and simvastatin. The NICE guidelines recommend that 20 mg atorvastatin daily should be offered to people with a 10% or greater risk of developing CVD within the next 10 years [190]. In people who already have pre-existing CVD, for example a previous stroke or heart attack, 80 mg atorvastatin is recommended daily dose. Atorvastatin has a higher potency than simvastatin, with the cholesterol lowering effects of atorvastatin at a 10 mg dose, being equal to those observed in simvastatin at 40 mg dose [190]. At doses between 20-80 mg daily of atorvastatin, and 80 mg simvastatin are classed as 'high-intensity' statins, reducing more than 40% of cholesterol production.

I started by researching the concentrations of atorvastatin and simvastatin used in previous biochemical studies of statin functions [191,192]. Based on these previous experiments, I used both atorvastatin and simvastatin dissolved in DMSO at 0.2 µM, 1 µM and 5 µM, along with a vehicle control of DMSO to ensure any effects on the cells were as a direct result of the statins. HUVEC were cultured at $1x10^5$/mL onto Transwell inserts in EGM-2, before refreshing with HIFA media after 24 hours. This method of Transwell cell culture had been optimised by previously by my laboratory group, as it had been shown to support the formation of a confluent monolayer. At the same time as refreshing with HIFA media, statins were added, and then added again after 24 hours at the concentrations shown. By using the FITC-dextran permeability assay as described in 3.2.2, I could effectively measure the permeability of the monolayer. Figure 4.1A shows that the addition of simvastatin at these concentrations showed increasing permeability with increasing concentrations of statins. However, this increase in permeability was not found to be statistically significant. To investigate this further, HUVEC were cultured on coverslips, and the simvastatin was applied at the same concentration as before, before fixing and staining. Cells were also counterstained with DAPI, in order to visualise their nuclei. As the concentration of simvastatin increases (Figure 4.1B), the junctions appear to become weaker, however HUVEC are still shown to form junctions, even at 5 µM. At 0.2 µM, the junctions appear similar the control (Figure 4B), especially in the distribution of

ZO-1. However, at 1 µM and 5 µM the junctions appear to be thinner than compared to the control (4.1B). This supports the permeability data that simvastatin at these concentrations, whilst affecting the EC monolayer, did not significantly affect the EC monolayer. Thus, I can be satisfied that at 0.2 µM, statins did not significantly affect the formation of the HUVEC

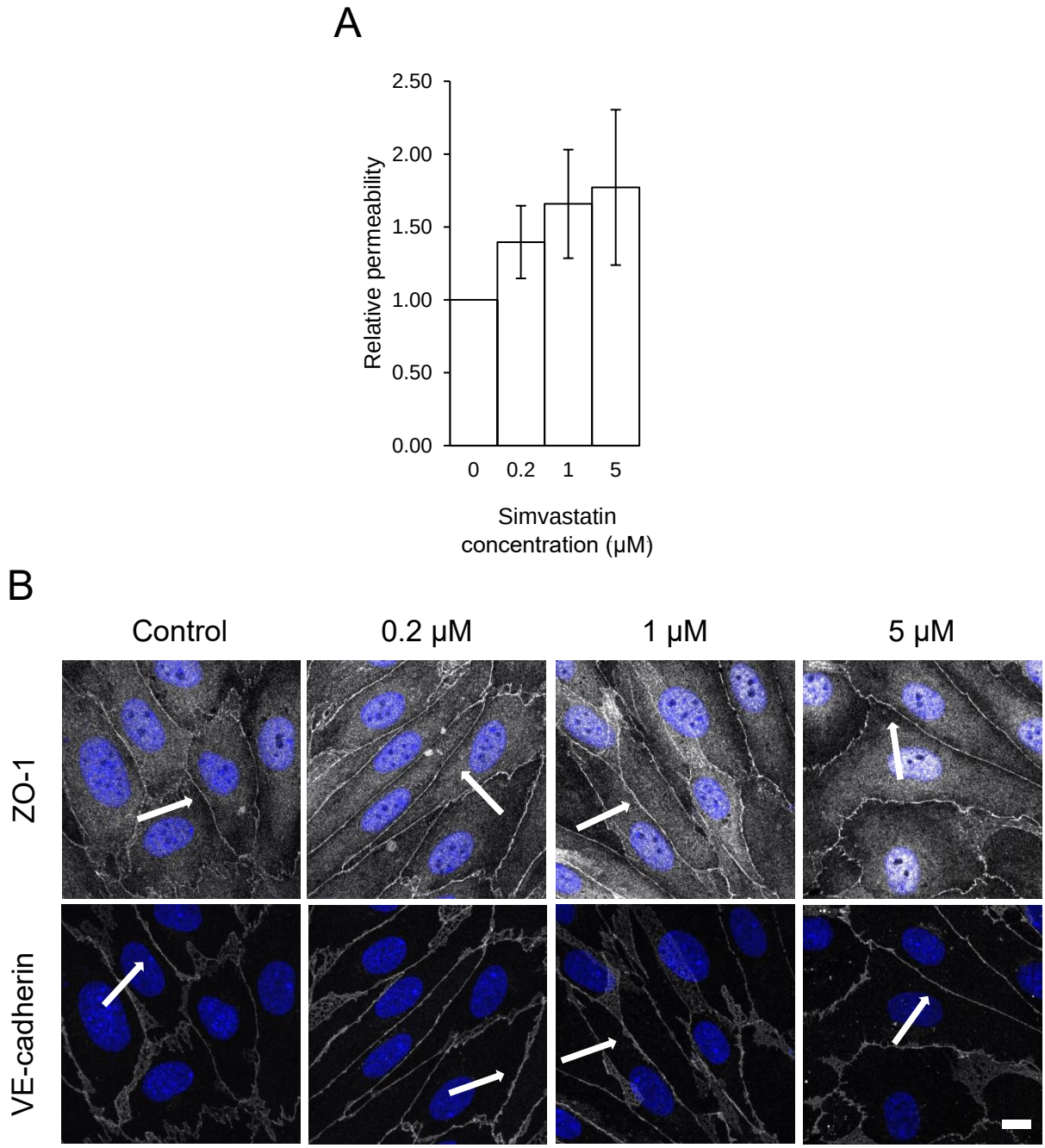

Figure 4.1. Addition of simvastatin has no significant effect on HUVEC cell:cell junctions. A) HUVEC were plated onto Transwell inserts, and simvastatin was added after 24 hours, then again after 48 hours at the concentrations shown. FITC-dextran was added to the upper compartment, and fluoresce intensity was measured after 24 hours, by removing media from the lower compartment. No results showed statistical significance. Graphs are plotted as means ± SEM (n=5), and data is normalised to the control. Statistical analysis performed using a repeated measures one-way ANOVA and Dunnett's multiple comparison post hoc test and P-values below 0.05 were considered to be statistically significant. B) HUVEC were grown on coverslips and treated after 24 hours and 48 hours with simvastatin, then fixed after a further 24 hours and stained for ZO-1 and VE-cadherin. ZO-1 and VE-cadherin showed similar distributions at all concentrations. White arrows show similarity of distribution of ZO-1 and VE-cadherin between all images. bar = 10 μm.

monolayer, and therefore forming a barrier preventing the diffusing of proteins between the medium. However, at increasing concentrations of simvastatin, I cannot be confident that the junctions are not affected.

This experimental design was also followed for atorvastatin, with the same concentrations and controls being applied. However, as shown in Figure 4.2A it was found that at 5 µM the permeability of the monolayer, when measured by FITC-dextran absorbance increased significantly, with no significant effect at any of the other concentrations shown. This was a surprising result, as in the literature other studies have used atorvastatin at up to 50 µM and the cells have been shown to be viable [193]. To validate this, confocal microscopy of atorvastatin treatment at the same time points was used (Figure 4.2B). At concentrations 0.2 µM and 1 µM, the distribution of ZO-1 and VE-cadherin suggest weaker junctions in comparison to the control, whilst at 5 µM HUVEC were shown to have completely retracted (Figure 4.2B), supporting the initial finding in the permeability assay. This was an unexpected result, as many previous studies, including by Zhang *et al* (2018) of atorvastatin on HUVEC have used concentrations much higher than 5 µM, and their cells were shown to be still viable at 50 µM treatment of atorvastatin [193]. However, the HUVEC in Zhang *et al* (2018) study were maintained in Dulbecco's modified Eagle's medium (DMEM) with 10% heat-inactivated fetal bovine serum (FBS), whilst the HUVEC in this study were maintained in HIFA, which contains no serum. This is one factor that may account for the difference in cell viability, as the presence of serum in the media may have affected the effect that statins have upon HUVEC. The atorvastatin used in their experiment was obtained from Pfizer and the purity was not stated, whilst the atorvastatin in my study was obtained from Sigma-Aldrich and had a purity of 99.93%. It is not surprising however, that simvastatin did not show the same effect at 5 µM as simvastatin has a lower potency than atorvastatin, with 40 mg of simvastatin showing the same effect on HMG-CoA as 10 and 20 mg of atorvastatin [190].

4.2.2 Optimisation of atorvastatin treatment for mass spectrometry

The permeability experiments allow us to know the integrity of the monolayer, which is vital if wanting to investigate the secreted proteome. If the monolayer did not have good cell:cell junctions, and was 'leaky,' it would be impossible to determine whether a protein truly had been secreted by the basolateral surface, or whether it merely passed through the poorly formed junctions of the monolayer to enter the basolateral media. These concentrations were used as the literature showed their use in other previous experiments into atorvastatin on HUVEC. The concentrations used of simvastatin up to 5 µM and atorvastatin up to 1 µM had

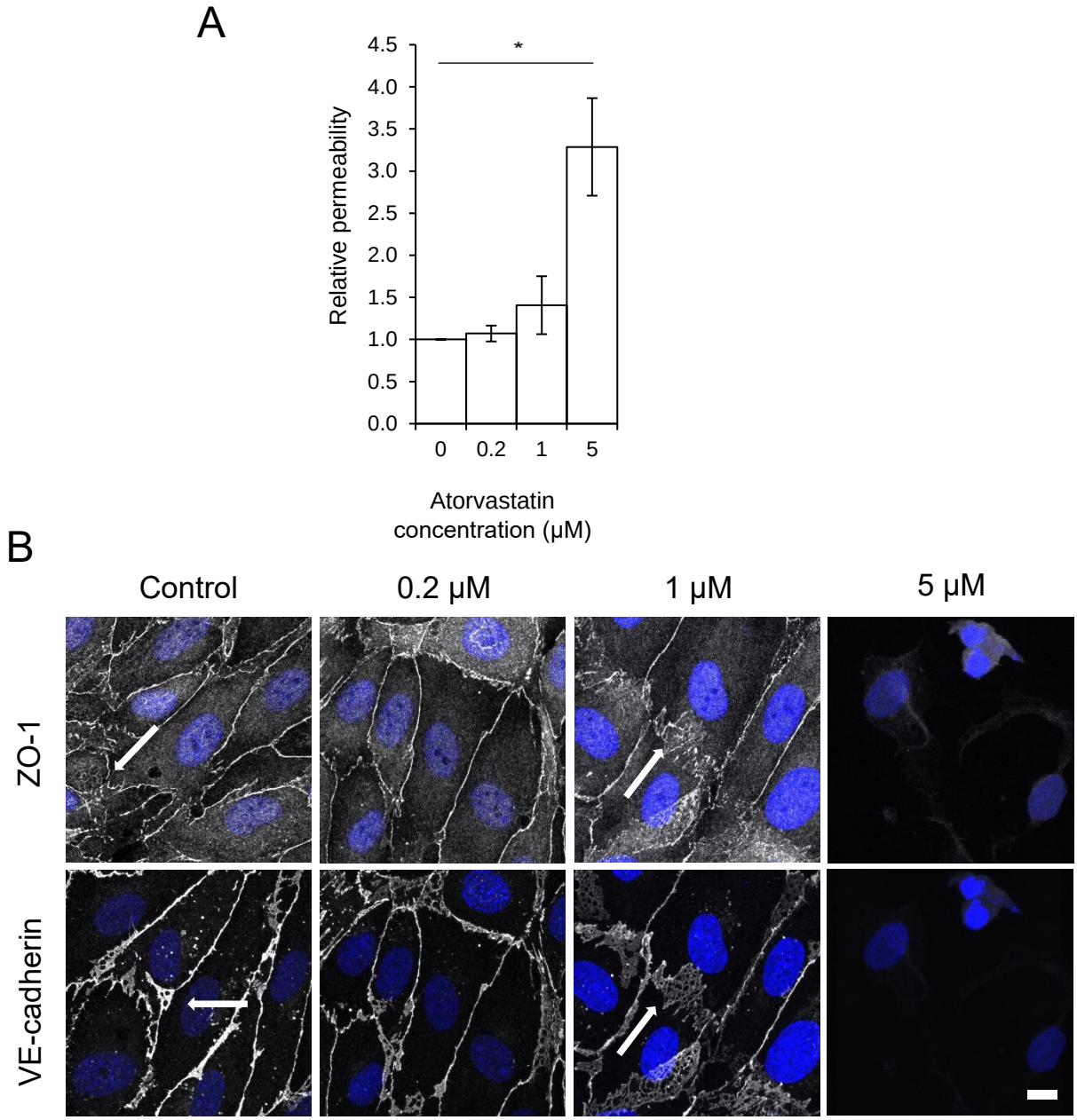

Figure 4.2. Atorvastatin disrupts cell junctions at high concentrations. A) HUVEC were plated onto Transwell inserts, and atorvastatin was added after 24 hours, and again 48 hours at the concentrations shown. FITC-dextran was added to the upper compartment, and fluoresce intensity was measured 24 hours after addition using media from the lower compartment. Atorvastatin at 5 μM had a significantly different permeability value to the control (P = 0.0147). Graphs are plotted as means ± SEM (n=5), and data is normalised to the control. Statistical analysis performed using a repeated measures one-way ANOVA and Dunnett's multiple comparison post hoc test and P-values below 0.05 were considered to be statistically significant. B) HUVEC were grown on coverslips and treated after 24 hours and 48 hours with statins, then fixed after a further 24 hours and stained for ZO-1 and VE-cadherin. Cells were then imaged using confocal microscopy. The distribution of ZO-1 and VE-cadherin appears different at 1 μM compared to the control. At 5 μM treatment with atorvastatin, cells were unable to form junctions. White arrows shows where cell:cell junctions are not as tight at 1 μM atorvastatin compared to control. Scale bar = 10 μm.

no significant effect on the appearance of HUVEC. However, despite the regular use of high concentrations of statins employed in cell experiments, these concentrations of statins are not the plasma concentrations seen in a patient undertaking statin treatment [192,194]. At a 20 mg dose of atorvastatin, the starting dose for the prevention of cardiovascular events in a patient who has never previously experienced a cardiovascular event, the maximum plasma concentration is around 40 nM, with a mean of 15 nM. [192].

To ensure these new concentrations (5 nM, 10 nM and 50 nM) also had no effect on the HUVEC monolayer, again permeability assays using simvastatin (Figure 4.3A) and atorvastatin (Figure 4.4A) were performed. None of these results were found to be significant when tested using ANOVA and Dunnett's post hoc test. HUVEC grown on coverslips were also treated with statins at the same time and dosage as the Transwell inserts. Neither simvastatin (Figure 4.3A) nor atorvastatin (Figure 4.4B) had a noticeable effect on the cell junctions when stained for ZO-1 and VE-cadherin. Images were not obtained for 5 nM simvastatin or atorvastatin, however, due to the images of HUVEC at 10 nM and 50 nM showing no noticeable difference in characteristics in comparison to the control, it was assumed that 5 nM statin treatment would also cause no noticeable difference.

As these initial experiments were involved in optimisation for further experiments in which the apical and basal media of the Transwell would be used, it was important to also investigate whether the integrity of the monolayer was also maintained on Transwell. This is important because the coverslips used in the imaging were made of glass and coated in fibronectin at 1 ng/mL, whilst Transwell inserts are 10 µM thick polyester membranes with 0.4 µm pores and are coated in a triple coat of fibronectin, gelatin and collagen. This could mean the images of the HUVEC grown on the coverslips may not be accurate for generalising to culture on Transwell. However, as shown in Figure 4.5, there is no noticeable difference between the ZO-1 and VE-cadherin on Transwell and the ZO-1 and VE-cadherin in HUVEC cultured on glass coverslips. One contrast between the images however is that in the Transwell images (Figure 4.5), DAPI staining appears to be very common and not focussed in the nuclei, as would be expected and is seen in the other Figures (4.1,4.2,4.3,4.4). This is a well-known issue with staining Transwell inserts, and pores are often visible in microscope images. Transwell inserts may possibly provide a superior image to that of glass coverslips, as the permeable membrane allows the basolateral side of the cells to also permeabilise when treated with Triton, which would otherwise be obscured by glass.

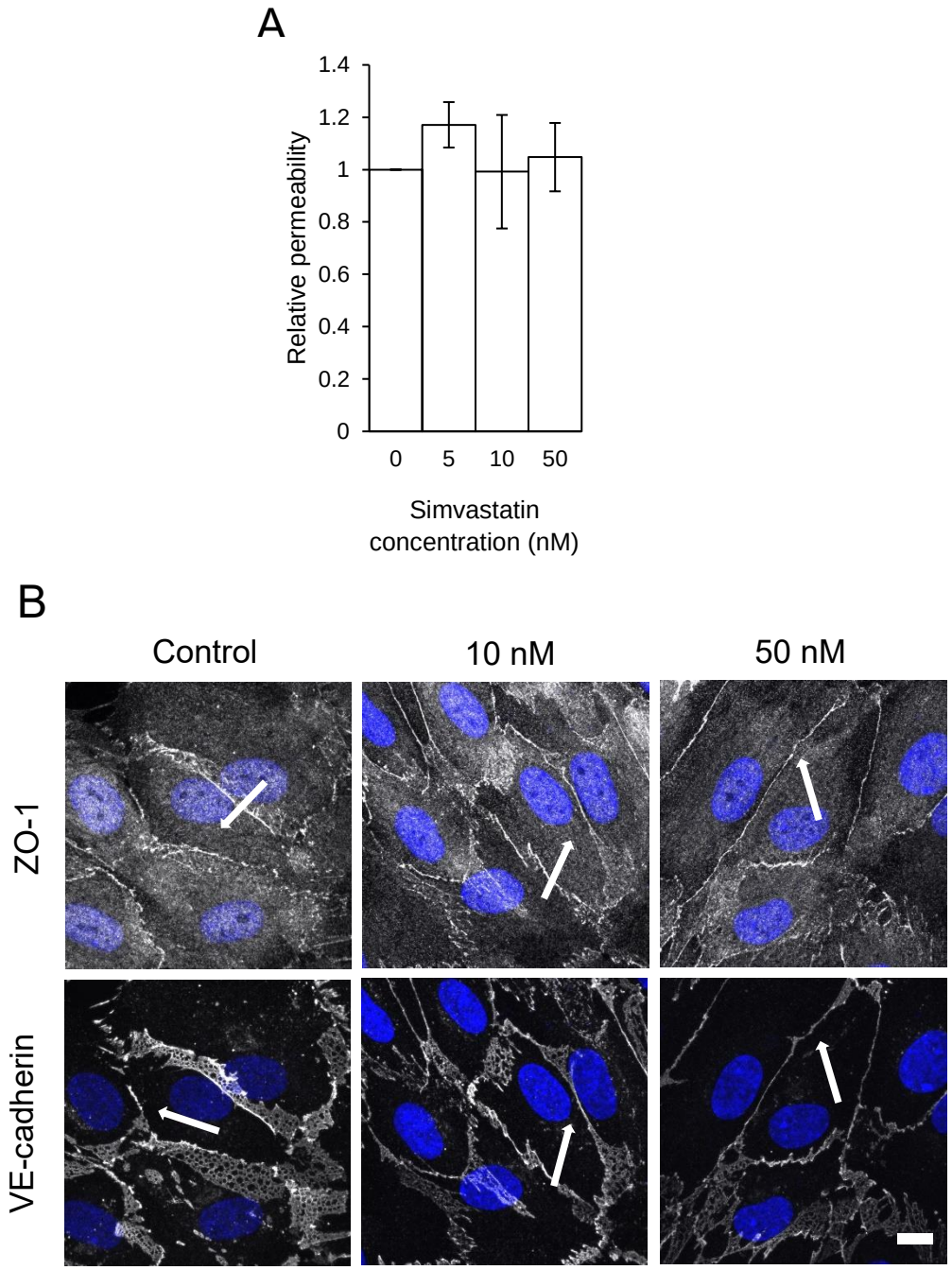

Figure 4.3. Low concentrations of simvastatin have no significant effect on HUVEC cell:cell junctions. A) HUVEC were plated onto Transwell inserts, and simvastatin was added after 24 hours, then again after 48 at the concentrations shown. FITC-dextran was added to the upper compartment, and fluorescence intensity was measured after 24 hours using media from the lower compartment. Graphs are plotted as means ± SEM (n=5), and data is normalised to the control. Statistical analysis performed using a repeated measures one-way ANOVA and Dunnett's multiple comparison post hoc test and P-values below 0.05 were considered to be statistically significant. B) HUVEC were grown on coverslips and treated after 24 hours and 48 hours with simvastatin, then fixed after a further 24 hours and stained for ZO-1 and VE-cadherin. Cells were then imaged using confocal microscopy. No concentration of simvastatin showed an obvious effect on the junctions. White arrows show similarities in cell:cell junctions between images. Scale bar = 10 μm.

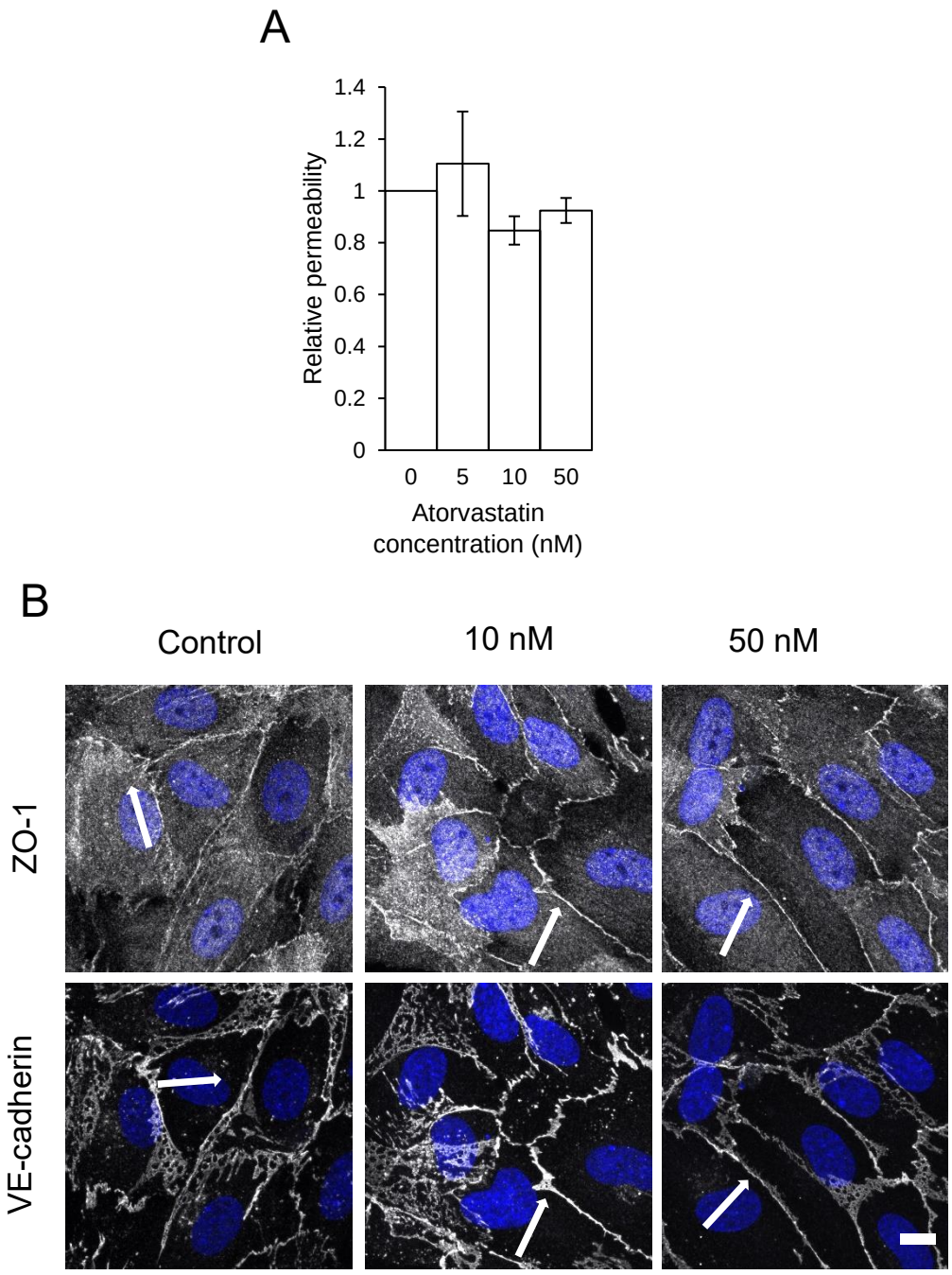

Figure 4.4. Low concentrations of atorvastatin have no significant effect on HUVEC cell:cell junctions. A) HUVEC were plated onto Transwell inserts, and atorvastatin was added after 24 hours, then again after 48 hours at the concentrations shown. FITC-dextran was added to the upper compartment, and fluorescence intensity was measured after 24 hours of media of the lower compartment. Graphs are plotted as means ± SEM (n=5), and data is normalised to the control. Statistical analysis performed using a repeated measures one-way ANOVA and Dunnett's multiple comparison post hoc test and P-values below 0.05 were considered to be statistically significant. B) HUVEC were grown on coverslips and treated after 24 hours and 48 hours with atorvastatin, then fixed after a further 24 hours and stained for ZO-1 and VE-cadherin. Cells were then imaged using confocal microscopy. No concentration of atorvastatin showed an obvious effect on the junctions. Scale bar = 10 μm.

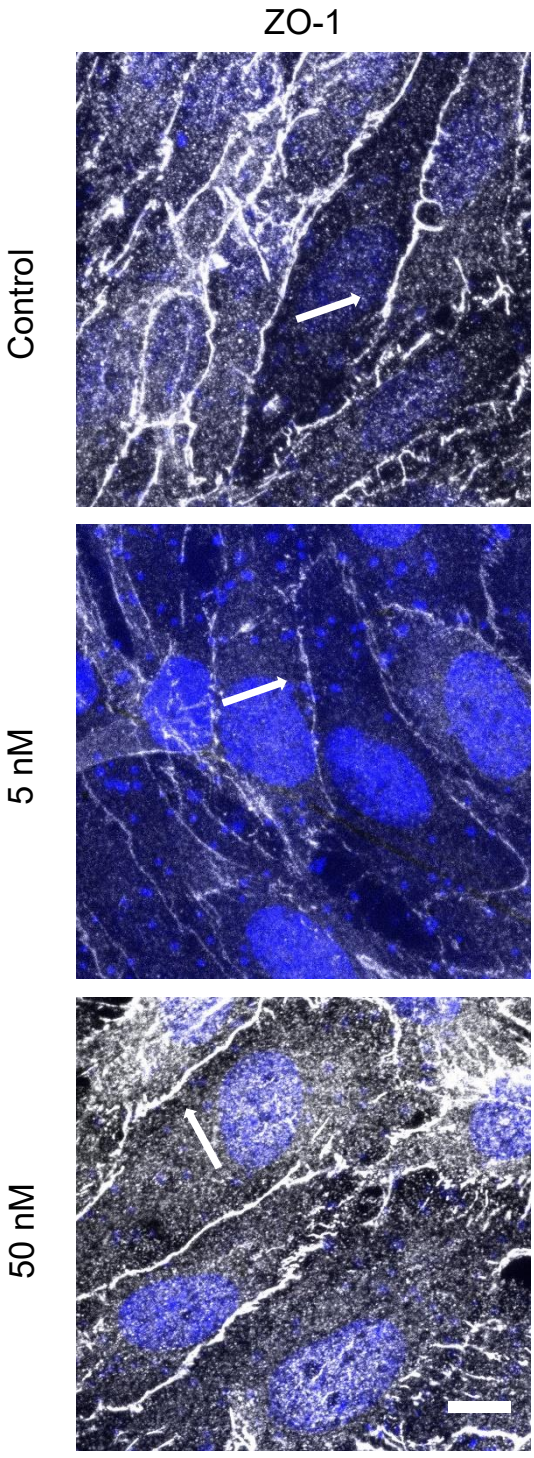

Figure 4.5. Atorvastatin has no significant effect on HUVEC cell:cell junctions when grown on Transwell. HUVEC were plated onto Transwell inserts, and atorvastatin was added after 24 hours, then again after 48 hours at the concentrations shown. Inserts were fixed using PFA and stained for ZO-1. Cells were then imaged using confocal microscopy. Like when grown on the coverslips, atorvastatin showed no effect on the ZO-1 distribution. DAPI nuclear staining also stains the pores on the Transwell insert. White arrows show similarities between ZO-1 distributions in images. Scale bar = 10 μm.

4.2.3 Atorvastatin treatment generally causes an increase of the apical/basolateral secretion ratio compared to the control

Performing the permeability experiments allowed optimisation of the experimental design for TMT mass spectrometry. The measurement of the effect at the higher concentrations of the permeability of HUVEC allowed understanding of the toxicity of statins on HUVEC and followed the other literature. However, for the results to be clinically relevant, the lower concentrations were used. Initially in the permeability experiments at the lower concentrations, 5 nM, 10 nM and 50 nM were used. However, with the difference of 5 nM and 10 nM being only two-fold, and the difference of 10 nM and 50 nM being five-fold, 15 nM replaced 10 nM, allowing for a three-fold difference between 5 nM and 15 nM, and almost a three-fold difference between 15 nM and 50 nM. 15 nM was not investigated for its effect on permeability but was considered suitable as a range of concentrations above and below 15 nM had shown no effect on the permeability.

During the preparations of samples for mass spectrometry, one of the ultracentrifuge tubes cracked, losing the 5 nM basolateral sample. Instead, a sample collected from a previous experiment was used. This previous experiment however, had used polycarbonate Transwell inserts as compared to permeability experiments that had used polyester (PET) inserts. As it is harder to see the cells monolayer upon a polycarbonate membrane as they are translucent, when taking the sample there was no idea about the integrity of the monolayer. However, a few permeability assays had previously been performed on polycarbonate Transwell inserts, and there had been no considerable difference in fluorescence absorbance in FITC-dextran compared to when the polyester Transwell inserts were used in other experiments, suggesting it was suitable as a replacement.

However, when the results from the mass spectrometry were returned, the result for 5 nM basolateral total abundance looked abnormal (Figure 4.6) when compared to the apical and basolateral samples of the control, 15 nM and 50 nM. Although the apical total abundance at 5 nM was comparable to the other three concentrations, the fact the 5 nM value was so obscure, and had come from a previous experiment with a different insert material that the 5 nM result was not used in any further analysis. To further support this decision, total abundance graphs and the corresponding R^2 value of the control vs 5 nM, 15 nM and 50 nM were created (Figure 4.7). R^2 values are statistical measurements that correspond to how much variation in the experimental (in this case the concentration of atorvastatin treatment) is due to the control data, and how well the data fits a regression line. The data was transformed to log2 values, as when plotted into a histogram the data was not normally distributed, and to

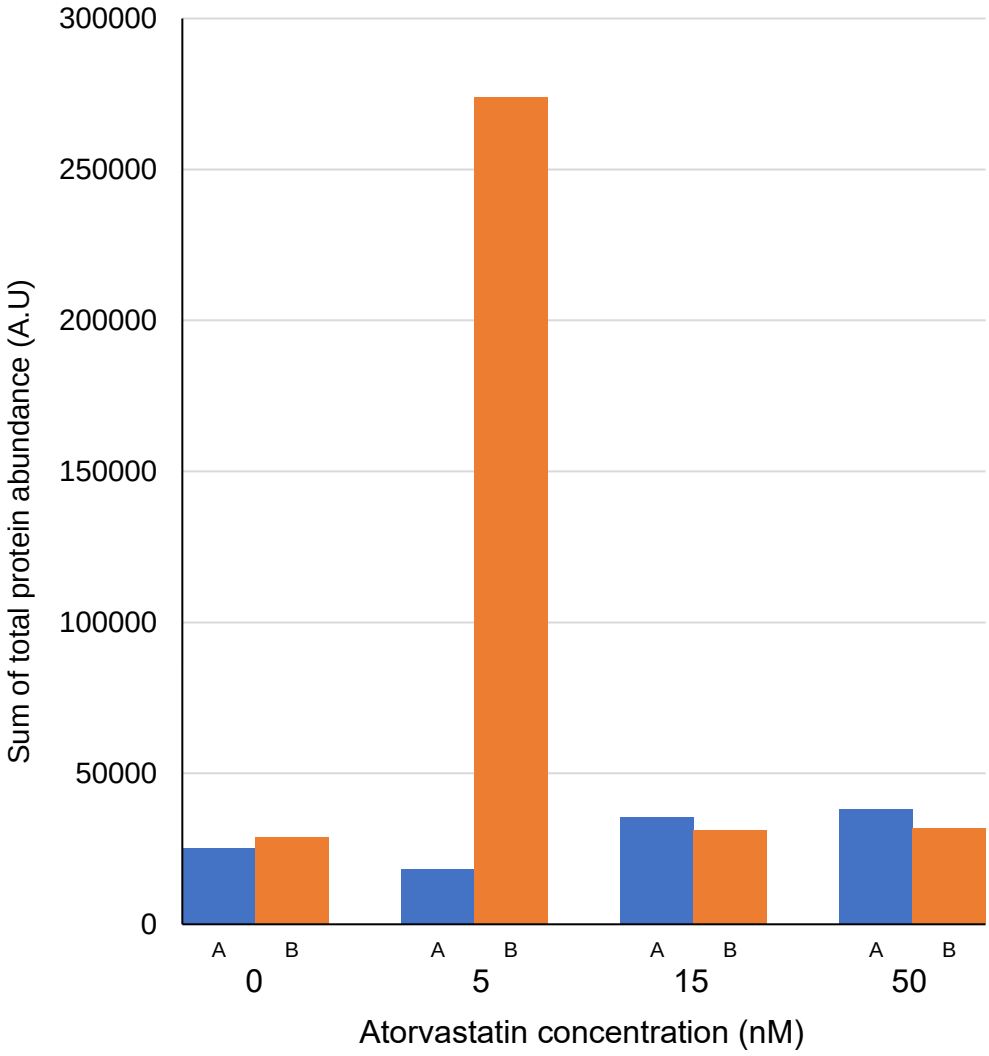

Figure 4.6. The total protein abundance was higher at 5 nM basolateral than any other condition. During the mass spectrometry preparation, the 5 nM atorvastatin sample was lost, and a replacement was used from a previous experiment. To investigate whether this sample was suitable to use in the analysis, the sum of the total abundance of the three different concentrations compared to the control was analysed. Generally, all apical and basolateral abundances were about equal, with the largest difference of samples of the same experiment (between 50 nM apical and control apical) being 1.5-fold, whilst the smallest difference between 5 nM basolateral and any other basolateral sample was at least 8.6-fold.

better visualise the differences between values. The values for 15 nM and 50 nM against the control gave very high R^2 values, both above 0.9 suggesting very high positive correlations between the variables, whilst for 5 nM, the R^2 value was 0.5178, suggesting a moderate correlation, and has high residuals (the distance between the regression line and the observed value). Whilst it is unknown whether the 5 nM sample was a true reflection of the clinical use of statins ECs, the substantial increase in abundance of the 5 nM sample, the moderate R^2 value and the high residuals compared to 15 nM and 50 nM meant there was considerable evidence for excluding 5 nM from the rest of the analysis.

In order to analyse the data further, all non-human proteins, such as bovine and contaminants such as keratin were removed from the data set, as defined in the mass spectrometry data, with 271 proteins remaining. Proteins which had missing abundances in any of the columns were also removed, as otherwise the data would be unable to be compared at different concentrations. The data was further processed by creating ratios of the apical/basolateral secretion of each protein, and plotted as values normalised to the control, and again, log2 values were used (Figure 4.8). Figure 4.8 shows that generally, the apical/basolateral ratio of the protein increased with increasing concentrations of atorvastatin. Highlighted in figure 4.8 are four proteins which show the highest effect on the ratio: collagen α1, a secreted protein that is the major component of type I collagen, which is found in most connective tissue; Chaperone containing TCP1, a molecular chaperone complex that assists protein folding normally present within the cytoplasm; Inter-α-trypsin inhibitor, a secreted protease inhibitor that is involved in the inflammatory response; and serine-tRNA ligase, a cytoplasmic enzyme that is involved in the metabolism of glycine, serine and threonine and aminoacyl-tRNA biosynthesis. Whilst this mass spectrometry purely looks at the secretome, sometimes cellular components can enter the media due to cell lysis before extraction of media, or cells not being removed during mass spectrometry sample preparation, which accounts for proteins such as Chaperone containing TCP1 and serine-tRNA ligase. However, these cytoplasmic proteins are of little interest, as they will only come from a few cells and therefore their abundance and ratios cannot be taken as reliable.

Using UniProt, the proteins were organised into whether they were known secreted proteins or not, and the proteins which were not secreted were ignored, reducing the data for 62 proteins (Figure 4.9). Again, generally the apical/basolateral secretion of proteins increased with atorvastatin treatment compared to the control, whilst a few proteins decreased.

Figure 4.10 shows the functions of the 52 known secreted proteins found in the HUVEC atorvastatin secretome using TMT mass spectrometry. Almost 30% of these proteins are proteins with are associated with the ECM, which, as one of the major secreted components

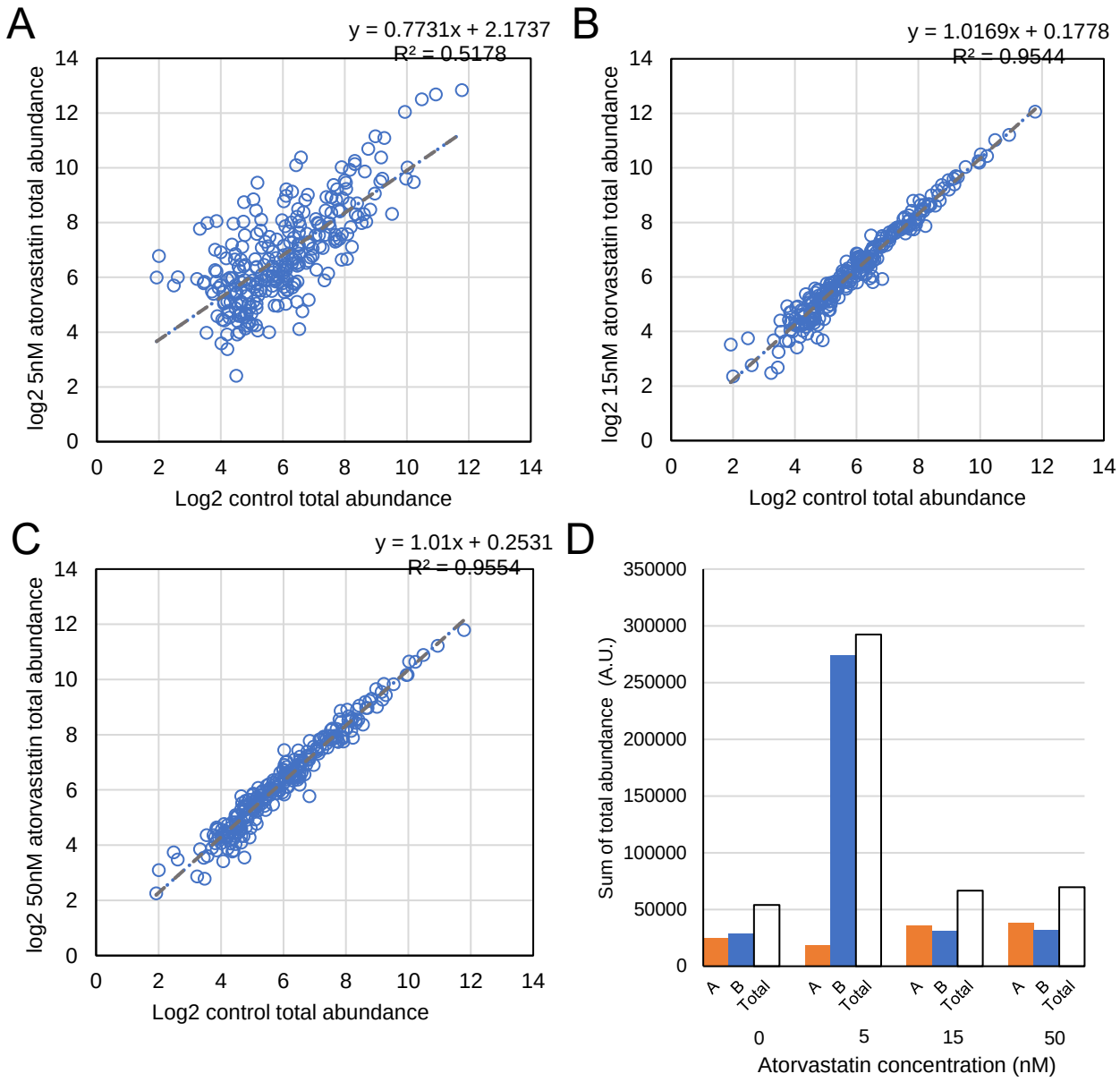

Figure 4.7. Total protein abundance at 5 nM atorvastatin is considerably different to any other protein abundance. During the mass spectrometry preparation, the 5 nM atorvastatin basal sample was lost, and a replacement was used from a previous experiment. To see whether this sample was suitable to use in the analysis, total abundance graphs of the treatment compared to the control was performed. A) The control apical and basal abundances were added together, and the log2 values plotted against the log2 value of apical and basal abundance at 5 nM. The graph has an R^2-value of 0.5178, suggesting there is a not a strong positive correlation between the 5 nM atorvastatin treatment and the control. B) The control apical and basal abundances were added together, and the log2 values plotted against the log2 value of apical and basal abundance at 15 nM and had an R^2-value of 0.9551, suggesting a strong positive correlation between the control and 15 nM total abundance. C) The control apical and basal abundances were added together, and the log2 values plotted against the log2 value of apical and basal abundances at 5 nM had an R^2-value of 0.9558, suggesting a strong positive correlation between the control and 50 nM total abundance. D) Apical, basal and total abundance values for each condition was plotted, showing the basolateral sample at 5 nM was considerably higher than any other condition, and as was the corresponding total protein abundance at 5 nM.

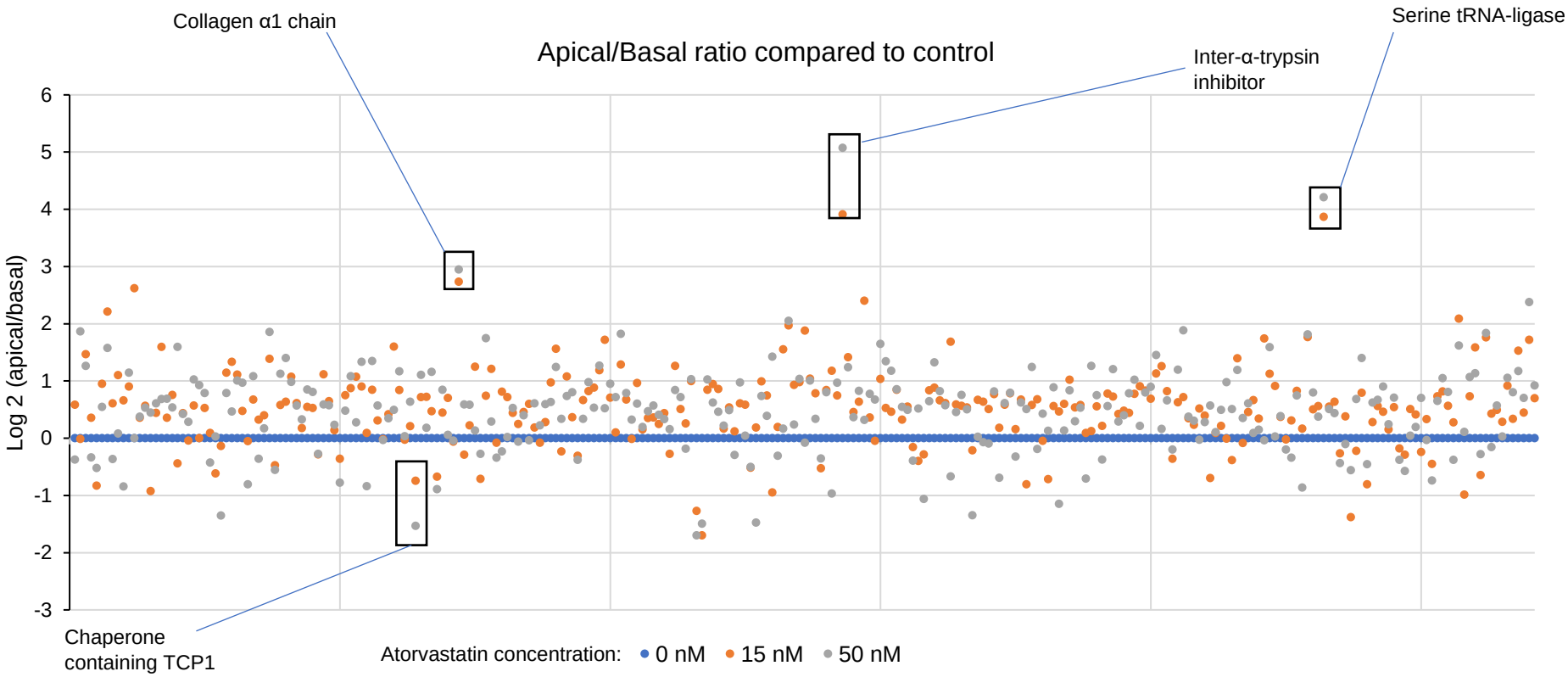

Figure 4.8. The apical/basolateral secreted ratio of 15 nM and 50 nM atorvastatin total mass spectrometry proteins differs to control ratio. The apical/basolateral ratios of 271 proteins for each condition were collated and the log2 values were plotted. Generally, atorvastatin treatment increases the apical/basolateral secreted ratio of the protein, whilst the apical/basolateral ratio of few proteins' decreases. All non-human proteins and contaminants were removed, as were proteins where one or more abundance values were absent. All data is n=1.

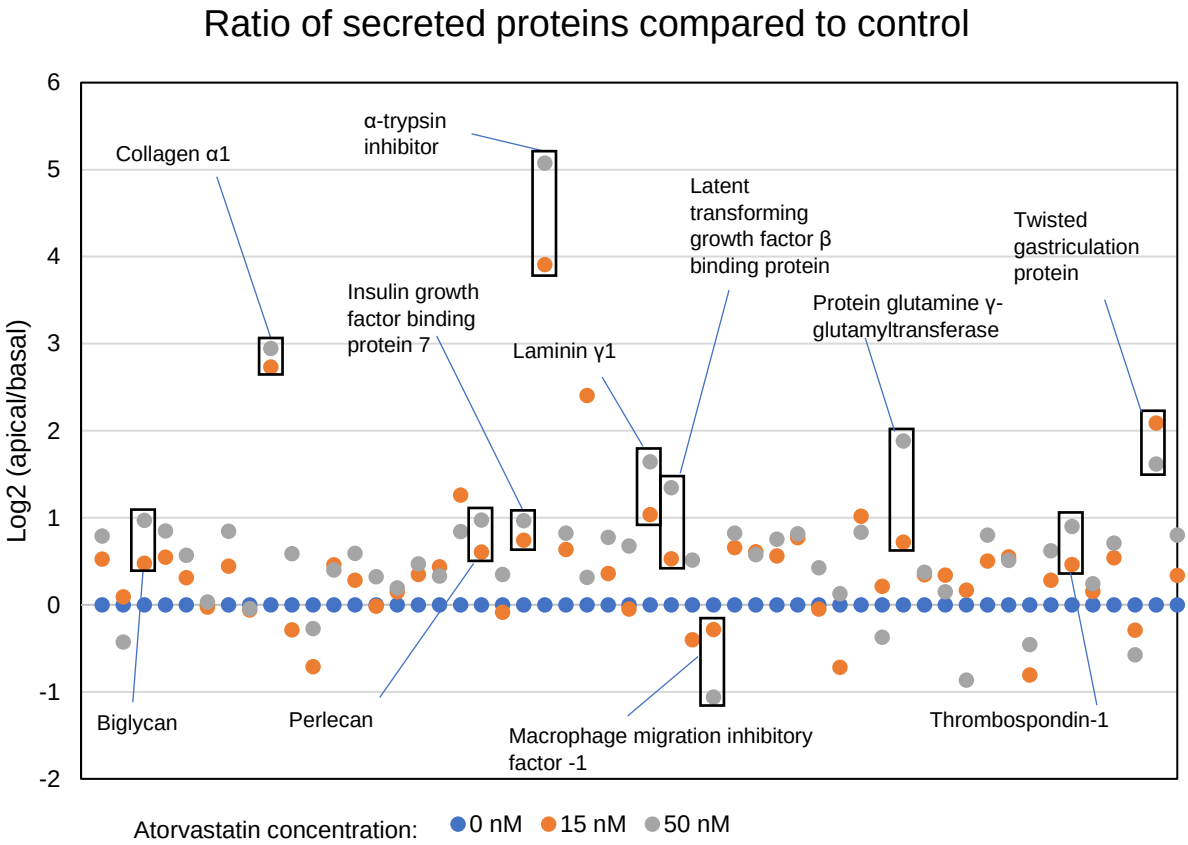

Figure 4.9. The apical/basal ratio of known secreted proteins generally increases with atorvastatin treatment compared to the control. The proteins shown in Figure 15. were analysed on whether they are a known secreted protein or not, and 52 proteins were found to be of this category. The log2 ratios of these proteins were plotted, and generally the apical/basal ratio increased in comparison to the control, with many proteins found to become more apical, causing the ratio to increase. Proteins highlighted are analysed futher in this thesis. All data is n=1.

of ECs are to be expected and shows the high range of genes that interact to form a stable ECM. Other popular proteins include enzymes, such as matrix metalloproteinase inhibitor TIMP1, which have a role in remodelling the ECM by controlling the activity of matrix metalloproteinases [195]. Growth factors, and proteins that bind growth factors are also secreted by ECs, including placental growth factor PGF, a member of the vascular endothelial growth family (VEGF) and associated with angiogenesis (Figure 4.10). Raised levels of PGF is implicated in chronic inflammatory disease, however, as the cells used in this experiment are HUVEC, it is highly likely these levels are just due to the cell type as these cells obviously play a large part in placental growth [196]. Another function of the secreted proteins is their role in haemostasis, controlling of the blood clotting pathways. One protein, vWF is an important protein in blood clotting, and deficiencies in this protein leads to the pathological condition vWF disease, symptoms of which include high risk of bleeding, and high levels are associated with thrombosis risk [39]. Other proteins include growth factors, immunity, and other secreted proteins include TCN2, a secreted transport protein.

However, in many of the proteins the secretion changed only slightly, and as shown in Figure 4.9, many of the protein's ratios are within 0 and 1 on the log2 scale, so their secretion was not substantially affected by the addition of atorvastatin.

4.2.4 Treatment with atorvastatin

Whilst the smaller list of proteins from the secretome obtained so far had been reduced to 59, many of these proteins' values fluctuated around 0-1 on the log scale, so did not show a substantial difference in their secretion. Also, other proteins showed that the 15 nM concentration caused a higher increase in secretion that the 50 nM concentration, and without a 5 nM sample any relationship cannot be strongly distinguished. Having only performed one experiment with no repeats, I cannot be sure whether it is correct to disregard these data points, or whether they are important. However, it would be unfeasible to repeat the mass spectrometry due to time constraints.

To evaluate the results, proteins were studied to see whether they had a log2 effect value of above or below 0.9 and -0.9 respectively, giving a final amount of 11 proteins which had successfully fulfilled all the criteria.

The proteins showed a range of effects with the addition of atorvastatin. In some proteins, the overall secretion of the protein increases with atorvastatin treatment, with both their apical and basal secretion increase (Figure 4.11). In some proteins, just the apical secretion increased

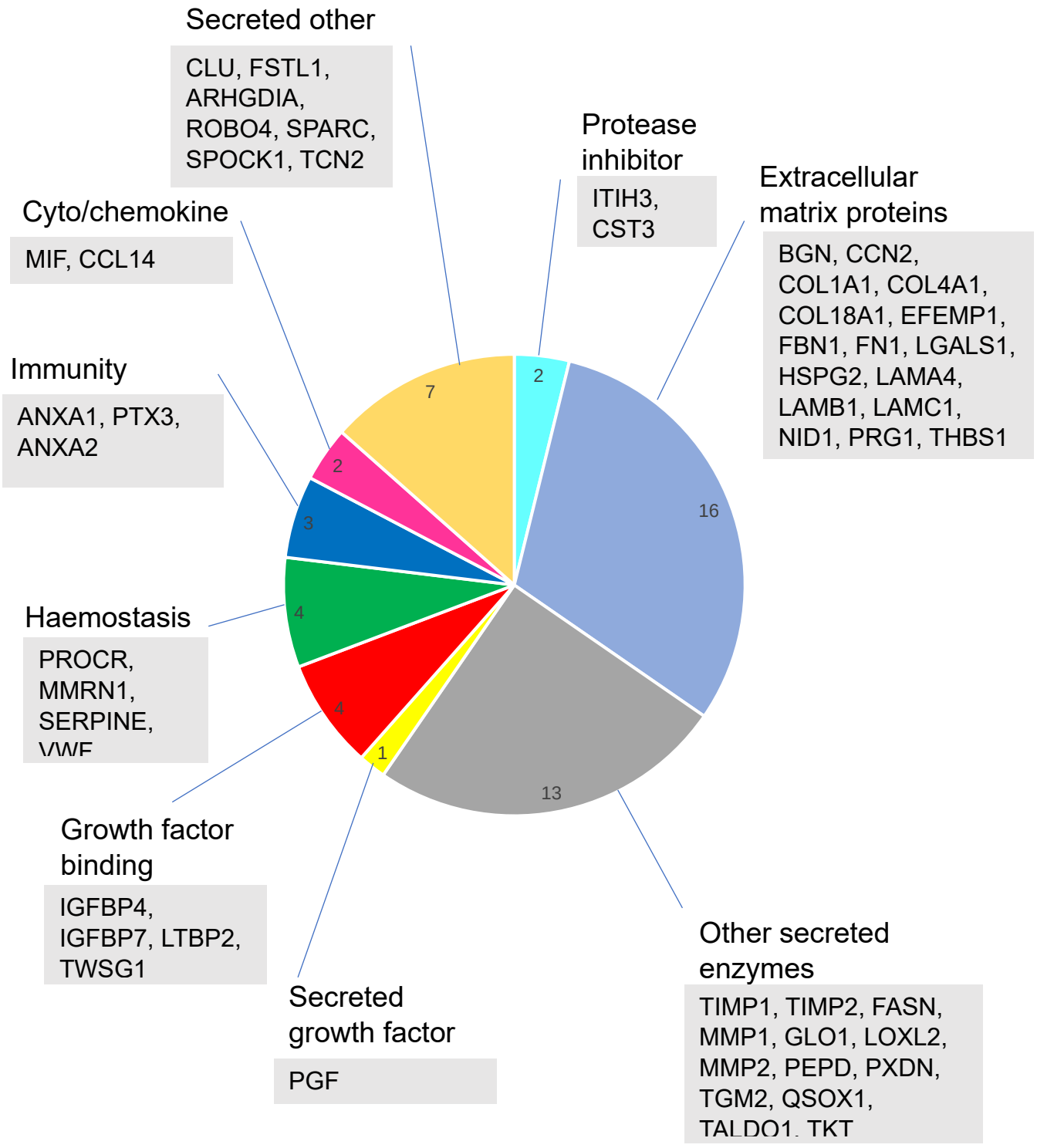

Figure 4.10. Function of proteins in the HUVEC atorvastatin secretome. HUVEC secretome was analysed using TMT mass spectrometry, then analysed for protein function using UniProt (www.uniprot.org)

and in others the basal secretion increased, with no effect on the overall secretion, suggesting atorvastatin changed the polarity of the protein secretion (Figure 4.12,4.15). However, in some proteins (Figure 4.14) the addition of atorvastatin showed a substantial change in the secretion of the protein.

Figure 4.11 shows proteins where the total secretion of the protein increases with atorvastatin treatment. The first protein shown is thrombospondin 1 (TSP1). TSP1 is an adhesive glycoprotein, that can bind to other proteins, including fibrinogen, laminin and collagen [197]. TSP1 levels have also been shown to affect angiogenesis, being antiangiogenic at high expression, and antiangiogenic at low expression [197]. When atorvastatin is added to HUVEC, the apical secretion of the TSP1 increases, whilst the basal secretion remains almost constant (Figure 4.11A). Despite this slight fall in basal secretion, the overall TSP1 abundance increases by about 1.25-fold between 0 nM and 15 nM, however, only increases slightly at addition of 50 nM. Studies by Keenan *et al* (2006), suggested that the addition of fluvastatin decreased levels of TSP1 [198]. However, they used much higher levels of statins that than used within this study, at 0.25 µM and 1 µM, so whilst the reduction in TSP1 may occur at these concentrations, at lower concentrations, such as the ones used with my study may have different effects. Another study by Zagorska *et al* (2006) also showed that at 1 µM atorvastatin treatment, expression of TSP1 also decreased, however, they did not show the effect at 10 nM. High levels of TSP1 are associated with decreased angiogenesis, and levels of TSP1 are found in increase after vascular injury [199]. TSP1 has also been shown to activate transforming growth factor (TGF-β), an anti-inflammatory factor, and it is suggested that activating TSP1 may be of therapeutic value in treatment of cardiovascular disease [199]. However, due to these conflicting findings in studies of TSP1 and its effect in disease, as well as the variety of concentrations atorvastatin used, my results do not show any clear indication of whether this increase of TSP1 has a positive or negative effect of statins.

Other proteins which follow this same pattern are ECM glycoproteins, laminin subunit γ-1, which is present in all basement membranes. The addition of atorvastatin causes an increase in the apical secretion of laminin (Figure 4.11C), and an increase in the overall secretion of atorvastatin (Figure 4.11D). At 15 nM, both the apical and basolateral secretion abundance increases steeply compared to the control, however at 50 nM the basal secretion falls back to a similar level as the control (Figure 4.11C). Overall, the total abundance of laminin subunit γ-1 increases with addition of atorvastatin, peaking at 15 nM (Figure 4.11D) However, secretion at 50 nM is still considerably more than the control secretion (Figure 4.11D).

Biglycan is a member of the small proteoglycan family, macromolecules of the ECM. Recently, evidence has shown that these components are not only for cellular support, but also involved

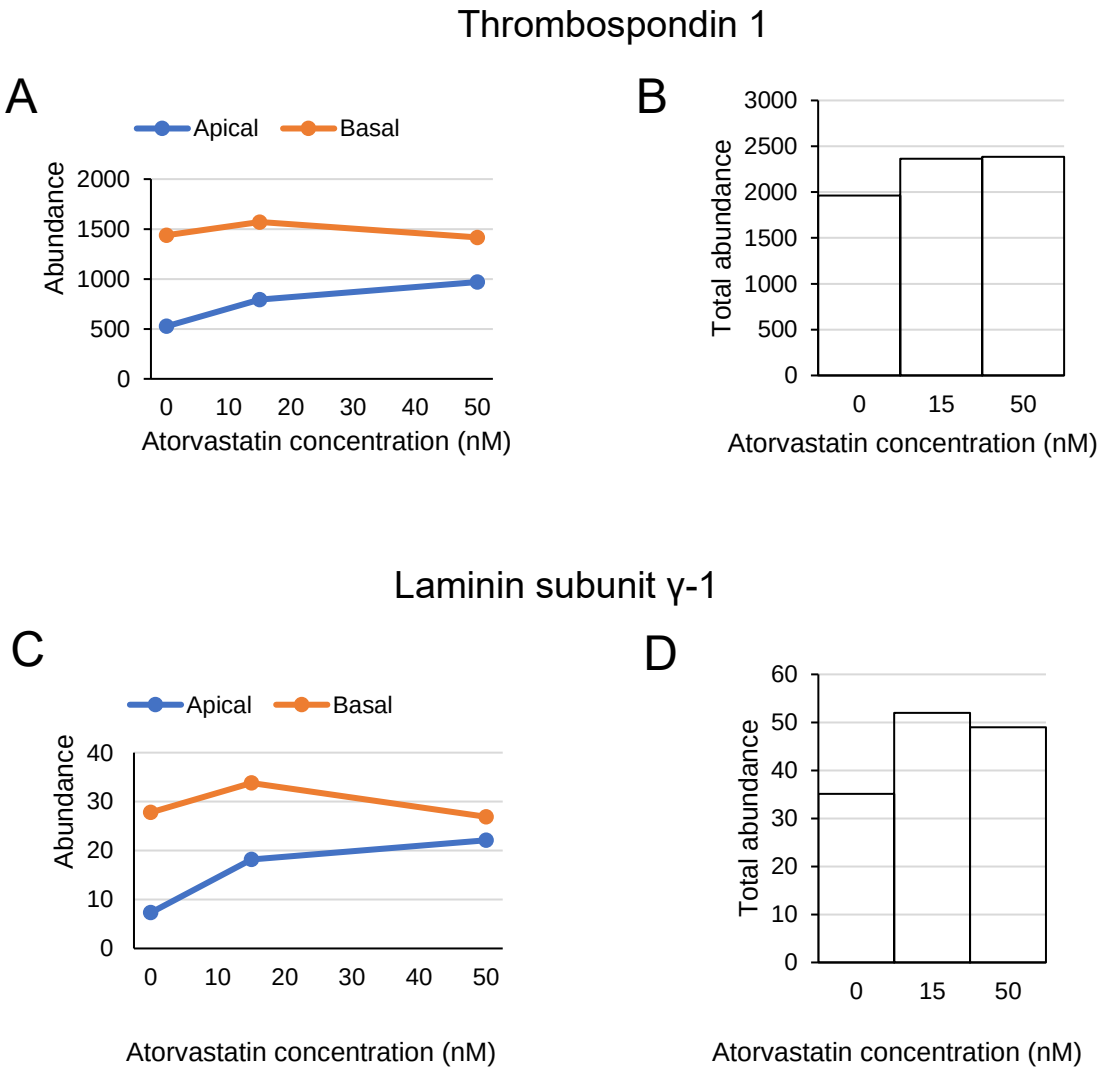

Figure 4.11 Total secretion of certain proteins increases with atorvastatin treatment. Change in the abundance of proteins in response to various concentrations of atorvastatin. (A, C) show the separate apical and basal abundance, and (B,D) show the pooled data of the separate abundances.

in depositions of collagens and mediation of cytokines and growth factors, amongst others. Previous studies have found that increased levels of vascular biglycan correlate with increased atherosclerosis in mice, and that accumulation of biglycan may contribute to the early stages of atherosclerosis [200,201]. This is due to biglycan being the most co-localised proteoglycan with apolipoprotein B which causes retention of low density lipoproteins (LDL), the 'bad' cholesterol, in the vessel wall, and vessels with increased biglycan have increased lipid retention [200]. Lipid retention is a contributing factor the initial stages of atherosclerosis. Increased levels of biglycan have also been associated with other contributing factors to atherosclerosis, including inflammation and regulation of growth factor availability, but also increased levels shows protection against hypoxia [200,202]. Whilst other studies have suggested that biglycan contributes to atherosclerosis, a study by Csont *et al* (2010), found that biglycan leads to protection against hypoxia/reoxygenation injury, by inducing cardioprotective genes such as NO synthases in the heart. This study found that it was the polarisation of biglycan secretion that changed, with the basolateral secretion of biglycan being almost 5-fold higher than the apical secretion at 0 nM (Figure 4.12A). At addition of 15 nM atorvastatin, both the apical and basal levels of secretion of biglycan rose, with the increase of apical secretion more substantial than the increase of the basal secretion (Figure 4.12A). However, my study showed at 50 nM atorvastatin, the basal levels of the protein secretion decreased, whilst the apical levels increase slightly compared to 15 nM (Figure 4.12A). I found that overall abundance of biglycan remains steady between the control and 50 nM, the total abundance peaks at 15 nM (Figure 4.12B). Overall, this study found that the apical secretion of biglycan increased, whilst the basolateral decreased, so further investigation is needed to examine whether it in increased secretion of biglycan from the apical surface is the significant factor in these effects shown.

Another protein indicated to be significant by my study was insulin-like growth factor-binding protein 7 (IGFBP7), which acts as a carrier protein for insulin-like growth factor (IGF-1) and insulin. IGFBP7 regulates cellular functions such as proliferation and adhesion, and has been proposed to regulate angiogenesis [203]. IGFBP7 is also a structural constituent of the ECM, as was biglycan, amongst others, suggesting that the basolateral secretion of these components is affected by atorvastatin addition. In Figure 4.12C, it shows that initially, the basolateral secretion of IGFBP7 is about three times more than the apical secretion. However, with the addition of 15 nM atorvastatin, this ratio changes, and the secretion of IGFBP7 from the basolateral surface becomes only twice the secretion from the apical surface (Figure 4.12C) as the apical secretion increases. At 50 nM atorvastatin, the apical secretion has remained similar to the secretion at 15 nM atorvastatin and the basolateral secretion fallen slightly, meaning the basal secretion is less than twice of the apical secretion (Figure 4.12C).

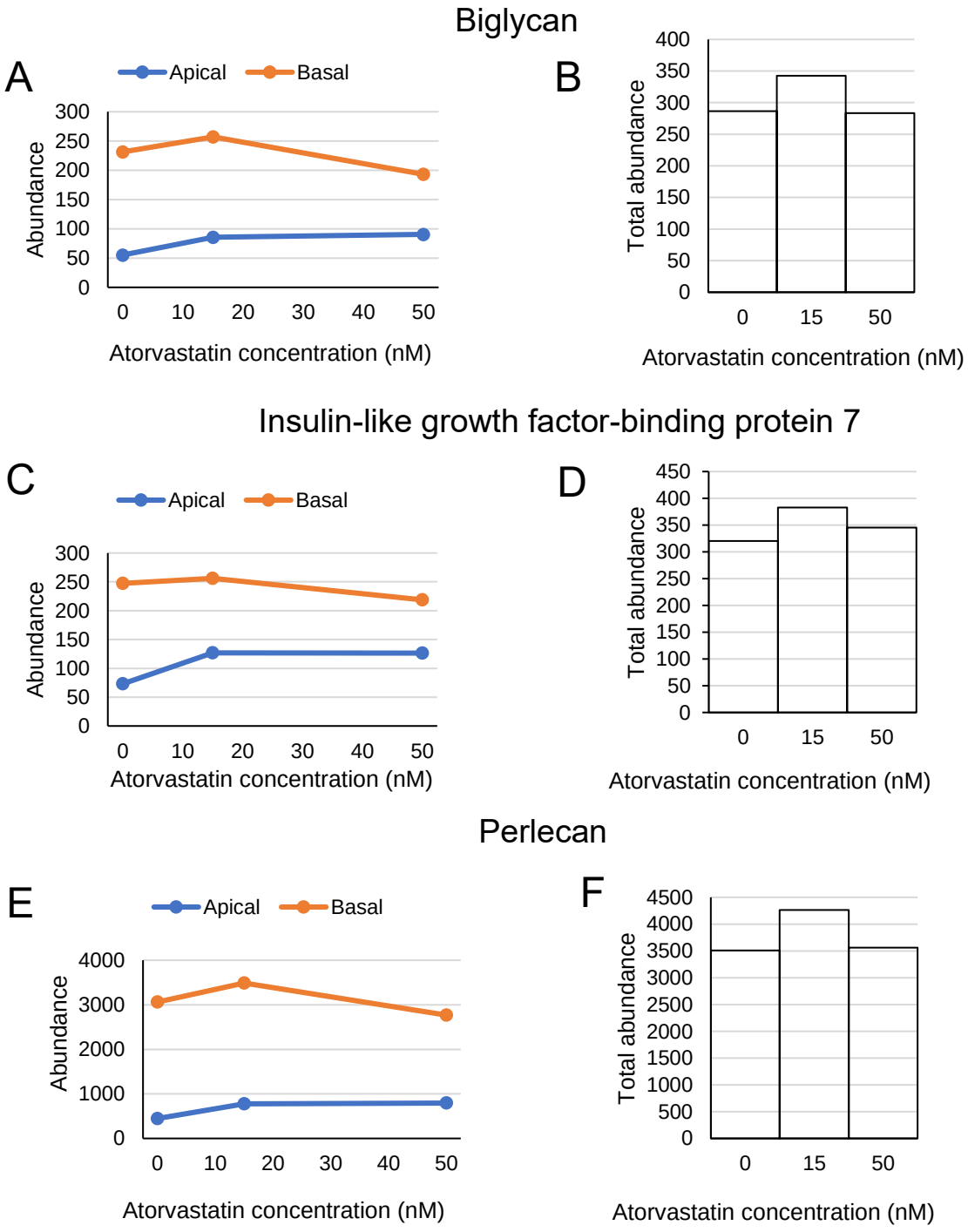

Figure 4.12 Apical secretion of certain proteins noticeably increases, whilst basal level decreases slightly with atorvastatin treatment. Change in the abundance of proteins in response to various concentrations of atorvastatin. (A,C,E) show the separate apical and basal abundance, and (B,D,F) show the pooled data of the separate abundances.

IGFBP7 is a marker of cell cycle arrest, and often shows increased levels in ischemic conditions, and is often used a marker for diagnosis of acute kidney injury [204]. IGFBP7 has also been shown to be a component of Weibel-Palade bodies, storage granules that contain von Willebrand factor (VWF), by binding to large vWF strings when they are released by ECs [205]. As VWF is a carrier for FVIII, which is involved in blood clotting, the increase in IGFBP7 secretion from the apical surface could allow for the rapid release of Weibel-Palade bodies from the apical surface, which may be crucial in maintaining vascular homeostasis [205]. The change in polarisation of IGFBP7 is not due to overall increased abundance (Figure 4.12D), as the total amount of IGFBP7 remains steady between 0 nM and 50 nM, however increases slightly between 0 nM and 15 nM, before decreasing back to the level at 0 nM at 50 nM atorvastatin. As Weibel-Palade body release is associated with thrombosis, the secretion of these may increase in atorvastatin treatment, which may increase the risk of thrombosis [150]. Whilst this may initially be positive as it could improve initial damage to the vessel by plugging damage with a clot, increased secretion may cause unwanted thrombosis and increased plaque formation [206].

Perlecan shows a similar pattern to that of biglycan and IGFBP7, where the apical secretion noticeably increases with increasing concentrations of atorvastatin, whilst the basal concentration slightly decreases (Figure 4.12). Perlecan, like biglycan is a component of the ECM and regulates many cellular processes, including cell adhesion, thrombosis and lipid metabolism [173]. Generally, perlecan is secreted basally into the underlying ECM and my data supports this (Figure 4.12E), which shows at 0 nM atorvastatin, the basal secretion is about seven-fold more than the apical secretion. This remains similar at 15 nM atorvastatin; however the basal secretion falls to less than 4.5-fold that of the apical (Figure 4.12E), and by 50 nM atorvastatin the basal secretion is only about 3.5-fold more than the apical (Figure 4.12E). This suggests that the addition of atorvastatin changes the polarisation of perlecan secretion as shown in Figure 4.12F, the overall abundance is similar at 0 nM and 50 nM, however, the abundance increases at 15 nM. This is a similar pattern also seen in both biglycan and IGFBP7 secretion, suggesting either the statins had a most considerable effect at 15 nM, or there was a difference in the initial loading of the samples for mass spectrometry. A study by Vikramadithyan *et al* (2004), found that in atherosclerosis that perlecan deficiency leads to less atherosclerosis [207]. However, whilst they found that loss of perlecan lead to less atherosclerosis in early lesions, in more advanced lesions, perlecan was found in the core regions of the atherosclerotic plaque, and perlecan was found to be a major component of more advanced plaques [207]. They also showed that decreased perlecan caused a dramatic and significant reduction in lesion in size in male mice, however, this result was not significant in female mice suggesting that, as men are more pre-disposed to cardiovascular disease than

women, perlecan secretion may play a part in this genetic difference [207,208]. Perlecan, along with other proteoglycans, is also associated with lipid retention in the subendothelial layer, which is a marker for early atherosclerosis [209]. One study found mice with proteoglycan binding defection LDL, developed significantly less atherosclerosis than wild-type LDL, suggesting that the subendothelial region, which contains perlecan, and the retention of lipids is an early step in atherogenesis [209]. This suggests that the decreased level of basal secretion of perlecan that treatment with atorvastatin showed could initially decrease the risk of atherosclerosis by reducing lipid retention, however, in more developed plaques, the increase apical secretion could contribute to plaques, as perlecan was found at the core of the atherosclerotic lesions.

Collagen-α1 is a component of the ECM, which is secreted by ECs. ECM deposition is an important contributor to the cardiac remodelling which is seen following myocardial injury, such as in myocardial infarction [210]. When atorvastatin is added to HUVEC, the basal secretion collagen is initially almost 10-fold that of the apical secretion. The addition of 15 nM atorvastatin reduces the basal secretion to less than 1.5-fold that of the apical secretion, and 50 nM is less than 1.25-fold (Figure 4.13A). The overall secretion of collagen decreases with increasing concentrations of atorvastatin (4.13B). A study by Martin *et al* (2005) found that atorvastatin appeared to directly inhibit the production of collagen by cardiac fibroblasts in a dose-dependent manner [210]. The data from this study suggested that statins could show mechanistic support for use in patients with heart failure. My data of the secretion of collagen supports their data, as it also showed a decrease in the overall secretion of collagen in a dose-dependent manner (Figure 13B). However, my data expands on the finding of Martin *et al* (2005), as it clearly shows the difference in both apical and basal secretion of collagen depending on dose, as well as the overall secretion. This is important as it shows whilst the basal secretion of collagen-α1 decreases, the apical levels increases, although the overall level decreases. Normally, the secretion of collagen is strongly polarised to the basolateral surface of the cell, but as the dose of atorvastatin increases, the basal secretion decreases. This could suggest that although atorvastatin decreases the overall secretion of collagen α1, the apical secretion of collagen could in fact increase, and the effects of this would have to be investigated further.

Another group of proteins showed that with atorvastatin treatment, the apical secretion of these proteins noticeably increased, whilst the basal secretion of these proteins noticeably decreased (Figure 4.14). One protein, latent-transforming growth factor β-binding protein 2 (LTBP2) was initially secreted twice as much basally than apically (Figure 4.14A), however, this ratio decreased at 15 nM, and again at 50 nM, where in fact the apical secretion is higher

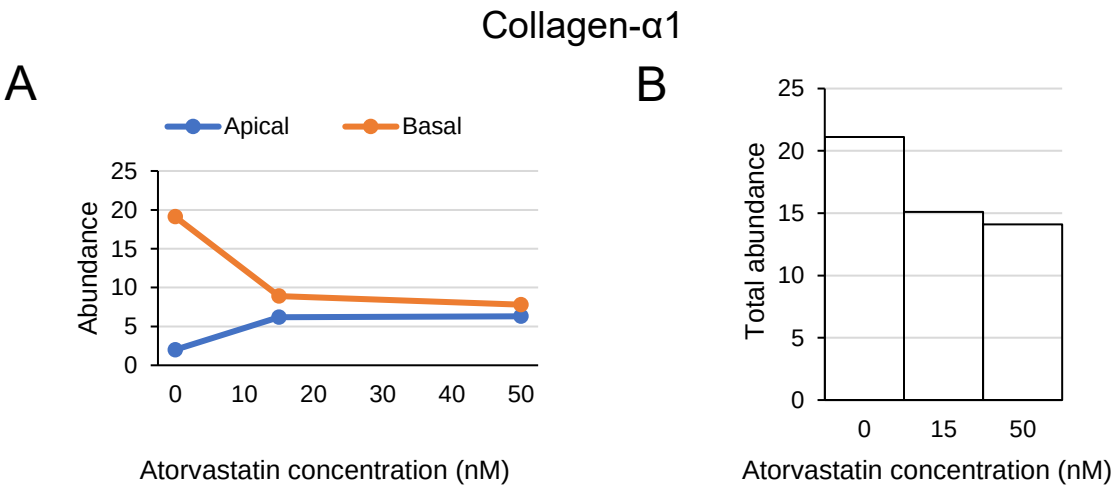

Figure 4.13 Apical secretion of collagen-α1 increases with atorvastatin treatment, whilst basal secretion decreases. Change in the abundance of collagen-α1 in response to various concentrations of atorvastatin. A) The separate apical and basal abundance B) Pooled data of the separate abundances.

Latent-transforming growth factor β-binding protein 2

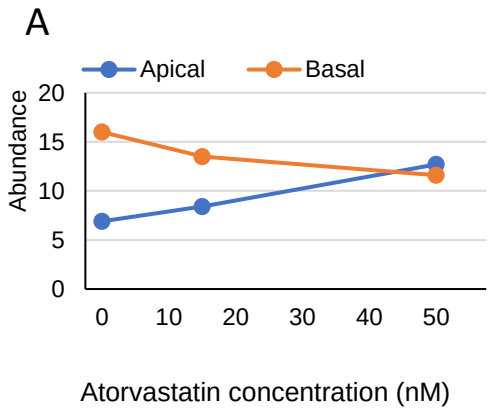

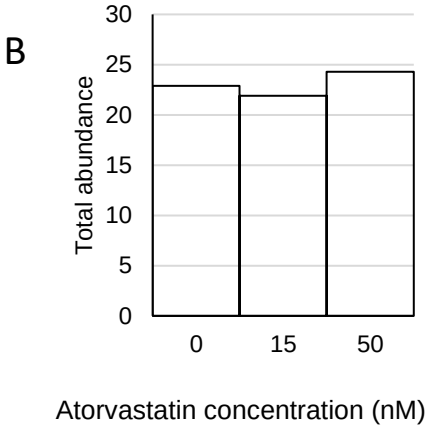

Twisted gastriculation protein homolog 1

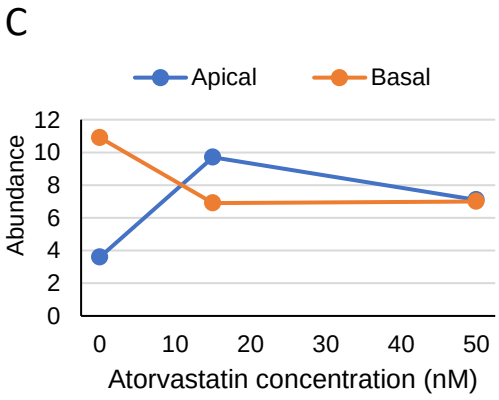

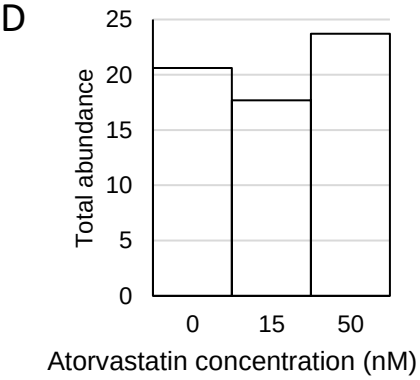

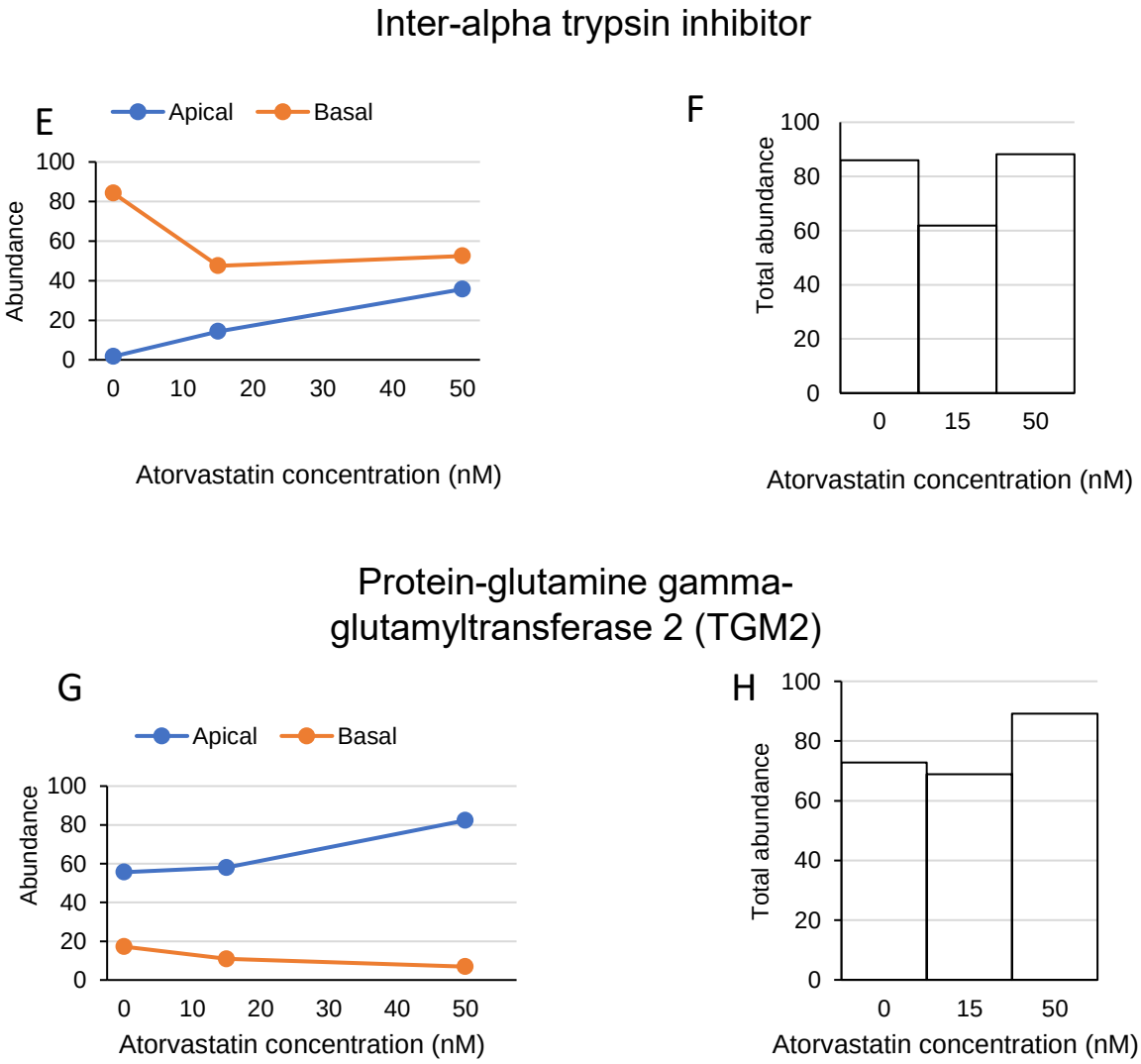

Figure 4.14 Apical secretion of certain proteins increases, whilst basal level decreases with atorvastatin treatment. Change in the abundance of proteins in response to various concentrations of atorvastatin. (A,C,E,G) show the separate apical and basal abundance, and (B,D,F,H) show the pooled data of the separate abundances.

than the basal secretion (Figure 4.14A). Unlike other members of the LTBP family, it is transforming growth factor-β independent. LTBP2 is also an ECM protein and interacts with fibrillin in the ECM, and is expressed abundantly in elastic tissues [211]. Studies have suggested that LTBP2 plays a role in the development of the extracellular fibrils, and may be involved in protecting these fibrils from enzyme degradation, rather than the formation of these fibrils [212]. Studies have also shown that LTBP2 could be an antiadhesive matrix component, and increased secretion from the apical surface could be angiogenic, which other studies have previously reported statins to be [213,214]. Like the other secreted proteins, the overall abundance of LTBP2 does not show a noticeable difference at any concentration (Figure 4.14B), suggesting that it is the change in polarised secretion of LTBP2 that could show these effects.

Twisted gastriculation protein homolog 1 (TWSG1) is a known antagonist of bone morphogenic protein 2 (BMP-2) activity [215]. BMPs are secreted by macrophages and are important regulators in blood vessel and vascular disease, and module vascular calcification [215–217]. BMPs are also involved in inflammation and have been shown to stabilise atherosclerotic plaques, by inducing vascular calcification [217]. In this study, at 0 nM the basal secretion of TWSG1 is twice as high as the apical secretion, however at 15 nM the apical secretion increases to higher than that of the basal secretion (Figure 4.14C). At 50 nM, the apical/basolateral secretion is equal (Figure 4.14C). BMP-2 secretion is downregulated in statin treatment, which suggests that statins affect proteins that are involved in the modulation of BMP [218]. However, TWSG1 is an antagonist of BMP, and my study shows that the total abundance of TWSG1 is only slightly upregulated at 15 nM atorvastatin, and decreases to below the 0 nM level at 50 nM (Figure 4.14D), it suggests that other proteins involved in the modulation of BMP-2 are involved. Causes of atherosclerosis, such as oxidised low-density lipoproteins induce the expression of BMP-2s, suggesting BMP2 is important in the development of atherosclerosis [217]. As my study found the overall secretion of TWSG1 did not markedly change with atorvastatin treatment, and the study by Zhang *et al* (2008) used higher concentrations of atorvastatin (1-10 μM), further investigations are needed to see whether this effect also occurs at lower concentrations, and whether this can give insight into other roles of statins on ECs [218].

Inter-α trypsin inhibitors (IαI) are plasma proteins that function as protease inhibitors. IαI forms complexes with hyaluronan, a component of the ECM to create serum-derived hyaluronan associated protein (SHAP)-HA complexes [219]. These complexes are found to be increasing in inflammatory conditions, including rheumatoid arthritis and Crohn's disease [219]. My study found that initially, the apical secretion of IαI is very low, however this increases at 15 nM, and increases again at 50 nM (Figure 4.14E). The basal secretion, however, decreases with

addition of atorvastatin (Figure 4.14F). There are very few studies into IαI, however, some studies have suggested it interacts with hyaluronan, which forms part of the ECM [219]. My study does not show the overall abundance of IαI confidently increasing or decreasing, so previous studies into IαI cannot be generalised to the effects on statins. However, as this protein plays a role in inflammation, and interacts with proteins within the ECM, it is reasonable to assume that statins would influence the polarised secretion of this protein [219]. Nonetheless, again, further investigations are needed into this protein.

Protein-glutamine gamma-glutamyl transferase 2 (TGM2), is also known as tissue glutaminase, a calcium dependent enzyme that crosslinks proteins between the amino lysine group and the carboxamide of glutamine. As an extracellular protein, TGM2 binds protein in the ECM, especially fibronectin, and plays roles in cell adhesion and wound healing [220]. My study shows that initially, the apical secretion of TGM2 was twice the amount of the basal secretion (Figure 4.14G), which is unlike many of the other proteins where the opposite occurred. With increasing concentrations of atorvastatin, the basal secretion of TGM2 decreased, however the apical secretion increased (Figure 4.14G), until it was over 10-fold higher than the basal secretion at 50 nM. Overall, the total abundance of atorvastatin increases with increasing concentrations of atorvastatin, however, at 15 nM atorvastatin the total abundance decreases slightly (Figure 4.14H). A previous study on the effect of TGM2 secretion on HUVEC treated with atorvastatin also found that atorvastatin treatment increased the expression of TGM2 [221]. This study showed that by cross-linking the ECM, TGM2 was able to indirectly stabilise the basement membrane, which could promote integrity of the vessel wall, providing previously unknown information about the pleiotropic effects of statins [221]. The study by Soehnlein *et al* (2004), used higher concentrations (1-10 μM) than my study, suggesting that the increase in TGM2 expression could occur at lower concentrations of atorvastatin than they used [221]. However, the effects of increased TGM2 showing stabilising effects mainly occurred in the ECM, by cross linking ECM components including fibronectin, whilst my study showed that the basal secretion of TGM2 decreased with increasing concentrations of atorvastatin. Whilst my study provides further evidence that atorvastatin does increase TGM2 expression, further studies are needed to investigate the stabilising effects of atorvastatin at the lower concentrations I used, and the significance of the changed polarisation. Studies also found that increased expression of TGM2 stabilised atherosclerotic plaques, decreasing their chance of rupture [221,222]. This suggests one of the positive effect's statins may have, endothelial stability.

Macrophage migration inhibitory factor (MIF) shows an increase in total abundance with increasing atorvastatin treatment (Figure 4.15B). Unlike the other proteins, the apical secretion

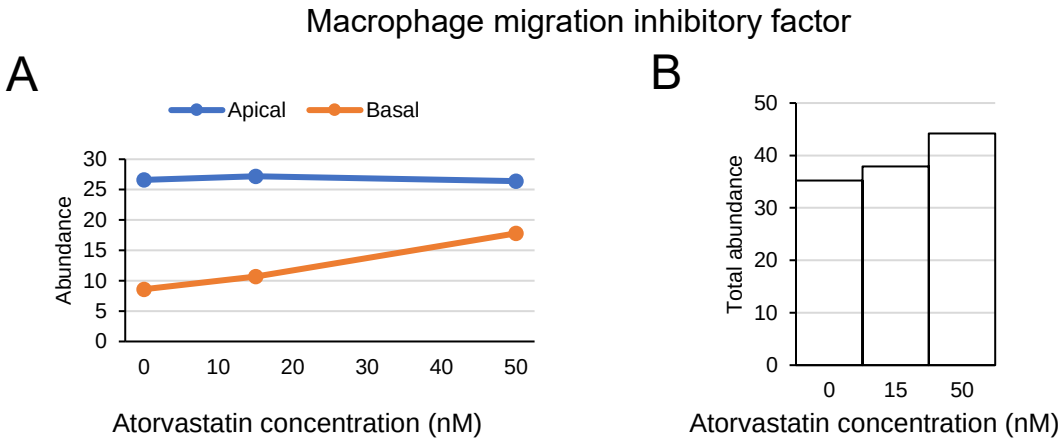

Figure 4.15 Apical secretion of macrophage migration inhibitory factor remains steady, whilst basal secretion noticeably changes with atorvastatin treatment. Change in the abundance of proteins in response to various concentrations of atorvastatin. (A) show the separate apical and basal abundance, and (B) show the pooled data of the separate abundances.

is higher than the basal at 0 nM (Figure 4.15A), and the apical secretion remains steady at increasing concentrations of atorvastatin (Figure 4.15A). However, unlike the other proteins which had their secretion changed by atorvastatin, the basal secretion of MIF increases with increasing concentrations of atorvastatin (Figure 4.15A). The role of MIF within the body is to prevent the macrophage migration out of capillaries. During times of stress, and pro-inflammatory mediators, MIF is rapidly released from ECs [223]. MIF is a key cytokine in inflammatory immune diseases, such as rheumatoid arthritis MIF has also been linked to the formation of atherosclerosis, and MIF has been shown to be functionally linked to atherosclerotic plaques *in vivo* [224]. Whilst this provides no suggestion of why the protein is upregulated with increasing additions of atorvastatin, MIF has been shown to stimulate the production of quiescent mouse fibroblasts, which are critical for wound healing, where it is rapidly released [225]. However, again the role in wound healing is uncertain, and needs to be ascertained by further research. However, as the increase in basal secretion is only two-fold (Figure 4.15A), the significance of these is unknown.

My results show that atorvastatin changes the polarised secretion of a subset of proteins. My optimisation for mass spectrometry involving the permeability experiments and images suggest that this is not due to leakage of the protein across the cell monolayer, but instead the addition of atorvastatin causes an internal change in the protein's delivery to the particular surface membrane. Previous studies have suggested that the addition of statins improve endothelial integrity, and that statins could be protective against atherosclerosis, in ways other than reduce cholesterol levels [226]. However, due to the current lack of studies into polarised secretion of ECs, further investigation is needed into these proteins, and whether their change in polarised secretion is implicated in improving endothelial function.

4.3 Conclusion

The importance of statins as a prescribed drug cannot be understated, with roughly 6 million people taking them each day. However, whilst the cholesterol lowering effects of statins are well known, there is limited understanding about the off-target effects. One of the main indications for statins is atherosclerosis, where the arteries become hardened and narrow, which can lead to myocardial infarction. As ECs line these vessels, any pleiotropic effects on the polarised secretion of ECs could be clinically relevant.

After finding the statins did not significantly affect the integrity of the EC monolayer, I was able to examine the polarised secretome of statin treated HUVEC. Using mass spectrometry, I compared the apical/basolateral secretion of HUVEC at 0 nM, 15 nM and 50 nM atorvastatin treatment. These results allowed me to investigate whether atorvastatin affected polarised secretion, and whether there was a relationship between the dose and how much the secretion was affected. Whilst much of the data in this chapter was at least n=3, the data obtained in my mass spectrometry was n=1, due to time limitations. Therefore, no clear conclusion or importance can be drawn from the analysis of this dataset. The proteins selected for analysis may not show any difference in secretion in another mass spectrometry experiment, and other proteins discarded may be of importance. If I did have time to make my data n=3, I would look at the proteins which the secretion changed consistently in all of the experiments, reducing variability and improving validity of my results.

In my analysis I also removed proteins with 0 abundance, in any of the conditions. As I had already had to disregard my results from the 5 nM sample, having a 0 value in any of the other samples would further reduce my ability to see any patterns within my results. It is debatable of whether this was the correct decision to make, as one of these proteins may have been so significantly affected by the addition of statins that the amount secreted dropped to 0. However, due to this being a preliminary study, it would not have been feasible to include any 0 values.

My results showed that atorvastatin mainly increased the apical/basolateral secretion of a subset of proteins, particularly of proteins involved in the ECM, such as biglycan and TSP1. I then analysed this subset further to find proteins with a relationship between the apical/basolateral ratio of protein secretion, and the increasing dose of atorvastatin treatment.

My research showed that atorvastatin increased the apical/basal polarised secretion of proteins including biglycan and perlecan, which have both been previously shown to increase the risk of atherosclerosis [200,207]. However, my research also showed that atorvastatin treatment increased the apical/basal secretion ratio of TGM2, as well as increasing the overall

secretion. Previous studies have shown that the increased secretion of TGM2 stabilises atherosclerotic plaques, decreasing their chance of rupture [221,222]. The rupture of atherosclerotic plaques often results in occurrence of a myocardial infarction, which can be fatal [169]. Other proteins affected by the addition of statins are TWSG1, an antagonist of the cytokine BMP-2 and the cytokine MIF. Increased secretion of BMP-2 and MIF is thought to be implicated in the progression of atherosclerotic plaques. However, the increased secretion of TWSG1 may decrease the secretion of BMP-2 therefore decreasing the risk of atherosclerosis [217].

The data from my study suggests that the addition of statins can have both a positive and negative effect on the formation, progression, and prognosis of atherosclerosis. However, there is limited understanding of the secretion of ECs, and even less into the polarised secretion. Further research is required to investigate the secretome of ECs, in order to really understand the implications of the altered secretion that occurs within the formation of atherosclerotic plaques. This research would allow us to understand the effect of statins upon the secretion of ECs in atherosclerosis, and the contribution to the disease progression. Further research could provide information about other therapeutic uses of statins, as well as potentially highlighting drug contraindications.

Chapter 5 Future Directions

Currently, few studies have investigated the polarised secretion of ECs, or how this process is regulated. My study provides information about the proteins which are secreted, and whether they are secreted from the apical or basolateral surface of ECs. As expected, the secretion of many ECM proteins such as perlecan were found to basolaterally polarised.

In order for the secretion to be polarised within the EC, the protein must have previously been sorted to the correct surface. There is currently limited information about the mechanisms involved in the polarised sorting of these proteins, however, a previous study has highlighted a mechanism involving the protein liprin-α1 has been shown to be involved in the sorting of fibronectin [35]. Fibronectin is a known component of the extracellular matrix which underlies endothelial cells, which I showed in my early analysis was basolaterally polarised. My data from my ELISA provides some evidence that liprin-α1 is involved in the secretion of FN from the basolateral surface. However, the fact I was coating my Transwell with FN, and the small change in secretion observed in my mass spectrometry data means further investigation is required.

Successfully culturing HUVEC can be difficult, and studies have shown that HUVEC have a higher proliferation rate when cell plates are coated with ECM substrates prior to cell seeding [227]. The culturing of HUVEC in our lab had been shown to be most successful when plastic culture dishes were coated with FN, and when Transwell inserts were coated in a triple coat of human FN, bovine collagen, and bovine gelatin.

When studying the effect of liprin-α1 depletion and statin treatment of HUVEC, my Transwells were each coated with this triple coat. Due to the cell culture substrate containing human FN, there is a possibility that the amount of FN secretion I recorded, both using ELISA and mass spectrometry may be inaccurate. The cell culture substrates also included bovine gelatin and collagen. Whilst I removed non-human contaminants from my mass spectrometry data during analysis, there is a possibility that this may have affect EC secretion, and the results found in my study would not be replicable without these substrates using for coating, and hence *in vivo*. However, due to time limitations, it was not possible to test and validate different methods for successfully culturing HUVEC.

The dysregulated secretion of fibronectin is known to be a contributing factor in the progression of atherosclerosis. In my study I aimed to find out whether depleting liprin-α1 affected the secretion of any other proteins. The depletion of liprin-α1 affected the apical/basolateral secretion of a subset of proteins, which could suggest liprin-α1 is involved

in the sorting of these proteins, the proteins are trafficked along with FN, or the proteins were compensating for the decreased FN secretion. To make my results more robust and to ensure I had identified correct proteins, I would repeat my mass spectrometry and perform ELISAs of the conditioned media. I could also examine if any of these proteins affected are involved in the formation of an atherosclerotic plaque, as this could provide further insight into the pathogenesis of atherosclerosis. For some of the proteins identified, the overall secretion decreased when liprin-α1 was depleted within HUVEC. A further investigation for these proteins could involve staining for the particular protein, to identify if it had accumulated within the cell.

For the next part of my study, I explored the effects of two statins upon HUVEC. Statins are currently one of the most commonly prescribed drugs in the UK, with factors such as an ageing population, increasing rates of obesity and increasing rates of heart disease, the number of statins prescribed is undoubtedly going to rise over the coming years. Whilst statins are well known for their plasma cholesterol lowering properties by inhibiting HMG-CoA reductase, there is widening interest into pleiotropic effects statins may have, especially in ECs. In my study, I focussed upon the effects of statins on ECs, and specifically the effect on the polarised secretion of proteins.

Throughout my study I experienced various limitations. The simvastatin powder used in my experiment had a 98% purity and the atorvastatin had a purity of 99.93%. Therefore, I cannot be certain whether the effects were a direct effect of the statin treatment, or whether the impurities in the sample affected this in any way. Repeating this experiment with a purer simvastatin sample would provide more accurate results, which could provide further insight into the proteins affected.

During the preparation for the mass spectrometry, the 5 nM atorvastatin treated HUVEC sample was lost, and I used a sample from a previous experiment. However, after comparing the results of the replacement 5 nM sample to the samples at other atorvastatin doses, I concluded the results were incomparable and could not be used. This reduced my ability to see relationships between the dose of statins and the polarised secretion ratios, meaning I could have missed some proteins which would have showed relationships. To continue this study, I would need to repeat this experiment with a 5 nM sample to fully investigate any effect. After this, western blots could be performed on the proteins indicated within the mass spectrometry to measure their expression. I could then use methods such as immunofluorescence to examine whether treatment with statins affected their location within the cell, in comparison to cells which had not been treated with statins. These proteins could also be depleted using CRISPR/cas9 to further study the role of the protein within ECs.

As all my current work has involved using HUVEC, the use of other cell lines could provide further validation, for example using human coronary artery endothelial cells (HCAEC). Using these cells may be more physiologically relevant, as atherosclerosis primarily occurs within the coronary arteries. Therefore, it would be interesting to see whether the same changes in polarised secretion were observed.

HUVEC have been shown to have sex differences [228]. As males have a higher risk of developing cardiovascular disease than women, I could use single donor HUVEC with a known sex to see whether the effects in male HUVEC differed from those in female HUVEC. These steps would improve the clinical validity of my results and could aid future studies into these effects. I could also expand the range of statins, examining the effects of the other common statins within the UK, such as pravastatin and rosuvastatin. This would allow me to analyse whether the effects seen could be generalised across all statins, or whether they were specific to particular statins.

There have already been some studies into effects of statins on EC function in apoE$^{-/-}$ mice, which have shown statins have a positive effect on ECs *in vivo,* such as promoting eNOS function, and enhancing the response to the vasoconstrictive ET-1 in the aorta [229,230] However, many of these studies have used concentrations well beyond those used for human treatment. Throughout my study I used clinically relevant concentrations of statins to investigate the effect on protein secretion. If my results were repeated and verified, these concentrations could be investigated in apoE$^{-/-}$ mice to provide more clinically valid results.

As currently there are few studies into the methods of protein sorting for polarised secretion, further studies would be needed in order to elucidate these methods, before investigations into changes in this pathway could be performed. These further suggestions and improvements would build a more solid basis for my results and could possibly indicate other clinical conditions statins could be used to treat.

References

1 Galley, H. F. and Webster, N. R. (2004) Physiology of the endothelium. Br. J. Anaesth. **93**, 105–113.

2 Chi, J.-T., Chang, H. Y., Haraldsen, G., Jahnsen, F. L., Troyanskaya, O. G., Chang, D. S., Wang, Z., Rockson, S. G., van de Rijn, M., Botstein, D., et al. (2003) Endothelial cell diversity revealed by global expression profiling. Proc. Natl. Acad. Sci. **100**, 10623–10628.

3 Sandoo, A., Veldhuijzen van Zanten, J. J. C. S., Metsios, G. S., Carroll, D. and Kitas, G. D. (2010) The Endothelium and Its Role in Regulating Vascular Tone. Open Cardiovasc. Med. J. **4**, 302–312.

4 Yuan, L., Chan, G. C., Beeler, D., Janes, L., Spokes, K. C., Dharaneeswaran, H., Mojiri, A., Adams, W. J., Sciuto, T., Garcia-Cardeña, G., et al. (2016) A role of stochastic phenotype switching in generating mosaic endothelial cell heterogeneity. Nat. Commun. **7**, 10160.

5 Bierhansl, L., Conradi, L.-C., Treps, L., Dewerchin, M. and Carmeliet, P. (2017) Central Role of Metabolism in Endothelial Cell Function and Vascular Disease. Physiology **32**, 126–140.

6 Yau, J. W., Teoh, H. and Verma, S. (2015) Endothelial cell control of thrombosis. BMC Cardiovasc. Disord. 130.

7 Cines, D. B., Pollak, E. S., Buck, C. A., Loscalzo, J., Zimmerman, G. A., McEver, R. P., Pober, J. S., Wick, T. M., Konkle, B. A., Schwartz, B. S., et al. (1998) Endothelial cells in physiology and in the pathophysiology of vascular disorders. Blood **91**, 3527–3561.

8 MacKman, N. (2009) The role of tissue factor and factor VIIa in hemostasis. Anesth. Analg. **108**, 1447–1452.

9 Minshall, R. D. and Malik, A. B. (2006) Transport across the endothelium: Regulation of endothelial permeability. Handb. Exp. Pharmacol. **176**, 107–144.

10 Daneman, R. and Prat, A. (2014) The Blood Brain Barrier (BBB). Cold Spring Harb. Perspect. Biol. **7**, a020412.

11 Mann, G. E., Yudilevich, D. L. and Sobrevia, L. (2003) Regulation of Amino Acid and Glucose Transporters in Endothelial and Smooth Muscle Cells. Physiol. Rev. **83**, 183–252.

12 Huang, Y., Lei, L., Liu, D. G., Jovin, I., Russell, R., Johnson, R. S., Di Lorenzo, A. and Giordano, F. J. (2012) Normal glucose uptake in the brain and heart requires an endothelial cell-specific HIF-1α-dependent function. Proc. Natl. Acad. Sci. U. S. A. **109**, 17478–17483.

13 Sweeney, M. D., Zhao, Z., Montagne, A., Nelson, A. R. and Zlokovic, B. V. (2019) Blood-brain barrier: From physiology to disease and back. Physiol. Rev. **99**, 21–78.

14 Klepper, J. and Voit, T. (2002) Facilitated glucose transporter protein type 1 (GLUT1) deficiency syndrome: Impaired glucose transport into brain - A review. Eur. J. Pediatr. **161**, 295–304.

15 McCall, A. L., Van Bueren, A. M., Huang, L., Stenbit, A., Celnik, E. and Charron, M. J. (1997) Forebrain endothelium expresses GLUT4, the insulin-responsive glucose

transporter. Brain Res. **744**, 318–326.

16 Theodorou, K. and Boon, R. A. (2018) Endothelial cell metabolism in atherosclerosis. Front. Cell Dev. Biol. **6**, 82.

17 Tousoulis, D., Kampoli, A.-M., Tentolouris, C., Papageorgiou, N. and Stefanadis, C. (2012) The role of nitric oxide on endothelial function. Curr. Vasc. Pharmacol. **10**, 4–18.

18 Van Winkle, L. J., Tesch, J. K., Shah, A. and Campione, A. L. (2006) System B0,+ amino acid transport regulates the penetration stage of blastocyst implantation with possible long-term developmental consequences through adulthood. Hum. Reprod. Update **12**, 145–157.

19 Smith, Q. R. (2000) Transport of Glutamate and Other Amino Acids at the Blood-Brain Barrier. J. Nutr. **130**, 1016S-1022S.

20 Caraceni, P., Tufoni, M. and Bonavita, M. E. (2013) Clinical use of albumin. Blood Transfus. **11**, s18–s25.

21 Millici, A. J., Watrous, N. E., Stukenbrok, H. and Palade, G. E. (1987) Transcytosis of albumin in capillary endothelium. J. Cell Biol. **105**, 2603–2612.

22 Sowa, G. (2012) Caveolae, caveolins, cavins, and endothelial cell function: New insights. Front. Physiol. **2**, 120.

23 Geith, S., Renner, B., Rabe, C., Stenzel, J. and Eyer, F. (2017) Ibuprofen plasma concentration profile in deliberate ibuprofen overdose with circulatory depression treated with therapeutic plasma exchange: A case report. BMC Pharmacol. Toxicol. **18**, 81.

24 Merlot, A. M., Kalinowski, D. S. and Richardson, D. R. (2014) Unraveling the mysteries of serum albumin-more than just a serum protein. Front. Physiol. **5**, 299.

25 Liu, Z., Liu, J., Wang, S., Liu, S. and Zhao, Y. (2016) Neuronal uptake of serum albumin is associated with neuron damage during the development of epilepsy. Exp. Ther. Med. **12**, 695–701.

26 Frantz, C., Stewart, K. M. and Weaver, V. M. (2010) The extracellular matrix at a glance. J. Cell Sci. **Pt 24**, 4195–4200.

27 Fidler, A. L., Boudko, S., Rokas, A. and Hudson, B. G. (2018) the triple helix of collagens - an ancient protein structure. J. Cell Sci. **131**, 2039250.

28 Mouw, J. K., Ou, G. and Weaver, V. M. (2014) Extracellular matrix assembly: A multiscale deconstruction. Nat. Rev. Mol. Cell Biol. **15**, 771–785.

29 Timpl, R., Rohde, H., Robey, P. G., Rennard, S. I., Foidart, J. M. and Martin, G. R. (1979) Laminin - A glycoprotein from basement membranes. J. Biol. Chem. **254**, 9933–9937.

30 Hohenester, E. and Yurchenco, P. D. (2013) Laminins in basement membrane assembly. Cell Adhes. Migr. **7**, 56–63.

31 Hamill, K. J., Kligys, K., Hopkinson, S. B. and Jones, J. C. R. (2009) Laminin deposition in the extracellular matrix: a complex picture emerges. J. Cell Sci. **122**, 4409–4417.

32 Parkin, J. Des, San Antonio, J. D., Pedchenko, V., Hudson, B., Jensen, S. T. and Savige, J. (2011) Mapping structural landmarks, ligand binding sites, and missense mutations to the collagen IV heterotrimers predicts major functional domains, novel

interactions, and variation in phenotypes in inherited diseases affecting basement membranes. Hum. Mutat. **32**, 127–143.

33 Kowalczyk, Andrew, Tulloh, Helen, and McKeown-Longo, P. J. (1990) Polarized fibronectin secretion and localized matrix assembly sites correlate with subendothelial matrix formation. Blood **75**, 2335–2342.

34 Pankov, R. (2002) Fibronectin at a glance. J. Cell Sci. **115**, 3861–3863.

35 Mana, G., Clapero, F., Panieri, E., Panero, V., Böttcher, R. T., Tseng, H. Y., Saltarin, F., Astanina, E., Wolanska, K. I., Morgan, M. R., et al. (2016) PPFIA1 drives active α5β1 integrin recycling and controls fibronectin fibrillogenesis and vascular morphogenesis. Nat. Commun. **7**, 1–20.

36 Ni, Y., Li, J. M., Liu, M. K., Zhang, T. T., Wang, D. P., Zhou, W. H., Hu, L. Z. and Lv, W. L. (2017) Pathological process of liver sinusoidal endothelial cells in liver diseases. World J. Gastroenterol. **23**, 7666–7677.

37 Michiels, C. (2003) Endothelial cell functions. J. Cell. Physiol. **196**, 430–443.

38 Federici, A. B. (2003) The factor VIII/von Willebrand factor complex: basic and clinical issues. Haematologica **88**, EREP02.

39 Peyvandi, F., Garagiola, I. and Baronciani, L. (2011) Role of von Willebrand factor in the haemostasis. Blood Transfus. **Suppl 2**, s3–s8.

40 Pearson, J. D. (2000) Normal endothelial cell function. Lupus **3**, 183–188.

41 Smith, S. A., Travers, R. J. and Morrissey, J. H. (2015) How it all starts: Initiation of the clotting cascade. Crit. Rev. Biochem. Mol. Biol. **50**, 326–336.

42 Lip, G. Y. H. and Blann, A. (1997) von Willebrand factor: A marker of endothelial dysfunction in vascular disorders? Cardiovasc. Res. **34**, 255–265.

43 James, P. D. and Goodeve, A. C. (2011) von Willebrand Disease. Genet. Med. **13**, 365–376.

44 Martin, F. A., Murphy, R. P. and Cummins, P. M. (2013) Thrombomodulin and the vascular endothelium: insights into functional, regulatory, and therapeutic aspects. Am. J. Physiol. Circ. Physiol. **304**, H1585–H1957.

45 Isermann, B., Hendrickson, S. B., Zogg, M., Wing, M., Cummiskey, M., Kisanuki, Y. Y., Yanagisawa, M. and Weiler, H. (2001) Endothelium-specific loss of murine thrombomodulin disrupts the protein C anticoagulant pathway and causes juvenile-onset thrombosis. J. Clin. Invest. **108**, 537–546.

46 Van Hinsbergh, V. W. M. (2012) Endothelium - Role in regulation of coagulation and inflammation. Semin. Immunopathol. **34**, 93–106.

47 Sprague, A. H. and Khalil, R. A. (2009) Inflammatory cytokines in vascular dysfunction and vascular disease. Biochem. Pharmacol. **78**, 539–552.

48 Vallance, P. and Chan, N. (2001) Endothelial function and nitric oxide: clinical relevance. Heart **85**, 342–350.

49 Zhang, C. (2008) The role of inflammatory cytokines in endothelial dysfunction. Basic Res. Cardiol. **103**, 398–406.

50 Hunt, B. J. and Jurd, K. M. (1998) Endothelial cell activation. A central pathophysiological process. BMJ **316**, 1328–1329.

51 Øynebråten, I., Bakke, O., Brandtzaeg, P., Johansen, F. E. and Haraldsen, G. (2004)

Rapid chemokine secretion from endothelial cells originates from 2 distinct compartments. Blood **104**, 314–320.

52 Swerlick, R. A. and Lawley, T. J. (1993) Role of microvascular endothelial cells in inflammation. J. Invest. Dermatol. **1**, 111S-115S.

53 Buzzeo, M. P., Yang, J., Casella, G. and Reddy, V. (2007) Hematopoietic stem cell mobilization with G-CSF induces innate inflammation yet suppresses adaptive immune gene expression as revealed by microarray analysis. Exp. Hematol. **35**, 1456–155.

54 Smith, C. (1993) Endothelial adhesion molecules and their role in inflammation. Can J Physiol Pharmacol. **71**, 76–87.

55 Jain, R. K. (2003) Molecular regulation of vessel maturation. Nat. Med. **9**, 685–693.

56 Biga, L., Dawson, S., Harwell, A., Hopkins, R., Kaufmann, J., LeMaster, M., Matern, P., Morrison-Graham, K., Quick, D. and Runyeon, J. (2012) 20.1 Structure and Function of Blood Vessels – Anatomy and Physiology. Anat. Physiol.

57 Chaudhry, R. and Rehman, A. (2018) Physiology, Cardiovascular. StatPearls.

58 Westerhof, N., Lankhaar, J. W. and Westerhof, B. E. (2009) The arterial windkessel. Med. Biol. Eng. Comput. **47**, 131–141.

59 Schöneberg, J., De Lorenzi, F., Theek, B., Blaeser, A., Rommel, D., Kuehne, A. J. C., Kießling, F. and Fischer, H. (2018) Engineering biofunctional in vitro vessel models using a multilayer bioprinting technique. Sci. Rep. **8**, 10430.

60 Tucker, W. D. and Mahajan, K. (2018) Anatomy, Blood Vessels. StatPearls.

61 Dela Paz, N. G. and D'Amore, P. A. (2009) Arterial versus venous endothelial cells. Cell Tissue Res. **335**, 5–16.

62 Martinez-Lemus, L. A. (2012) The dynamic structure of arterioles. Basic Clin. Pharmacol. Toxicol. **1**, 5–11.

63 Rajendran, P., Rengarajan, T., Thangavel, J., Nishigaki, Y., Sakthisekaran, D., Sethi, G. and Nishigaki, I. (2013) The vascular endothelium and human diseases. Int. J. Biol. Sci. **9**, 1057–1069.

64 Gimbrone, M. A. and García-Cardeña, G. (2016) Endothelial Cell Dysfunction and the Pathobiology of Atherosclerosis. Circ. Res. **4**, 620–636.

65 Rafieian-Kopaei, M., Setorki, M., Doudi, M., Baradaran, A. and Nasri, H. (2014) Atherosclerosis: Process, indicators, risk factors and new hopes. Int. J. Prev. Med. **5**, 927–946.

66 Singh, R. B., Mengi, S. A., Xu, Y. J., Arneja, A. S. and Dhalla, N. S. (2002) Pathogenesis of atherosclerosis: A multifactorial process. Exp. Clin. Cardiol. **7**, 40–53.

67 Satchell, S. C. and Braet, F. (2009) Glomerular endothelial cell fenestrations: An integral component of the glomerular filtration barrier. Am. J. Physiol. - Ren. Physiol. **296**, F947–F956.

68 Perlin, J. R., Sporrij, A. and Zon, L. I. (2017) Blood on the tracks: hematopoietic stem cell-endothelial cell interactions in homing and engraftment. J. Mol. Med. **95**, 809–819.

69 Meissner, M. H. (2005) Lower extremity venous anatomy. Semin. Intervent. Radiol. **3**, 147–156.

70 van Bemmelen, P. S. (1990) The Mechanism of Venous Valve Closure. Arch. Surg. **5**, 617–619.

71 Spiridon, M. and Corduneanu, D. (2017) Chronic Venous Insufficiency: a Frequently Underdiagnosed and Undertreated Pathology. Maedica (Buchar). **12**, 59–61.

72 Campbell, B. (2006) Clinical review Varicose veins and their management. Bmj **752**, 287–292.

73 Pocock, G., Richards, C. D. and Richards, D. A. (2013) Human physiology.

74 Randolph, G. J. and Miller, N. E. (2014) Lymphatic transport of high-density lipoproteins and chylomicrons. J. Clin. Invest. **124**, 929–935.

75 Alexander, J. S., Ganta, V. C., Jordan, P. A. and Witte, M. H. (2010) Gastrointestinal lymphatics in health and disease. Pathophysiology **17**, 315–335.

76 Null, M. and Agarwal, M. (2019) Anatomy, Lymphatic System. StatPearls.

77 Kvietys, P. R. and Granger, D. N. (2010) Role of intestinal lymphatics in interstitial volume regulation and transmucosal water transport. Ann. N. Y. Acad. Sci. **1297**, E29–E43.

78 Hansen, K. C., D'Alessandro, A., Clement, C. C. and Santambrogio, L. (2015) Lymph formation, composition and circulation: A proteomics perspective. Int. Immunol. **27**, 219–227.

79 Elmore, S. A. (2006) Histopathology of the Lymph Nodes. Toxicol. Pathol. **34**, 425–454.

80 Haig, D. M., Hopkins, J. and Miller, H. R. P. (1999) Local immune responses in afferent and efferent lymph. Immunology **96**, 155–163.

81 Scallan, J. P., Zawieja, S. D., Castorena-Gonzalez, J. A. and Davis, M. J. (2016) Lymphatic pumping: mechanics, mechanisms and malfunction. J. Physiol. **594**, 5749–5768.

82 Wiig, H. and Swartz, M. A. (2012) Interstitial fluid and lymph formation and transport: Physiological regulation and roles in inflammation and cancer. Physiol. Rev. **92**, 1005–1060.

83 Wang, S., Nie, D., Rubin, J. P. and Kokai, L. (2017) Lymphatic Endothelial Cells under Mechanical Stress: Altered Expression of Inflammatory Cytokines and Fibrosis. Lymphat. Res. Biol. **15**, 130–135.

84 Aird, W. C. (2012) Endothelial cell heterogeneity. Cold Spring Harb. Perspect. Med. **2**, a006429.

85 Aird, W. C. (2007) Phenotypic heterogeneity of the endothelium: I. Structure, function, and mechanisms. Circ. Res. **100**, 158–173.

86 Minagar, A. and Alexander, J. S. (2003) Blood-brain barrier disruption in multiple sclerosis. Mult. Scler. **9**, 540–549.

87 Nag, S. (2017) The Blood–Brain Barrier: An Overview. In Reference Module in Neuroscience and Biobehavioral Psychology, pp 434–440.

88 Stamatovic, S. M., Keep, R. F. and Andjelkovic, A. V. (2008) Brain endothelial cell-cell junctions: how to "open" the blood brain barrier. Curr. Neuropharmacol. **6**, 179–192.

89 Stamatovic, S. M., Johnson, A. M., Keep, R. F. and Andjelkovic, A. V. (2016) Junctional proteins of the blood-brain barrier: New insights into function and

dysfunction. Tissue Barriers **4**, e1154641.

90 Qosa, H., Miller, D. S., Pasinelli, P. and Trotti, D. (2015) Regulation of ABC efflux transporters at blood-brain barrier in health and neurological disorders. Brain Res. **0**, 298–316.

91 Miller, D. S. (2010) Regulation of P-glycoprotein and other ABC drug transporters at the blood-brain barrier. Trends Pharmacol. Sci. **31**, 246–254.

92 Vogelgesang, S., Cascorbi, I., Schroeder, E., Pahnke, J., Kroemer, H. K., Siegmund, W., Kunert-Keil, C., Walker, L. C. and Warzok, R. W. (2002) Deposition of Alzheimer's β-amyloid is inversely correlated with P-glycoprotein expression in the brains of elderly non-demented humans. Pharmacogenetics **12**, 535–541.

93 Grant, D. M. (1991) Detoxification pathways in the liver. J. Inherit. Metab. Dis. **14**, 421–430.

94 Bilzer, M., Roggel, F. and Gerbes, A. L. (2006) Role of Kupffer cells in host defense and liver disease. Liver Int. **26**, 1175–1186.

95 Poisson, J., Lemoinne, S., Boulanger, C., Durand, F., Moreau, R., Valla, D. and Rautou, P. E. (2017) Liver sinusoidal endothelial cells: Physiology and role in liver diseases. J. Hepatol. **66**, 212–227.

96 DeLeve, L. D. and Maretti-Mira, A. C. (2017) Liver Sinusoidal Endothelial Cell: An Update. Semin. Liver Dis. **37**, 377–387.

97 Schuppan, D. and Afdhal, N. H. (2008) Liver cirrhosis. Lancet **371**, 838-851wi.

98 Jelkmann, W. (2011) Regulation of erythropoietin production. J. Physiol. **589**, 1251–1258.

99 Deen, W. M., Lazzara, M. J. and Myers, B. D. (2001) Structural determinants of glomerular permeability. Am. J. Physiol. - Ren. Physiol. **281**, F579–F596.

100 Ballermann, B. J. (2005) Glomerular endothelial cell differentiation. Kidney Int. **67**, 1668–1671.

101 Satchell, S. C. (2012) The glomerular endothelium emerges as a key player in diabetic nephropathy. Kidney Int. **82**, 949–951.

102 Atkins, G. B., Jain, M. K. and Hamik, A. (2011) Endothelial differentiation: Molecular mechanisms of specification and heterogeneity. Arterioscler. Thromb. Vasc. Biol. **31**, 1476–1484.

103 Lewis, E. J. and Xu, X. (2008) Abnormal glomerular permeability characteristics in diabetic nephropathy: implications for the therapeutic use of low-molecular weight heparin. Diabetes Care **31**, S202–S207.

104 Hill-Felberg, S., Wu, H. H., Toms, S. A. and Dehdashti, A. R. (2015) Notch receptor expression in human brain arteriovenous malformations. J. Cell. Mol. Med. **19**, 1986–1993.

105 Gimbrone, M. A., Topper, J., Nagel, T., Anderson, K. and Garcia-Cardeña, G. (2006) Endothelial Dysfunction, Hemodynamic Forces, and Atherogenesisa. Ann. N. Y. Acad. Sci. **902**, 230–239.

106 Turgeon, P. J., Sukumar, A. N. and Marsden, P. A. (2014) Epigenetics of cardiovascular disease: A new "beat" in coronary artery disease. Med. Epigenetics **2**, 37–52.

107 Brönneke, S., Brückner, B., Peters, N., Bosch, T. C. G., Stäb, F., Wenck, H., Hagemann, S. and Winnefeld, M. (2012) DNA methylation regulates lineage-specifying genes in primary lymphatic and blood endothelial cells. Angiogenesis **15**, 317–329.

108 Lee, J. L. and Streuli, C. H. (2014) Integrins and epithelial cell polarity. J. Cell Sci. **127**, 3217–3225.

109 Apodaca, G. (2018) Role of polarity proteins in the generation and organization of apical surface protrusions. Cold Spring Harb. Perspect. Biol. **10**, a027813.

110 Worzfeld, T. and Schwaninger, M. (2016) Apicobasal polarity of brain endothelial cells. J. Cereb. Blood Flow Metab. **36**, 340–362.

111 Campanale, J. P., Sun, T. Y. and Montell, D. J. (2017) Development and dynamics of cell polarity at a glance. J. Cell Sci. **130**, 1201–1207.

112 Bulgakova, N. A. and Knust, E. (2009) The Crumbs complex: from epithelial-cell polarity to retinal degeneration. J. Cell Sci. **122**, 2587–296.

113 Ngok, S. P., Lin, W. H. and Anastasiadis, P. Z. (2014) Establishment of epithelial polarity - GEF who's minding the GAP? J. Cell Sci. **127**, 3205–3215.

114 Cao, X., Surma, M. A. and Simons, K. (2012) Polarized sorting and trafficking in epithelial cells. Cell Res. **22**, 793–805.

115 Shin, K., Fogg, V. C. and Margolis, B. (2006) Tight Junctions and Cell Polarity. Annu. Rev. Cell Dev. Biol. **22**, 207–235.

116 Vogel, G. F., Klee, K. M. C., Janecke, A. R., Müller, T., Hess, M. W. and Huber, L. A. (2015) Cargo-selective apical exocytosis in epithelial cells is conducted by Myo5B, Slp4a, Vamp7, and Syntaxin 3. J. Cell Biol. **211**, 587–604.

117 Ang, S. F. and Fölsch, H. (2012) The role of secretory and endocytic pathways in the maintenance of cell polarity. Essays Biochem. **53**, 29–39.

118 Muse, M. E. and Crane, J. S. (2019) Physiology, Epithelialization. StatPearls.

119 Mutsaers, S. E. (2004) The mesothelial cell. Int. J. Biochem. Cell Biol. **36**, 9–16.

120 Bragulla, H. H. and Homberger, D. G. (2009) Structure and functions of keratin proteins in simple, stratified, keratinized and cornified epithelia. J. Anat. **214**, 516–559.

121 Matter, K. and Mellman, I. (1994) Mechamisms of cell polarity: sorting and transport in epithelial cells. Curr. Opin. Cell Biol. **6**, 545–554.

122 Paladino, S., Pocard, T., Catino, M. A. and Zurzolo, C. (2006) GPI-anchored proteins are directly targeted to the apical surface in fully polarized MDCK cells. J. Cell Biol. **172**, 1023–1034.

123 Vagin, O., Kraut, J. A. and Sachs, G. (2009) Role of N-glycosylation in trafficking of apical membrane proteins in epithelia. Am. J. Physiol. - Ren. Physiol. **296**, F459–F469.

124 Hara-Kuge, S., Ohkura, T., Ideo, H., Shimada, O., Atsumi, S. and Yamashita, K. (2002) Involvement of VIP36 in intracellular transport and secretion of glycoproteins in polarized madin-darby canine kidney (MDCK) cells. J. Biol. Chem. **277**, 16332–16339.

125 Delacour, D., Cramm-Behrens, C. I., Drobecq, H., Le Bivic, A., Naim, H. Y. and

Jacob, R. (2006) Requirement for galectin-3 in apical protein sorting. Curr. Biol. **16**, 408–414.

126 Vagin, O., Turdikulova, S. and Sachs, G. (2004) The H,K-ATPase β subunit as a model to study the role of N-glycosylation in membrane trafficking and apical sorting. J. Biol. Chem. **279**, 39026–39034.

127 Stoops, E. H. and Caplan, M. J. (2014) Trafficking to the Apical and Basolateral Membranes in Polarized Epithelial Cells. J. Am. Soc. Nephrol. **25**, 1375–1386.

128 Prydz, K., Live, G. and Tveit, H. (2012) The Role of Glycans in Apical Sorting of Proteins in Polarized Epithelial Cells. In Glycosylation (Petrescu, S., ed.), IntechOpen.

129 Gu, F., Crump, C. M. and Thomas, G. (2001) Trans-Golgi network sorting. Cell. Mol. Life Sci. **58**, 1067–1084.

130 Becherer, U., Moser, T., Stühmer, W. and Oheim, M. (2003) Calcium regulates exocytosis at the level of single vesicles. Nat. Neurosci. **6**, 846–853.

131 Schneeberger, K., Roth, S., Nieuwenhuis, E. E. S. and Middendorp, S. (2018) Intestinal epithelial cell polarity defects in disease: Lessons from microvillus inclusion disease. DMM Dis. Model. Mech. **11**, dmm031088.

132 Clevers, H. C. and Bevins, C. L. (2013) Paneth Cells: Maestros of the Small Intestinal Crypts. Annu. Rev. Physiol. **75**, 289–311.

133 Husain, S. and Thrower, E. (2009) Molecular and cellular regulation of pancreatic acinar cell function. Curr. Opin. Gastroenterol. **25**, 466–471.

134 Grapin-Botton, A. (2005) Ductal cells of the pancreas. Int. J. Biochem. Cell Biol. **37**, 504–10.

135 Gutierrez-Aguilar, R. and Woods, S. C. (2011) Nutrition and L and K-enteroendocrine cells. Curr. Opin. Endocrinol. Diabetes Obes. **18**, 35–41.

136 Raposo, G. and Stoorvogel, W. (2013) Extracellular vesicles: Exosomes, microvesicles, and friends. J. Cell Biol. **200**, 373–383.

137 Tung, K., Ernstoff, M., Allen, C. and Shu, S. (2019) A Review of Exosomes and their Role in The Tumor Microenvironment and Host-Tumor “Macroenvironment.” J. Immunol. Sci. **3**, 4–8.

138 Edgar, J. R. (2016) Q & A: What are exosomes, exactly? BMC Biol. **14**.

139 Bunggulawa, E. J., Wang, W., Yin, T., Wang, N., Durkan, C., Wang, Y. and Wang, G. (2018) Recent advancements in the use of exosomes as drug delivery systems. J. Nanobiotechnology **16**.

140 Chen, Y., Li, G. and Liu, M. L. (2018) Microvesicles as Emerging Biomarkers and Therapeutic Targets in Cardiometabolic Diseases. Genomics, Proteomics Bioinforma. **16**, 50–62.

141 Davidson, S. M., Riquelme, J. A., Zheng, Y., Vicencio, J. M., Lavandero, S. and Yellon, D. M. (2018) Endothelial cells release cardioprotective exosomes that may contribute to ischaemic preconditioning. Sci. Rep. **8**.

142 Gomari, H., Moghadam, M. F. and Soleimani, M. (2018) Targeted cancer therapy using engineered exosome as a natural drug delivery vehicle. Onco. Targets. Ther. **11**, 5753–5762.

143 Sáez, T., de Vos, P., Kuipers, J., Sobrevia, L. and Faas, M. M. (2019) Exosomes

derived from monocytes and from endothelial cells mediate monocyte and endothelial cell activation under high D-glucose conditions. Immunobiology **224**, 325–333.

144 Saeedi, S., Israel, S., Nagy, C. and Turecki, G. (2019) The emerging role of exosomes in mental disorders. Transl. Psychiatry **9**.

145 Ståhl, A. lie, Johansson, K., Mossberg, M., Kahn, R. and Karpman, D. (2019) Exosomes and microvesicles in normal physiology, pathophysiology, and renal diseases. Pediatr. Nephrol. **34**, 11–30.

146 Muralidharan-Chari, V., Clancy, J. W., Sedgwick, A. and D'Souza-Schorey, C. (2010) Microvesicles: Mediators of extracellular communication during cancer progression. J. Cell Sci. **123**, 1603–1611.

147 Neumüller, J. and Ellinger, A. (2008) Secretion and endocytosis in endothelial cells. In The Golgi Apparatus: State of the Art 110 Years after Camillo Golgi's Discovery.

148 Giblin, J. P., Hewlett, L. J. and Hannah, M. J. (2008) Basal secretion of von willebrand factor from human endothelial cells. Blood **112**, 957–964.

149 Schillemans, M., Karampini, E., Van Den Eshof, B. L., Gangaev, A., Hofman, M., Van Breevoort, D., Meems, H., Janssen, H., Mulder, A. A., Jost, C. R., et al. (2018) Weibel-palade body localized syntaxin-3 modulates von willebrand factor secretion from endothelial cells. Arterioscler. Thromb. Vasc. Biol. **38**, 1549–1561.

150 Da Silva, M. L. and Cutler, D. F. (2016) Von Willebrand factor multimerization and the polarity of secretory pathways in endothelial cells. Blood **128**, 277–285.

151 Greenlee, K. J., Werb, Z. and Kheradmand, F. (2007) Matrix metalloproteinases in lung: Multiple, multifarious, and multifaceted. Physiol. Rev. **81**, 69–98.

152 Ding, B. Sen, Nolan, D. J., Guo, P., Babazadeh, A. O., Cao, Z., Rosenwaks, Z., Crystal, R. G., Simons, M., Sato, T. N., Worgall, S., et al. (2011) Endothelial-derived angiocrine signals induce and sustain regenerative lung alveolarization. Cell **147**, 539–553.

153 Ding, B. Sen, Nolan, D. J., Butler, J. M., James, D., Babazadeh, A. O., Rosenwaks, Z., Mittal, V., Kobayashi, H., Shido, K., Lyden, D., et al. (2010) Inductive angiocrine signals from sinusoidal endothelium are required for liver regeneration. Nature **468**, 310–315.

154 Dardik, A., Yamashita, A., Aziz, F., Asada, H. and Sumpio, B. E. (2005) Shear stress-stimulated endothelial cells induce smooth muscle cell chemotaxis via platelet-derived growth factor-BB and interleukin-1α. J. Vasc. Surg. **41**, 321–331.

155 Zhao, Y., Biswas, S. K., McNulty, P. H., Kozak, M., Jun, J. Y. and Segar, L. (2011) PDGF-induced vascular smooth muscle cell proliferation is associated with dysregulation of insulin receptor substrates. Am. J. Physiol. - Cell Physiol. **300**, C1375–C1385.

156 Magid, R., Murphy, T. J. and Galis, Z. S. (2003) Expression of matrix metalloproteinase-9 in endothelial cells is differentially regulated by shear stress: Role of c-Myc. J. Biol. Chem. **278**, 32994–32999.

157 Muniyappa, R. and Sowers, J. R. (2013) Role of insulin resistance in endothelial dysfunction. Rev. Endocr. Metab. Disord. **14**, 5–12.

158 Böhm, F. and Pernow, J. (2007) The importance of endothelin-1 for vascular dysfunction in cardiovascular disease. Cardiovasc. Res. **76**, 8–18.

159 Kowalczyk, A., Kleniewska, P., Kolodziejczyk, M., Skibska, B. and Goraca, A. (2015)

The role of endothelin-1 and endothelin receptor antagonists in inflammatory response and sepsis. Arch. Immunol. Ther. Exp. (Warsz). **63**, 41–52.

160 Jurczyluk, J., Brown, D. and Stanley, K. K. (2003) Polarised secretion of cytokines in primary human microvascular endothelial cells is not dependent on N-linked glycosylation. Cell Biol. Int. **27**, 997–1003.

161 Verma, S., Nakaoke, R., Dohgu, S. and Banks, W. A. (2006) Release of cytokines by brain endothelial cells: A polarized response to lipopolysaccharide. Brain. Behav. Immun. **20**, 449–455.

162 Wagner, O. F., Christ, G., Wojta, J., Vierhapper, H., Parzer, S., Nowotny, P. J., Schneider, B., Waldhäusl, W. and Binder, B. R. (1992) Polar secretion of endothelin-1 by cultured endothelial cells. J. Biol. Chem. **267**, 16066–16068.

163 Su, J. B. (2015) Vascular endothelial dysfunction and pharmacological treatment. World J. Cardiol. **7**, 719–741.

164 Ii, M. and Losordo, D. W. (2007) Statins and the endothelium. Vascul. Pharmacol. **46**, 1–9.

165 Liao, J. K. (2002) Isoprenoids as mediators of the biological effects of statins. J. Clin. Invest. **110**, 285–8.

166 Pinal-Fernandez, I., Casal-Dominguez, M. and Mammen, A. L. (2018) Statins: pros and cons. Med. Clin. (Barc). **150**, 398–402.

167 Burghoff, S. and Schrader, J. (2011) Secretome of human endothelial cells under shear stress. J. Proteome Res. **10**, 1160–1169.

168 Muller, W. A. and Gimbrone, M. A. (1986) Plasmalemmal proteins of cultured vascular endothelial cells exhibit apical-basal polarity: Analysis by surface-selective iodination. J. Cell Biol. **103**, 2389–402.

169 Rohwedder, I., Montanez, E., Beckmann, K., Bengtsson, E., Dunér, P., Nilsson, J., Soehnlein, O. and Fässler, R. (2012) Plasma fibronectin deficiency impedes atherosclerosis progression and fibrous cap formation. EMBO Mol. Med. **7**, 564–576.

170 Dick, M., MacDonald, K., Tardif, J. C. and Leask, R. L. (2015) The effect of simvastatin treatment on endothelial cell response to shear stress and tumor necrosis factor alpha stimulation. Biomed. Eng. Online **14**, 1.

171 Park, H. J., Zhang, Y., Georgescu, S. P., Johnson, K. L., Kong, D. and Galper, J. B. (2006) Human umbilical vein endothelial cells and human dermal microvascular endothelial cells offer new insights into the relationship between lipid metabolism and angiogenesis. Stem Cell Rev. **2**, 93–102.

172 Gospodarowicz, D., Greenburg, G., Foidart, J. M. and Savion, N. (1981) The production and localization of laminin in cultured vascular and corneal endothelial cells. J. Cell. Physiol. **2**, 171–183.

173 Gubbiotti, M. A., Neill, T. and Iozzo, R. V. (2017) A current view of perlecan in physiology and pathology: A mosaic of functions. Matrix Biol. **57**–**58**, 285–298.

174 Bignon, M., Pichol-Thievend, C., Hardouin, J., Malbouyres, M., Bréchot, N., Nasciutti, L., Barret, A., Teillon, J., Guillon, E., Etienne, E., et al. (2011) Lysyl oxidase-like protein-2 regulates sprouting angiogenesis and type IV collagen assembly in the endothelial basement membrane. Blood **14**, 3979–3989.

175 McNeil, E. (2006) Zonula Occludens-1 Function in the Assembly of Tight Junctions in Madin-Darby Canine Kidney Epithelial Cells. Mol. Biol. Cell **4**, 1922–1932.

176 Giannotta, M., Trani, M. and Dejana, E. (2013) VE-cadherin and endothelial adherens junctions: Active guardians of vascular integrity. Dev. Cell **5**, 441–454.

177 Lemańska-Perek, A., Krzyżanowska-Gołąb, D., Pupek, M., Klimeczek, P., Witkiewicz, W. and Kątnik-Prastowska, I. (2016) Analysis of Soluble Molecular Fibronectin-Fibrin Complexes and EDA-Fibronectin Concentration in Plasma of Patients with Atherosclerosis. Inflammation **39**, 1059–1068.

178 Mc Namara, K., Alzubaidi, H. and Jackson, J. K. (2019) Cardiovascular disease as a leading cause of death: how are pharmacists getting involved? Integr. Pharm. Res. Pract. 1–11.

179 Pauty, J., Usuba, R., Takahashi, H., Suehiro, J., Fujisawa, K., Yano, K., Nishizawa, T. and Matsunaga, Y. T. (2017) A vascular permeability assay using an in vitro human microvessel model mimicking the inflammatory condition. Nanotheranostics **1**, 103–113.

180 Jiménez, N., Krouwer, V. J. D. and Post, J. A. (2013) A new, rapid and reproducible method to obtain high quality endothelium in vitro. Cytotechnology **65**, 1–14.

181 Kocherova, I., Bryja, A., Mozdziak, P., Angelova Volponi, A., Dyszkiewicz-Konwińska, M., Piotrowska-Kempisty, H., Antosik, P., Bukowska, D., Bruska, M., Iżycki, D., et al. (2019) Human Umbilical Vein Endothelial Cells (HUVECs) Co-Culture with Osteogenic Cells: From Molecular Communication to Engineering Prevascularised Bone Grafts. J. Clin. Med. **8**, 1602.

182 Srinivasan, B., Kolli, A. R., Esch, M. B., Abaci, H. E., Shuler, M. L. and Hickman, J. J. (2015) TEER Measurement Techniques for In Vitro Barrier Model Systems. J. Lab. Autom. **20**, 107–126.

183 Higdon, R. and Kolker, E. (2007) A predictive model for identifying proteins by a single peptide match. Bioinformatics **23**, 277–280.

184 Lu, P., Takai, K., Weaver, V. M. and Werb, Z. (2011) Extracellular Matrix degradation and remodeling in development and disease. Cold Spring Harb. Perspect. Biol. **3**, a005058.

185 Taylor, F., Af, M., Thm, M., Burke, M., G, D. S. and Ward, K. (2013) Statins for the primary prevention of cardiovascular disease. Cochrane Collab. **1**.

186 O'Keeffe, A. G., Nazareth, I. and Petersen, I. (2016) Time trends in the prescription of statins for the primary prevention of cardiovascular disease in the United Kingdom: A cohort study using The Health Improvement Network primary care data. Clin. Epidemiol. **8**, 123–132.

187 Farmer, J. (2000) Pleiotropic Effects of Statins. Curr. Atheroscler. Rep. **2**, 208–217.

188 Vestweber, D. (2008) VE-cadherin: The major endothelial adhesion molecule controlling cellular junctions and blood vessel formation. Arterioscler. Thromb. Vasc. Biol. **28**, 223–232.

189 Tornavaca, O., Chia, M., Dufton, N., Almagro, L. O., Conway, D. E., Randi, A. M., Schwartz, M. A., Matter, K. and Balda, M. S. (2015) ZO-1 controls endothelial adherens junctions, cell-cell tension, angiogenesis, and barrier formation. J. Cell Biol. **208**, 821–838.

190 Moon, J. C. and Bogle, R. G. (2006) Switching statins. BMJ **7554**, 1344–345.

191 Chang, Y., Li, Y., Ye, N., Guo, X., Li, Z., Sun, G. and Sun, Y. (2018) Atorvastatin protects the proliferative ability of human umbilical vein endothelial cells inhibited by

angiotensin II by changing mitochondrial energy metabolism. Int. J. Mol. Med. **1**, 33–42.

192 Björkhem-Bergman, L., Lindh, J. D. and Bergman, P. (2011) What is a relevant statin concentration in cell experiments claiming pleiotropic effects? Br. J. Clin. Pharmacol. **1**, 164–165.

193 Dang, H., Song, B., Dong, R. A. N. and Zhang, H. (2018) Atorvastatin reverses the dysfunction of human umbilical vein endothelial cells induced by angiotensin ii. Exp. Ther. Med. **16**, 5286–5297.

194 Lins, R. L., Matthys, K. E., Verpooten, G. A., Peeters, P. C., Dratwa, M., Stolear, J. C. and Lameire, N. H. (2003) Pharmacokinetics of atorvastatin and its metabolites after single and multiple dosing in hypercholesterolaemic haemodialysis patients. Nephrol. Dial. Transplant. **18**, 967–976.

195 Ries, C. (2014) Cytokine functions of TIMP-1. Cell. Mol. Life Sci. **54**, 1468–1479.

196 Khurana, R., Moons, L., Shafi, S., Luttun, A., Collen, D., Martin, J. F., Carmeliet, P. and Zachary, I. C. (2005) Placental growth factor promotes atherosclerotic intimal thickening and macrophage accumulation. Circulation **21**, 2828–2836.

197 Ioachim, E., Damala, K., Tsanou, E., Briasoulis, E., Papadiotis, E., Mitselou, A., Charhanti, A., Doukas, M., Lampri, L. and Arvanitis, D. L. (2012) Thrombospondin-1 expression in breast cancer: Prognostic significance and association with p53 alterations, tumour angiogenesis and extracellular matrix components. Histol. Histopathol. **2**, 209–216.

198 McGillicuddy, F. C., O'Toole, D., Hickey, J. A., Gallagher, W. M., Dawson, K. A. and Keenan, A. K. (2006) TGF-β1-induced thrombospondin-1 expression through the p38 MAPK pathway is abolished by fluvastatin in human coronary artery smooth muscle cells. Vascul. Pharmacol. **44**, 469–475.

199 Chistiakov, D. A., Melnichenko, A. A., Myasoedova, V. A., Grechko, A. V. and Orekhov, A. N. (2017) Thrombospondins: A role in cardiovascular disease. Int. J. Mol. Sci. **7**, 1540.

200 Thompson, J. C., Tang, T., Wilson, P. G., Yoder, M. H. and Tannock, L. R. (2014) Increased atherosclerosis in mice with increased vascular biglycan content. Atherosclerosis **1**, 71–75.

201 Kunjathoor, V. V., Chiu, D. S., O'Brien, K. D. and LeBoeuf, R. C. (2002) Accumulation of biglycan and perlecan, but not versican, in lesions of murine models of atherosclerosis. Arterioscler. Thromb. Vasc. Biol. **3**, 462–468.

202 Csont, T., Görbe, A., Bereczki, E., Szunyog, A., Aypar, E., Tóth, M. E., Varga, Z. V., Csonka, C., Fülöp, F., Sántha, M., et al. (2010) Biglycan protects cardiomyocytes against hypoxia/reoxygenation injury: Role of nitric oxide. J. Mol. Cell. Cardiol. **48**, 649–652.

203 Tamura, K., Yoshie, M., Hashimoto, K. and Tachikawa, E. (2014) Inhibitory effect of insulin-like growth factor-binding protein-7 (IGFBP7) on in vitro angiogenesis of vascular endothelial cells in the rat corpus luteum. J. Reprod. Dev. **6**, 447–453.

204 Saad, A., Wang, W., Herrmann, S. M. S., Glockner, J. F., McKusick, M. A., Misra, S., Bjarnason, H., Lerman, L. O. and Textor, S. C. (2016) Atherosclerotic renal artery stenosis is associated with elevated cell cycle arrest markers related to reduced renal blood flow and postcontrast hypoxia. Nephrol. Dial. Transplant. **11**, 1855–1863.

205 Van Breevoort, D., Van Agtmaal, E. L., Dragt, B. S., Gebbinck, J. K., Dienava-

Verdoold, I., Kragt, A., Bierings, R., Horrevoets, A. J. G., Valentijn, K. M., Eikenboom, J. C., et al. (2012) Proteomic screen identifies IGFBP7 as a novel component of endothelial cell-specific weibel-palade bodies. J. Proteome Res. **11**, 2925–2936.

206 Chambers, R. C. (2003) Role of coagulation cascade proteases in lung repair and fibrosis. Eur. Respir. J. **22**, 33s-35s.

207 Vikramadithyan, R. K., Kako, Y., Chen, G., Hu, Y., Arikawa-Hirasawa, E., Yamada, Y. and Goldberg, I. J. (2004) Atherosclerosis in perlecan heterozygous mice. J. Lipid Res. **45**, 1806–1812.

208 Mosca, L., Barrett-Connor, E. and Kass Wenger, N. (2011) Sex/gender differences in cardiovascular disease prevention: What a difference a decade makes. Circulation **124**, 2145–2154.

209 Skålén, K., Gustafsson, M., Knutsen Rydberg, E., Hultén, L. M., Wiklund, O., Innerarity, T. L. and Boren, J. (2002) Subendothelial retention of atherogenic lipoproteins in early atherosclerosis. Nature **417**, 750–754.

210 Martin, J., Denver, R., Bailey, M. and Krum, H. (2005) In vitro inhibitory effects of atorvastatin on cardiac fibroblasts: Implications for ventricular remodelling. Clin. Exp. Pharmacol. Physiol. **32**, 697–701.

211 Robertson, I. B., Horiguchi, M., Zilberberg, L., Dabovic, B., Hadjiolova, K. and Rifkin, D. B. (2015) Latent TGF-β-binding proteins. Matrix Biol. **47**, 44–53.

212 Fujikawa, Y., Yoshida, H., Inoue, T., Ohbayashi, T., Noda, K., Von Melchner, H., Iwasaka, T., Shiojima, I., Akama, T. O. and Nakamura, T. (2017) Latent TGF-β binding protein 2 and 4 have essential overlapping functions in microfibril development. Sci. Rep. **7**, 43714.

213 Hyytiäinen, M. and Keski-Oja, J. (2003) Latent TGF-β binding protein LTBP-2 decreases fibroblast adhesion to fibronectin. J. Cell Biol. **6**, 1363–1374.

214 Zhu, L., Gu, Q. and Fang, L. (2019) Cholesterol-mediated regulation of angiogenesis: An emerging paradigm. Cardiol. Plus **1**, 1.

215 Helbing, T., Rothweiler, R., Ketterer, E., Goetz, L., Heinke, J., Grundmann, S., Duerschmied, D., Patterson, C., Bode, C. and Moser, M. (2011) BMP activity controlled by BMPER regulates the proinflammatory phenotype of endothelium. Blood **18**, 5040–5049.

216 Scott, I. C., Blitz, I. L., Pappano, W. N., Maas, S. A., Cho, K. W. Y. and Greenspan, D. S. (2001) Homologues of twisted gastrulation am extracellular cofactors in antagonism of BMP signalling. Nature **6827**, 475–478.

217 Su, X., Ao, L., Shi, Y., Johnson, T. R., Fullerton, D. A. and Meng, X. (2011) Oxidized low density lipoprotein induces bone morphogenetic protein-2 in coronary artery endothelial cells via toll-like receptors 2 and 4. J. Biol. Chem. **14**, 12213–12220.

218 Zhang, M., Zhou, S.-H., Li, X.-P., Shen, X.-Q., Fang, Z.-F., Liu, Q.-M., Qiu, S.-F. and Zhao, S.-P. (2008) Atorvastatin Downregulates BMP-2 Expression Induced by Oxidized Low-Density Lipoprotein in Human Umbilical Vein Endothelial Cells. Circ. J. **5**, 807–812.

219 Zhuo, L., Hascall, V. C. and Kimata, K. (2004) Inter-α-trypsin inhibitor, a covalent protein-glycosaminoglycan- protein complex. J. Biol. Chem. **37**, 38079–38082.

220 Lortat-Jacob, H., Burhan, I., Scarpellini, A., Thomas, A., Imberty, A., Vivès, R. R., Johnson, T., Gutierrez, A. and Verderio, E. A. M. (2012) Transglutaminase-2

interaction with heparin: Identification of a heparin binding site that regulates cell adhesion to fibronectin-transglutaminase-2 matrix. J. Biol. Chem. **22**, 18005–18017.

221 Soehnlein, O., Eskafi, S., Schmeisser, A., Kloos, H., Daniel, W. G. and Garlichs, C. D. (2004) Atorvastatin induces tissue transglutaminase in human endothelial cells. Biochem. Biophys. Res. Commun. **1**, 105–109.

222 Sumi, Y., Inoue, N., Azumi, H., Seno, T., Okuda, M., Hirata, K., Kawashima, S., Hayashi, Y., Itoh, H. and Yokoyama, M. (2002) Expression of tissue transglutaminase and elafin in human coronary artery: Implication for plaque instability. Atherosclerosis **160**, 31–39.

223 Simons, D., Grieb, G., Hristov, M., Pallua, N., Weber, C., Bernhagen, J. and Steffens, G. (2011) Hypoxia-induced endothelial secretion of macrophage migration inhibitory factor and role in endothelial progenitor cell recruitment. J. Cell. Mol. Med. **3**, 668–678.

224 Morand, E. F., Leech, M. and Bernhagen, J. (2006) MIF: A new cytokine link between rheumatoid arthritis and atherosclerosis. Nat. Rev. Drug Discov. **5**, 399–411.

225 Mitchell, R. A., Metz, C. N., Peng, T. and Bucala, R. (1999) Sustained mitogen-activated protein kinase (MAPK) and cytoplasmic phospholipase A2 activation by macrophage migration inhibitory factor (MIF): Regulatory role in cell proliferation and glucocorticoid action. J. Biol. Chem. **25**, 18100–18106.

226 Greenwood, J. and Mason, J. C. (2007) Statins and the vascular endothelial inflammatory response. Trends Immunol. **28**, 88–98.

227 Relou, I. A. M., Damen, C. A., Van Der Schaft, D. W. J., Groenewegen, G. and Griffioen, A. W. (1998) Effect of culture conditions on endothelial cell growth and responsiveness. Tissue Cell **30**, 525–530.

228 Addis, R., Campesi, I., Fois, M., Capobianco, G., Dessole, S., Fenu, G., Montella, A., Cattaneo, M. G., Vicentini, L. M. and Franconi, F. (2014) Human umbilical endothelial cells (HUVECs) have a sex: Characterisation of the phenotype of male and female cells. Biol. Sex Differ. **5**, 18.

229 Pelat, M., Dessy, C., Massion, P., Desager, J. P., Feron, O. and Balligand, J. L. (2003) Rosuvastatin decreases caveolin-1 and improves nitric oxide-dependent heart rate and blood pressure variability in apolipoprotein E-/- mice in vivo. Circulation **107**, 2480–2486.

230 Maguire, J. J., Wiley, K. E., Kuc, R. E., Stoneman, V. E. A., Bennett, M. R. and Davenport, A. P. (2006) Endothelin-mediated vasoconstriction in early atherosclerosis is markedly increased in ApoE-/- mouse but prevented by atorvastatin. Exp. Biol. Med. **231**, 806–812.

231 Elsadek, B. and Kratz, F. (2012) Impact of albumin on drug delivery - New applications on the horizon. J. Control. Release **157**, 4–28.

232 Barber, T., Esteban-Pretel, G., Marín, M. P. and Timoneda, J. (2014) Vitamin A deficiency and alterations in the extracellular matrix. Nutrients **6**, 4984–5017.

233 Augustin, H. G. and Koh, G. Y. (2017) Organotypic vasculature: From descriptive heterogeneity to functional pathophysiology. Science (80-.). **357**, eaal2379.

234 Al-Kofahi, M., Yun, J. W., Minagar, A. and Alexander, J. S. (2017) Anatomy and roles of lymphatics in inflammatory diseases. Clin. Exp. Neuroimmunol. **8**, 199–214.